Source-to-Outcome Modeling Physiologically Based Pharmacokinetic/Pharmacodynamic (PBPK/PD) Model Linked to a Dietary Exposure Model: Chlorpyrifos as a Case Study

Science Issues Paper for SAP Meeting on
Chlorpyrifos Physiologically Based Pharmacokinetic/Pharmacodynamic (PBPK/PD) Model linked to the Cumulative and Aggregate Risk Evaluation System (CARES)
February 15-18, 2011, Washington, D.C.

Dow AgroSciences

The Dow Chemical Company

Battelle Pacific Northwest National Laboratory

January 7, 2011

Table of Contents

Page

Page

Page

Terminology

AChE – acetylcholinesterase

ADME – adsorption, distribution, metabolism, and excretion

BuChE – butyrylcholinesterase

CARES: Cumulative and Aggregate Risk Evaluation System, a dietary exposure software program

CNS - Central Nervous System

CPF – Chlorpyrifos

CPF-oxon – Chlorpyrifos oxon

CYP – Cytochrome P450

Dietary exposure software: A software program that relates data on pesticide residues in agricultural commodities to daily doses for one or more consecutive days in populations of individuals of a specific age. Examples of these models include CARES, LifeLine, DEEM™ and SHEDS.

Gompertz function: A mathematical equation of a specific form. Used for fitting increases in volume as s function of weight or age.

LifeLine: A dietary exposure software program

NHANES – National Health and Nutrition Examination Survey

PBPK/PD- physiologically based pharmacokinetic and pharmacodynamic

RBC – red blood cell

Sensitivity: a) A measure of the correlation of a change in one variable and another in a model, and b) A measure of the toxicological change from a given dose.

SHEDS: Stochastic Human Exposure and Dose Simulation, a dietary exposure program

Source-to-outcome model: a model (composed of exposure and PBPK/PD software) that allows the direct determination of the potential for the occurrence of apical effects from levels of residues in foods.

TCPy - 3, 5, 6-trichloro-2-pyridinol

Typical Adult model: A PBPK/PD program that describes the pharmacokinetics and pharmacodynamics of CPF, its major metabolites, and cholinesterase for a typical adult from oral doses of CPF, based on the model first described by Timchalk et al, (2002).

LifeStage model: PBPK/PD program expanded to include the ontogeny of enzymes and tissue compartments with age to describe the pharmacokinetics and pharmacodynamics of CPF from oral doses.

Longitudinal dietary simulations: The statistical processes used to construct individuals' dietary intakes over 2 or more consecutive days based on data on multiple individuals collected in dietary surveys that only determined data on two non-consecutive days.

Uncertainty: Epistemic uncertainty arising from incomplete knowledge.

Variation model: a PBPK/PD program that includes interindividual variation in response to oral doses of CPF in populations of individuals of specified ages, an expansion of the LifeStage model.

Variability: Aleatory uncertainty, arising from actual differences in dose received or response to those doses due to differences in individuals.

Z-score: A method of describing variation in terms of a distribution's mean and standard deviation. Z-scores of -2, -1, 0, 1, 2 are values that fall at two standard deviations below the mean, one standard deviation below the mean, the mean value, one standard deviation above

the mean and two standard deviations above the mean. The following table gives the Z-scores that correspond to various percentiles for normal distributions.

Percentiles	Z-score
1	-2.3
5	-1.6
10	-1.3
25	-0.7
50	0
75	0.7
90	1.3
95	1.6
99	2.3

Plotting the values of a distribution against their Z-score produces a straight line if the data are normally distributed. Plotting the logs of data against Z-scores produces a straight line when the data are log-normally distributed.

Project Contributors

A variety of scientists made important contributions to the successful development and implementation of this project.

Dow AgroSciences

Dr. Daland Juberg

Dr. Cheryl Cleveland

The Dow Chemical Company

Paul Price M.S.

Dr. Michael Bartels

Battelle Pacific Northwest National Laboratory

Dr. Torka Poet

Dr. Paul Hinderliter

Dr. Charles Timchalk

Executive Summary

This case study presents the results of the continued development of the scientific database for a particular chemical and shows how using new tools and conceptual approaches can bring objective, data driven insights, to the risk assessment process. The development of data to replace uncertainty represents advancement in knowledge. Specifically, this project links data, computer simulation models, and new analyses to improve risk assessment for a chemical, chlorpyrifos (CPF), which has as database that is sufficiently robust to support these new modeling techniques.

In this paper we describe the methodologies and data used to create a process that captures the events in the pathway that begins with data on residue levels and ends with predictions of cholinesterase inhibition across the U.S. population, a source-to-outcome model. The source-to-outcome model consists of two publically available software programs. The first program can be any of the dietary exposure software programs that produce estimates of longitudinal dietary exposures (the specific model used here is CARES). The second program is the Variation model, a program created to run on acslXtreme, a publically available software platform for PBPK modeling. A copy of the Variation model is provided in Attachment C of this report.

The steps in the creation of the source-to-outcome model are outlined in detail in this report and this approach can be applied to other chemicals with other toxicological endpoints of interest. Using this approach, key events in the toxicity pathway are identified that are as close to the initial interaction between the biological targets/molecules in the body and the chemical, or its active metabolite (see Section 2). Once this has occurred, a physiologically based pharmacokinetic/pharmacodynamic (PBPK/PD) model is developed and used to predict the dose response for the key event (see Section 3). Once the PBPK/PD model is in place, a sensitivity analysis is performed that identifies the factors that drive variation in response (see Section 4). Information on the interindividual variation in these factors is obtained from published sources and is used to create simulation models of interindividual variation in the relationship between dose and the key event.

The two models define dose and the individual in very specific ways. The exposure portions of the source-to-outcome models need to be matched to the specific needs of the PBPK/PD models of variation. In this project an existing dietary model was used to characterize exposure (see Section 5). The linkage between the two models was achieved by a careful consideration of the physiological processes involved in the exposure event (see Section 6).

In Sections 3, 4, 5, and 8 we investigated the ability of the model to predict changes in levels of cholinesterase inhibition and findings such as distribution of blood concentrations of chlorpyrifos and its metabolites. These predictions can be evaluated using other modeled and measured data. In general, we have demonstrated that the various predictions of the source-to-outcome model are consistent with empirical data reported in the literature. However, these model-to-measurement comparisons were limited by the relevance of the measurement data. Because of this, we conclude that the final predictions of impacts on AChE in the general population are likely to be within an order of magnitude of actual levels but additional monitoring data are required in order to determine if the models are in fact more precise.

Once the source-to-outcome model is completed, it can be used in a variety of ways. We believe that the value of a source-to-outcome model is fully realized when the model is used as a tool for exploring the processes that determine the source-to-outcome pathway rather than just as a risk "calculator." In this project the source-to-outcome model has been used in a number of ways and has demonstrated a number of novel and potentially valuable findings.

- Age related differences in sensitivity to CPF were found to be small (less than 2 fold) and to differ with dose and endpoint (Section 4).
- The models found that variation in metabolism but not variation in physiology or level of physical activity were important for infants. For adults, variation in physiology had some effect but was still minor compared to metabolism (see Section 4).

- The source-to-outcome model allowed the investigation of the impact of repeated doses of CPF on blood levels of CPF and CPF–oxon and the impact on cholinesterases (see Section 7).
    - This work indicated that neither CPF nor CPF-oxon accumulated over time.
    - The inhibition of AChE increased over time when the same doses occurred on multiple days. At the dose levels that currently occur from exposure to dietary residues the inhibition of RBC AChE was approximately 3-fold. Increases of inhibition in brain AChE inhibition less than 3-fold across all doses.
    - When day-to-day variation in dietary exposure was considered, the increase in impact from one to multiple days was found to be less than 3-fold.
    - The impact of multi-day exposures was much smaller for individuals with high exposures. The impact of dietary exposures on the RBC and brain AChE inhibition for these individuals was dominated (90% of the impact) by the dose received from a single day.
- At current dietary levels of exposure the difference between the responses of the typical and sensitive individual (resulting from differences in metabolism, physiology, and activity) was less than 2 (Section 10).

The source-to-outcome model was used to evaluate the impact of the current dietary exposure on RBC and brain AChE inhibition. This was done in two ways. First the model investigated the impacts in three age groups after quasi-steady state conditions were obtained (see Section 9). The peak inhibitions did not exceed 0.01% inhibition for either RBC or brain inhibition. The second way the models were used was to determine age-specific values for the interspecies and interindividual uncertainty factors (Section 10). This assessment found that models prediction of variation in response overlapped with the responses seen in recent animal studies (Attachment G). In addition, human variation in response was found to be modest (less than a factor of 2 between the responses in a typical adult or infant and a sensitive adult or infant) for doses that cause 10% or less RBC AChE inhibition in humans. As a result, the values of age-specific interspecies and interindividual uncertainty factors were small and ranged between 1 and 2.

The case study achieved its goals. A key event, AChE inhibition, was identified and models of interindividual variation in both dose and response were constructed. The combined models form a complete source-to-outcome model. The final source-to-outcome model's quantitative predictions of the AChE inhibition and internal concentrations of CPF and its metabolites were evaluated. The final source-to-outcome model provided a framework that has allowed diverse information from *in vitro* studies of metabolism, biomonitoring studies in humans, test animal data, and statistical tools to come together to provide quantitative insights on the impacts posed by a chemical to the general U.S. population.

The value in this project relates not to CPF as such, but rather in showcasing how both empirical and modeled data can be leveraged and linked to inform and advance our insight on the risk assessment of specific chemicals. The hope is that continued discussion and refinement of the techniques and thinking brought forward in this project will allow multiple stakeholders to utilize these and similar approaches for advancing risk assessment and aiding regulatory decision-making, goals that align with and that have been embraced by the broader scientific community.

1. Introduction

1.1 Report objectives

Risk assessments of dietary exposures to pesticides have used detailed characterization of variation in age-specific dietary exposures, but have relied on data from test animals and default values for uncertainty factors when characterizing the toxicity of pesticides. These default values do not necessarily reflect specific knowledge of a chemical's mechanism of action, or our increased ability to quantitatively predict internal doses and responses in humans.

This paper summarizes the development of a source-to-outcome model that provides a single consistent analysis of both toxicity and exposure and specifically includes data on mechanism of action. The source-to-outcome model provides a quantitative relationship between the amount of a pesticide, in this case chlorpyrifos (CPF), in food, and the probability of the occurrence of cholinesterase inhibition in humans. CPF is used as the example chemical because the molecule has a rich data set including:

- A well-defined metabolism and mechanism of action
- Multiple markers for exposure and effect
- A well-defined pharmacokinetic/pharmacodynamic model that quantitatively predicts markers of early effects (e.g., inhibition of RBC and plasma cholinesterases)
- Multiple human data sets available for model calibration and evaluation of model predictions

This document and its attachments provide a detailed description of the source-to-outcome model and information on the uncertainty in the model's predictions. The source-to-outcome model is composed of any of the existing dietary exposure software that can produce estimates of longitudinal exposure and a pharmacokinetic/pharmacodynamic model of response. Together these programs relate data on residues on crops to predictions of inhibition of cholinesterases (Figure 1).

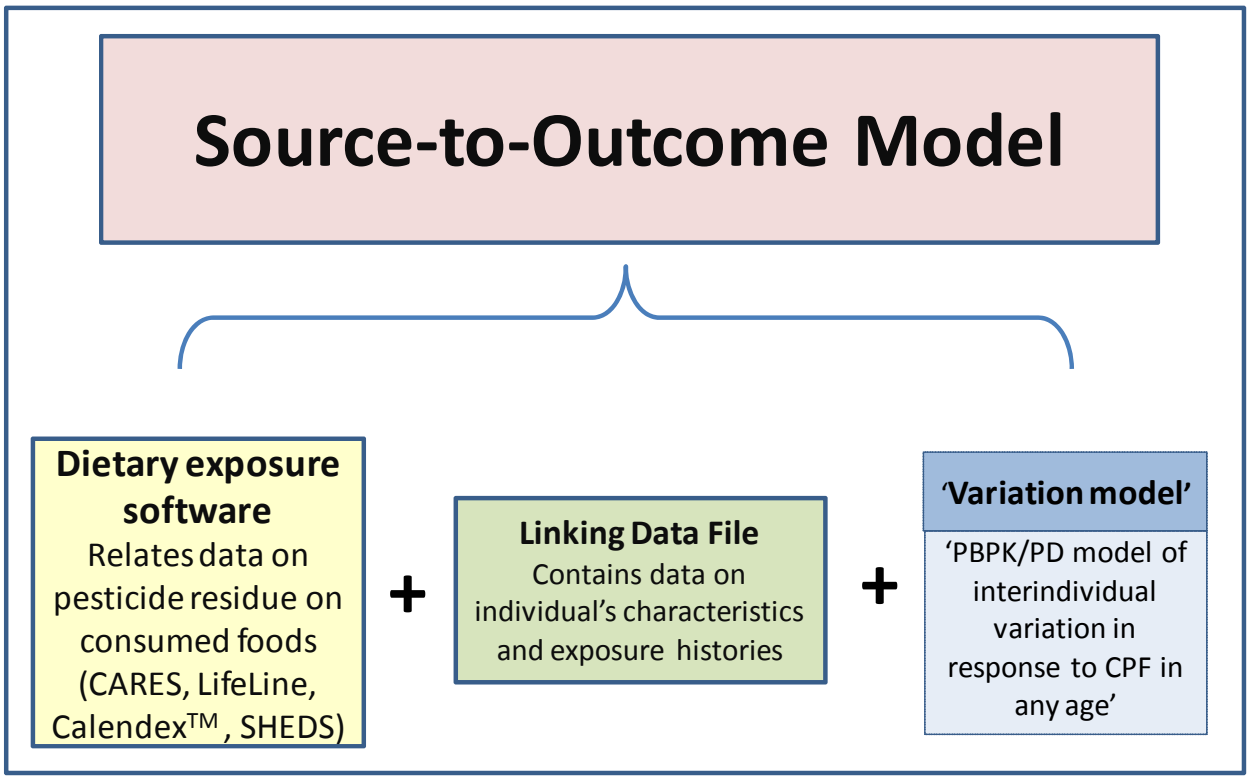

Figure 1. Components of the source-to-outcome model

The source-to-outcome model is used to investigate of the impact of current dietary exposures on three different age groups (thirty year-olds, three year-olds, and six month-olds). In addition, the document presents examples by which predictions of the model could be used in an assessment of the potential effects using dietary residues of CPF as an example. Other examples showcasing the utility of the model include an analysis of the factors that influence the relative sensitivity of individuals, predictions of the impacts of longitudinal dietary exposures, and the development of chemical- and age-specific uncertainty factors.

The analysis in this document focuses on measures of internal dose and key events in the toxicity pathway that lead to inhibition of cholinesterases. The specific targets are the characterization of the dose response for the inhibition of acetyl cholinesterase (AChE) in red blood cells and brain from exposures to dietary residues by the oral route. The document does not address effects that may be associated with non-cholinergic

mechanisms[1], nor does it directly address exposures that occur from other sources, by other routes, or to other age groups.

1.2 *Document organization*

The paper begins with a review of the relevant information on the absorption, distribution, metabolism, and excretion (ADME) and mechanism of action for CPF (Section 2). We next describe the creation and final characteristics of the various components of the source-to-outcome model (Sections 3 through 7).

One component in the source-to-outcome model is the software program that determines the relationship of the oral dose to the inhibition of cholinesterase. The development of this component is presented in a series of three steps (Figure 2).

Step 1 (Section 3): a PBPK/PD model of the relationship between oral doses and 1) internal concentrations of CPF and its metabolites and 2) markers of the key event, brain AChE, is described for a generic adult (Typical Adult model).

Step 2 (Section 3): the expansion of this model to investigate age-related changes and specifically to predict dose-response relationships in children and infants is described. This expanded model is called the "LifeStage" model.

Step 3 (Section 4): the LifeStage model is expanded to address interindividual variability in dose response that occurs from differences in physical activity, physiology, and metabolism in specific age groups. This final version is called the "Variation" model, and is used as the PBPK/PD component of the final source-to-outcome model.

1 This project has determined internal concentrations of CPF and CPF oxon that are measures of internal dose that could be used to evaluate the potential for the occurrence of other endpoints.

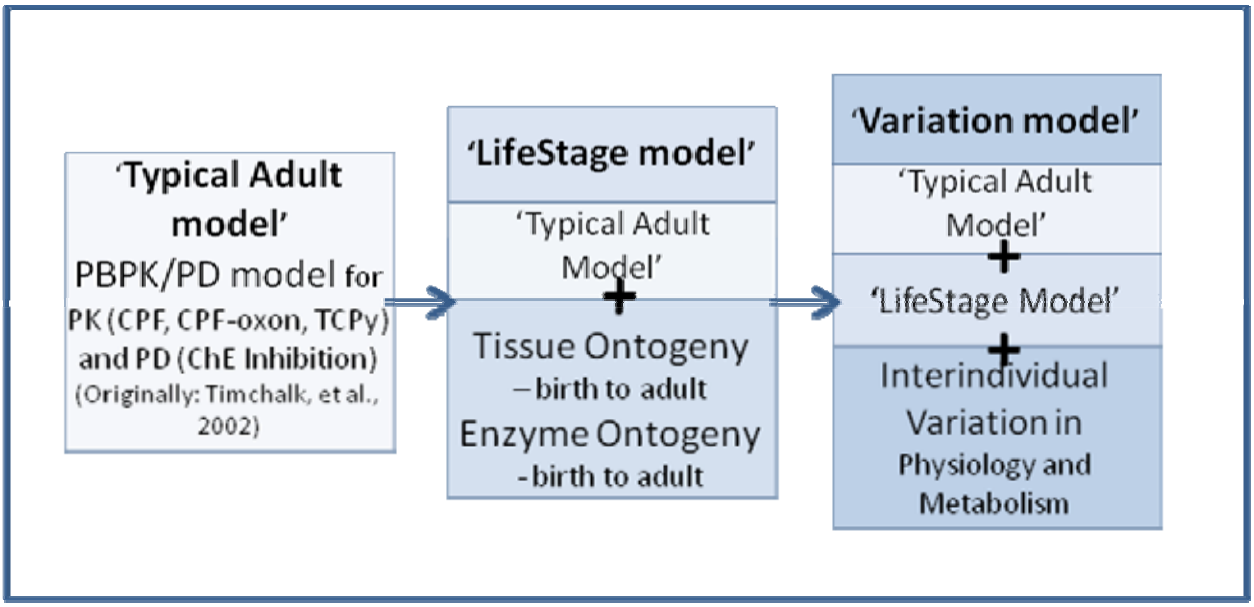

Figure 2. Steps in the creation of the Variation model. The variation model consists of the original "Typical Adult Model" with added parameterization to describe growth in tissues and enzymes with age and finally variability around important physiological and biochemical factors.

Sections 3 and 4 also include a series of model-to-measurement exercises that demonstrate the LifeStage and Variation's models' ability to predict age-related variation in physiology and the effects of CPF in human volunteer studies. Finally, in Section 4 the Variation model is used to investigate the interindividual variation of the dose response of RBC and brain AChE.

Section 5 presents the dietary exposure component of the source-to-outcome model. The modeling of CPF is described along with the data on residues used in this analysis. The issue of the uncertainty in characterizing longitudinal exposures is addressed and multiple approaches of characterizing longitudinal exposure are investigated. Section 6 presents the process used to link the dietary exposure software and the PBPK/PD component of the Variation model.

The uncertainty in the source-to-outcome model's predictions of internal dose and biomarkers of exposure are evaluated in Section 7 using a series of model-to-measurement

exercises. The purpose of these exercises is to demonstrate how data can be used to evaluate the predictions of present and future source-to-outcome models.

The document then describes the use of the complete source-to-outcome model to characterize the impacts of dietary exposures using CPF as a case study. This description begins in Section 8 with the use of the source-to-outcome model to analyze the impact of longitudinal exposures on predictions of impact of dietary doses. The model is then used to directly predict the impacts of current dietary exposures on AChE in different age groups (Section 9). Finally, the source-to-outcome model is used to develop age-specific uncertainty factors for the interspecies and interindividual uncertainty factors (Section 10). The paper concludes with a summary of work presented in this paper (Section 11).

1.3 *The use of a source-to-outcome model and the future of risk assessment*

Risk assessments of chemicals are undergoing a transition. New tools and approaches are enabling assessors to directly characterize the impact of factors such as extrapolation from toxicity in animals to humans, age-related differences, human variation, and variation in dose over time. At the same time the expectations for risk assessments have increased. Assessments are expected to produce quantitative estimates of risk and descriptions of how these risks vary across individuals. Finally, future risk assessments will be expected to minimize the use of animals and maximize the use of *in vitro* and *in silico* tools. These changes have been discussed in two recent National Academies Reports (National Research Council, 2007; National Research Council, 2008). The source-to outcome model described in this paper meets a number of the goals identified in these reports.

In the National Academies of Science report, *Toxicity Testing in the 21st Century,* toxicology is challenged to understand toxicity in terms of toxicity pathways (National Research Council, 2007). These pathways begin with early perturbations of cellular response networks that precede the apical events in time and are necessary for the occurrence of the apical effects. The authors state that toxicological investigations of a chemical should focus on the early events in the pathways rather than on apical effects and that dose response modeling should be informed by data on the mechanism of action rather

than the simple empirical fitting of response data. This may be achieved by constructing quantitative dose response relationships for those perturbations using PBPK/PD models. The concept of a perturbation in a cellular response network that is "obligatory" for the occurrence of apical effects is also parallel to the "key event" concept in the carcinogen mode of action risk assessment (U.S. EPA, 2005). A key event is defined as an empirically observable precursor step that is itself a necessary element of the mode of action or is a biological marker for such an element (U.S. EPA, 2005).

As the NAS report indicates creating a dose response model for key events in a toxicity pathway provides a number of advantages. First, early key events provide more tractable targets for building pharmacodynamic (PD) models. This allows the PD models to avoid having to predict the complexity of the complete pathway. Second, early key events are easier to study with *in vitro* techniques. Finally, for chemicals in commerce, human biomonitoring of the key event (or the absence of the event) may provide data to inform the PD modeling.

In this assessment we use an organophosphorus insecticide, CPF, as an example to illustrate the methodology of the source-to-outcome model. Similar to numerous organophosphorous pesticides, high doses of CPF may be associated with a range of apical effects in mammals that occur as a result of the compound's effect on the cholinergic system. However the initial perturbation of the cholinergic system that leads to these apical effects is the inhibition of AChE in the central nervous system and in other tissues. Thus, this change is an example of the "obligatory perturbation" concept identified in the National Academies of Science report.

The source-to-outcome model discussed in this paper is based on three key events. The first is brain AChE inhibition, which is a necessary event in the toxicity pathway for CNS apical effects. The other two key events (inhibition of AChE in RBCs and BuChE in plasma) are not part of the toxicity pathway related to cholinergic effects but represent conservative markers of exposure, since inhibition of these blood enzymes likely occurs presystemically in the liver during oxon metabolite production.

Figure 3 presents a source-to-outcome model built on the mode of action for CPF's effects on the cholinergic system. While a detailed description of CPF's mode of action is described in Section 2, the process can be summarized as follows. CPF is converted to the oxon which inhibits a variety of cholinesterases. Inhibition of AChE in the central nervous system leads to accumulation of acetylcholine at neuronal junctions in target tissues. As Figure 3 indicates, the PBPD models do not include processes in the toxicity pathway beyond the key event. The PBPD model does make quantitative predictions of when the key event occurs in an individual based on the mechanisms of metabolism and interaction with cholinesterase. Thus the PBPD model fulfills the goal of extrapolation as stated on page 9 of the National Academies of Sciences report *Toxicity Testing in the 21st Century*, to provide a quantitative, mechanistic understanding of the dose-response relationship.

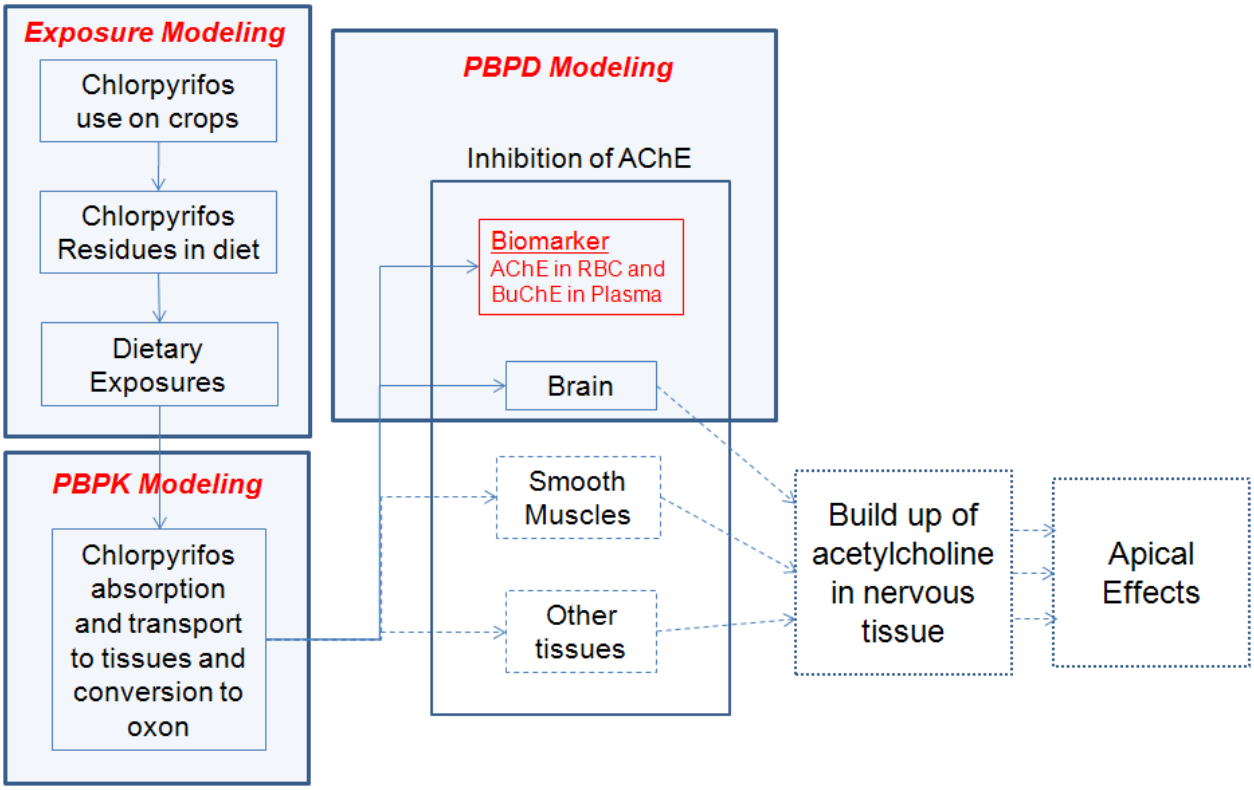

Figure 3. Source-to-outcome model for the key events of CPF and the subsequent portions of the toxicity pathway. Portions enclosed in shaded areas are included in the source-to-outcome model.

This project also addresses concerns raised in the National Academy of Sciences report Science and Decisions: Advancing *Risk Assessment (National Research Council, 2008)*. In chapter 5 of the report, the panel members expressed concern that current RfD-based risk characterizations do not provide information on the fraction of the population adversely affected by a given dose or on any other direct measure of risk.

The source-to-outcome model produces quantitative estimates of key events (inhibition of AChE) that are required steps in the pathway that lead to cholinergic effects or are conservative markers for such steps. By demonstrating when blood and brain AChE are unchanged, the models are able to predict when cholinergic effects may or may not occur.

A second issue raised in Science and Decisions: Advancing Risk Assessment, is the importance of considering population variability in humans. As discussed in detail in Sections 3 and 4 of this paper, the source-to-outcome model allows for a systematic examination of the factors that affect variation in dose, ADME, and responses in the key events. These models allow the direct investigation of sensitive subpopulations defined by age, variation in enzyme activity, or other factors.

Finally, Science and Decisions: Advancing Risk Assessment, raises the issue of default assumptions in risk assessment and the level of theory and evidence that is required to deviate from a default. In Section 10 of this paper, we present an illustration of how the source-to-outcome models can be used for setting values of interspecies and interindividual uncertainty factors that differ from the default values. This presentation occurs at the end of the paper after the technical basis for the model and its predictions are presented. Thus, the findings of the modeling project provide a basis for determining if the proposed uncertainty factor values meet the suggested criteria of "transparency, clarity, consistency, and reasonableness" suggested by the Academy panel report.

In summary, while the basic mechanism of action for CPF effects on the cholinergic system has been understood for decades, the development of quantitative models of the key event is an example of the future of toxicology as envisioned by recent National Academies of Sciences reports.

2. CPF metabolism/mechanism of action

Section overview

This section presents information on the pharmacokinetics and metabolism of CPF. The chapter begins with a review of the previously reported animal and human PK/metabolism data, then discusses new *in vitro* metabolism data obtained with human donor tissues from humans of various ages that was used in the development of the LifeStage PBPK model.

CPF exerts its biological effects through a complex pathway that includes metabolic bioactivation to CPF-oxon and detoxification to trichloropyridinol (TCPy) and dialkylphosphate metabolites (diethylphosphate (DEP) and diethylthiophosphate (DETP)) (Figure 4). Since the concentration of CPF-oxon is the crucial dose metric leading to the toxicity of CPF (Amitai *et al.*, 1998; Chambers *et al.*, 1994), it is important to understand the metabolic fate of CPF in humans and any dose- or species-differences in activation and detoxification of CPF. *In vitro* studies of metabolism of CPF were performed to better understand interindividual and age related variation. The results of the studies are also presented.

2.1 Chemical properties

CPF is one of a series of phosphate triesters that are used as pesticides. The specific structure of CPF (below) includes a phosphothioate functionality, two ethoxy moieties, and a trichloropyridinol leaving group. CPF is fairly lipophilic with a log K_{ow} value of 4.96 (Sangster, 1994), whereas the CPF-oxon and hydrolysis metabolites TCPy, DETP and DEP are substantially more polar. The parent compound; containing the P=S bond is more chemically stable than the reactive CPF-oxon, due to the P=S bond being less electronegative than the corresponding P=O moiety of the oxon metabolite, which stabilizes CPF from loss of TCPy (Ballantyne and Marrs, 1992; Chambers and Levi, 1992). As a result, toxicological effects are generally ascribed to the more reactive CPF-oxon than the parent compound (Sultatos, 1994).

Toxicological effects arising from formation of the CPF-oxon metabolite are primarily via inhibition of acetylcholinesterase (AChE) activity, through covalent binding of CPF-oxon to the serine active site of this class of enzymes (Thompson *et al.*, 2010). This inhibition of the enzyme results in accumulation of acetylcholine at neuronal junctions. Covalent binding of CPF-oxon has also been shown to occur to serine, tyrosine or lysine residues of butyrylcholinesterase (BuChE), albumin, tubulin and numerous other proteins (Albers *et al.*, 2010; Chiu *et al.*, 2007; Grigoryan *et al.*, 2009; Grigoryan *et al.*, 2008; Noort *et al.*, 2009). These non-ChE protein targets are consistent with reports of effects of CPF in various *in vivo* or *in vitro* test systems that are not mediated by inhibition of AChE (Moreira *et al.*, 2010; Nomura and Casida, 2010; Ray *et al.*, 2010; Yang *et al.*, 2008).

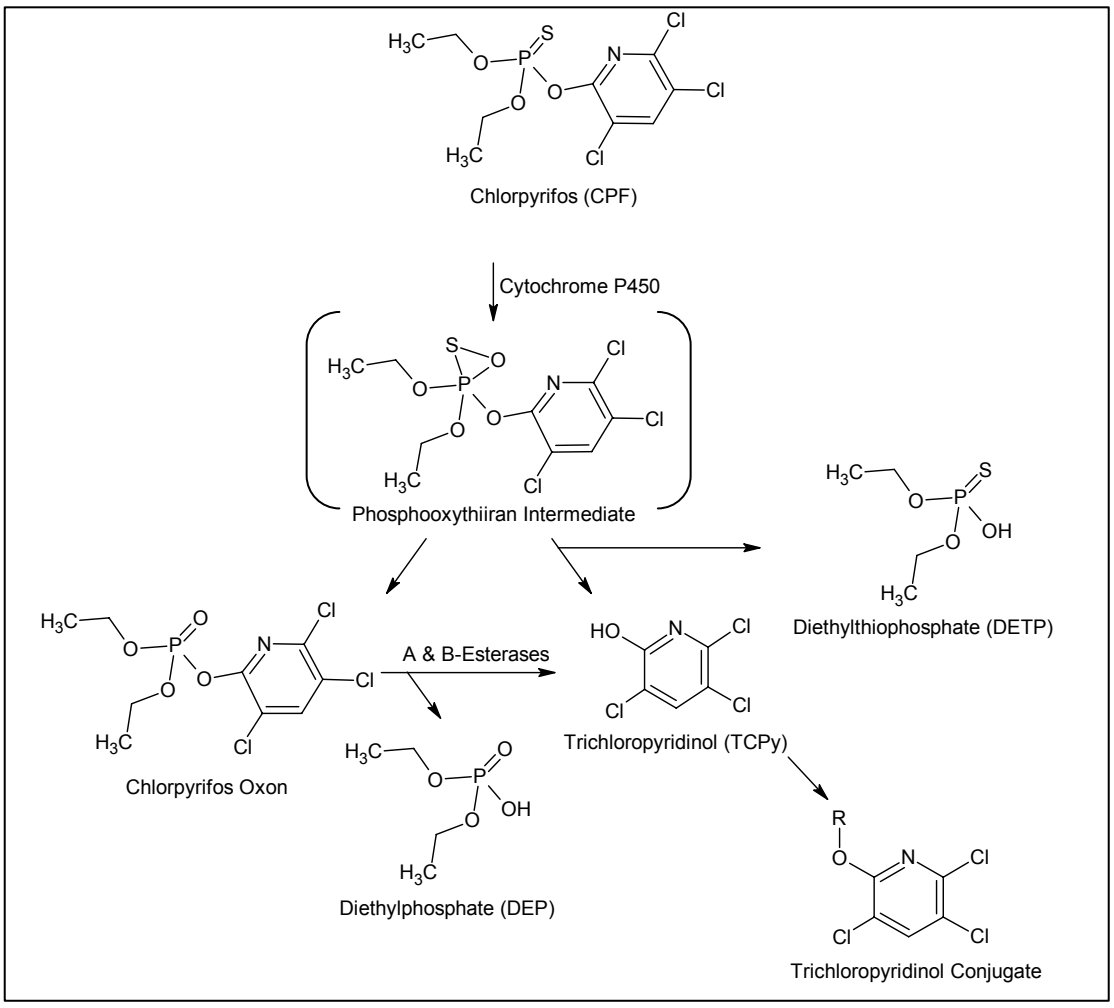

Figure 4. Metabolic scheme for CPF in mammals.

2.2 Metabolism studies

In rats, CPF is well absorbed and excreted primarily in the urine as conjugates of TCPy (Bakke and Price, 1976; Smith *et al.*, 1967). Nolan *et al.* (1987) also studied CPF metabolism in the rat and found that it undergoes high first-pass metabolism to TCPy, with no parent compound excreted in urine. These authors reported the major urinary metabolite to be TCPy-glucuronide, with lesser amounts of TCPy-sulfate and free TCPy (Nolan *et al.*, 1987). Sunaga, *et al.* (1989) report similar findings, following inter-peritoneal administration of CPF to rats, showing urinary TCPy accounted for >85% of the administered dose of CPF, with lower percentages of the DETP and DEP metabolites recovered. A subsequent study by Mendrala and Brzak was conducted to evaluate the time-course of blood metabolites following oral administration of 0.5-100 mg CPF/kg body weight. The authors found 99% of blood metabolites as TCPy with only 1% as parent compound. Trace levels of CPF-oxon levels were found, generally 100-fold lower than CPF levels (Mendrala and Brzak, 1998). These trace levels of the oxon metabolite are consistent with the report of high first-pass metabolism of CPF by the liver (Sultatos, 1994).

The metabolism and pharmacokinetics of CPF have also been evaluated in several human volunteer studies. Nolan *et al.* found at least 70% of an orally administered dose of CPF (0.5 mg/kg) was absorbed and excreted in the urine, primarily as acid-labile conjugates of TCPy. Trace levels of CPF were found in this study, with no measurements conducted for CPF-oxon. Griffin *et al.* measured the urinary DEP metabolites of CPF following oral or dermal administration of the parent compound, showing these dialkylphosphate metabolites represent 93% of the administered dose in humans (Griffin *et al.*, 1999). In a later multi-dose level pharmacokinetic study, Kisicki *et al.*, (1999) found that following oral administration of 0.5, 1.0 or 2.0 mg CPF/kg body weight, TCPy was again the major metabolite in blood, with CPF levels <1% of TCPy concentrations. No CPF-oxon was detected in blood samples from this study, with the 1 ng/ml LOQ value 3-18-fold lower than the highest CPF concentrations observed. These CPF-oxon results are quite consistent with the rat pharmacokinetic results of Mendrala, discussed above, and indicate that CPF undergoes high first-pass metabolism in humans as well as animals.

Any minor variations in the hepatic or extrahepatic formation and/or degradation of CPF-oxon would have an impact on systemically available levels of this trace, reactive metabolite. It is therefore important to understand the differences in enzymatic activity that affect the rates of CPF-oxon formation and hydrolysis to be able to accurately predict variations in systemic CPF-oxon levels and the resulting biological effects across the population. This evaluation is further discussed in Section 5 of this report.

Minor metabolites of CPF have also been reported. Additional metabolic routes, involving GSH conjugation with the TCPy ring and glucuronide phenolic conjugates of TCPy have been seen in human liver S9 and or hepatocyte incubations with CPF (Choi *et al.*, 2006). GSH conjugates have been also seen *in vivo* (Bicker *et al.*, 2005) and in mice dosed with 100 mg CPF/kg (Fujioka and Casida, 2007). While the potential toxicity of these GSH conjugates is not known, the fact that they have not been seen in lower dose animal studies and that protein adducts identified so far arise from reaction with CPF-oxon, would suggest that GSH conjugation of CPF or CPF-oxon is not relevant for the mechanism of action for this compound at doses commonly used in toxicity studies or from environmental exposures.

Direct evaluation of the *in vivo* stability of the CPF metabolites has also been examined. Timchalk *et al.*, (2007) conducted *in vivo* pharmacokinetic studies with TCPy, DETP and DEP in rats, and compared the results to animals dosed directly with CPF. These authors found 100% of the administered TCPy was recovered in the 0-72 hr urine, and 65% and 86% of the DETP and DEP, respectively, remained unchanged. These data indicate that the majority of these CPF hydrolysis products are excreted without further Phase I metabolism. In a more recent Comparative Cholinesterase Assay study, CPF or CPF-oxon was administered to adult or PND-11 rats (Marty and Andrus, 2010). At 6-8 hr post-dosing, detectable levels of CPF were found in the blood of rats dosed with 0.5 mg/kg CPF, while no detectable CPF-oxon was found 4 hr post-dosing in adult or neonatal rats dosed with 0.5 mg CPF-oxon/kg. In addition, TCPy was found to be a major blood metabolite in the CPF-oxon dosed rats as well as the CPF-dose group. Since CPF has been previously shown to be highly metabolized in the rat, and these new data show comparable TCPy blood levels from CPF and CPF-oxon, these results indicate that CPF-oxon also

undergoes high first-pass metabolism in the adult and neonatal rat. A more thorough overview of these animal and human metabolism/kinetic studies can be found in recent reviews of CPF metabolism (US EPA, 2008b; Eaton *et al.*, 2008).

Dose-dependent kinetics

Since the first steps in CPF metabolism involve CYP oxidation, it would be expected that the rate of metabolism of this compound could be dependent on concentration. A comparison of the ratio of blood TCPy/CPF concentrations from various toxicokinetic studies in rats (Mendrala *et al.*, 1998; Timchalk *et al.*, 2006; Marty *et al.*, 2010) was therefore conducted to evaluate this issue (Figure 5).

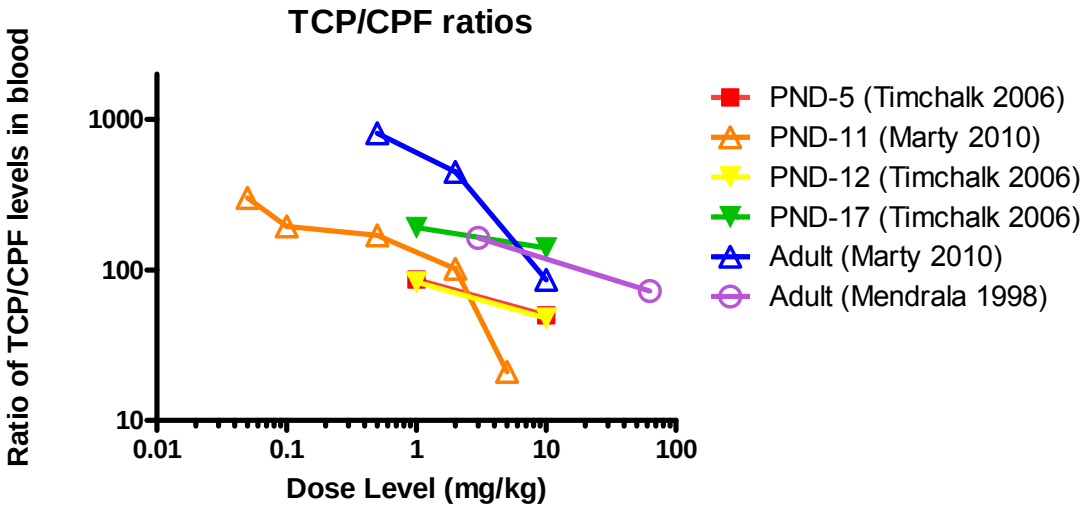

Figure 5. Dose-dependent pharmacokinetics of CPF and TCPy in the rat.

As shown in Figure 5, the ratio of TCPy vs. CPF decreases with increased dose in each of the six datasets from the three studies evaluated. Overall, the PND-5 to PND-12 rats show lower metabolism rates than the PND-17 and adult datasets. However, all of the experimental results show a good correlation of increased CPF metabolism as dose levels decrease. The most complete data are the PND-11 blood data from the recent Marty 2010 study. The TCPy/CPF ratio increased from 21 to 300 for the dose levels of 5 mg/kg down

to 0.05 mg/kg. Examination of both the adult and PND-11 data from this study show a point of inflection for this metabolite ratio above 1 mg/kg dose levels. One would expect that a similar phenomenon of CYP-based metabolic saturation would occur in humans. Therefore, an important validation check for the LifeStage model will be to evaluate this metabolic saturation in simulations of human systemic dose.

2.3 *Sites of metabolism*

The primary site of CPF metabolism has been shown to be the liver in numerous *in vivo* and *in vitro* studies (Chambers and Chambers, 1989; Sultatos, 1994; Poet *et al.*, 2003). Poet *et al.* have also found that the enterocytes of the small intestine have measurable cytochrome P450 (CYP) activity to form both CPF-oxon and TCPy from CPF (Poet *et al.*, 2003). Numerous groups have reported on the various esterases in blood that can hydrolyze CPF-oxon (Pond *et al.*, 1995; Jokanović, 2001). Finally, several researchers have postulated or provided data supporting some oxidation of CPF to the oxon or esterase hydrolysis of oxon in peripheral tissues such as brain and intestines (Chambers and Chambers, 1989; Poet *et al.*, 2003).

Metabolizing enzymes

The hepatic metabolism of CPF occurs via CYP-mediated desulfurylation and dearylation, affording CPF-oxon and TCPy, respectively. Many investigators have studied both the rates of microsomal metabolism of CPF, as well as the specific CYPs responsible (Ma and Chambers, 1994; Tang *et al.*, 2001; Buratti *et al.*, 2003; Sams *et al.*, 2004; Mutch and Williams, 2006; Foxenberg *et al.*, 2007; Croom *et al.*, 2010). CPF desulfurylation is most likely due to CYP2B6, 3A4/5, and 2D6 (Croom et al., 2010; Foxenberg et al., 2007; Mutch and Williams, 2006; Sams et al., 2004; Tang et al., 2001). For CPF dearylation, CYP2C19 was the primary CYP, CYP2D6 and 3A4/5 apparently have significant capacity to metabolize CPF. Overall, these investigators have found that CPF metabolism in human liver microsomes favors dearylation to TCPy over desulfurylation to CPF-oxon, by a factor of 3 to 6-fold, based on Vmax or pseudo-first order rates of metabolism. What is important to population modeling, however, is the inter-subject variability in metabolic rates. The highest variability seen in microsomal formation of CPF-oxon was that of Buratti *et al.*

(2003), in which the authors report a 30-fold difference in oxon production between the least and most active human hepatic microsomes. While this variability definitely should be taken into account in the Variation model, Foxenberg notes that some variability seen in metabolic rates between different sources may be due to artifacts in microsomal viability because of varying tissue isolation and microsomal preparation conditions.

The degradation of CPF-oxon occurs primarily via esterase activity, in the liver, blood and various tissues. Some authors report microsomal-based hydrolysis of CPF-oxon (Sams *et al.*, 2004). The primary enzymes responsible for CPF-oxon hydrolysis are the calcium-dependent A-esterases (PON1) and B-esterases (cholinesterases) (Pond *et al.*, 1995). Other proteins like serum albumin have also been shown to have esterase activity against CPF-oxon (Sogorb *et al.*, 2008). As with the CYP activities discussed above, substantial variability has been observed in PON1 activity between human donors. Mutch *et al.* evaluated variation in CPF-oxon hydrolysis in liver microsomes from 27 human donors, with various SNP 192 PON1 phenotypes (Mutch *et al.*, 2006). A 16-fold variation was observed between low and high activities, with a high degree of overlap between phenotypes. Huen *et al.* discuss 4 to 34-fold variation in CPF-oxon hydrolysis in plasma from newborns, 7-year-old s and pregnant mothers, who express one of the five known phenotypes of the PON-1 enzyme (Huen *et al.*, 2010). The variations in PON1 and other esterase-mediated hydrolysis of CPF-oxon have been included in the Variation model (see Section 4). Recent *in vitro* experiments, discussed below, provide data on the esterase capacity of liver and plasma from numerous human donors, both infant and adult.

Age-dependent kinetics

Several groups have published data showing age-dependent differences in sensitivity to CPF in animals (Timchalk *et al.*, 2006; Marty *et al.*, 2010; Pope *et al.*, 1991; Moser *et al.*, 1998; Padilla *et al.*, 2000; Timchalk *et al.*, 2006). This differential sensitivity may be due to CYP or esterase deficiencies in the young, affording higher levels of CPF and/or CPF-oxon. Researchers studying the ontogeny of metabolic systems have reported that individual CYP enzymes maturate at different rates (Alcorn and McNamara, 2002; Johnson *et al.*, 2006). Some CYPs (e.g. CYP2C9) will mature to adult levels in as little as half a week, while others (e.g. CYP2C19) will take 2 years or longer to reach adult levels

(Johnson *et al.*, 2006; Koukouritaki *et al.*, 2004; Tateishi *et al.*, 1997; Treluyer *et al.*, 1997). Other CYP enzymes yet (e.g. CYP3A7) may be present during infancy and not present in adults (Tateishi *et al.*, 1997). In a similar vein, PON1 and other esterase activities have been shown to increase with age, in both animals and humans (Augustinsson and Barr, 1963; Timchalk *et al.*, 2006). Any age-based differences in CPF metabolism need to be included in the LifeStage model for appropriate predictions of systemic dose in infants, children and adults. Age-specific metabolic parameters for this model were therefore obtained by a new *in vitro* metabolism study, described in the following subsection.

2.4 New data on age-dependent metabolic rates

As discussed above, age-dependent changes in CPF metabolism have been reported in rodents (Zemke *et al.*, 2009). While age-dependent changes have been indicated in rodents, there has not been a full characterization of enzymatic activity (i.e. Michaelis-Menten enzymatic kinetics) with regards to age in humans. Therefore, a new study was conducted to quantify age-dependent enzymatic metabolism of CPF and CPF-oxon *in vitro* using human hepatic microsomes and plasma. The rates of CPF conversion to CPF-oxon and TCPy in liver microsomes, as well as the hydrolysis of CPF-oxon to TCPy in microsomes and plasma were measured. A detailed report on this study is given in Attachment A of this report. The following is a brief summary of the study and its findings.

Materials and methods for in vitro study

Thirty human hepatic microsome samples were obtained from XenoTech, LLC (Lenexa, KS, USA). Microsomes were selected to maximize the number of samples for humans less than 12 years of age (n=20), and match those pediatric samples with 10 adult (17 years or older) samples. Overall age range of hepatic microsome donors was 13 d-75 y. Both oxidative desulfurylation (CPF to CPF-oxon) and dearylation (CPF to TCPy) pathways of CPF metabolism were measured by quantifying product formation from *in vitro* incubations of hepatic microsomes with CPF. Microsomes (0.5 mg protein) were incubated in 50 mM HEPES buffer (7.4 pH) containing 15 mM $MgCl_2$•$6H_2O$ (Poet *et al.*,

2003; Lee *et al.*, 2009) and 1 mM ethylenediaminetetraacetic acid (EDTA, to inhibit PON1 activity (Furlong *et al.*, 1989) with 20, 50, 125, 315.5, or 781.25 μM CPF. Incubations were conducted at 37º C, initiated with the addition of 1 mM nicotinamide adenine dinucleotide phosphate (NADPH) after a 3 min pre-incubation to allow samples to reach temperature equilibrium, and terminated with the addition of 0.25 ml of 3 M HCl saturated with NaCl at 15 min after the addition of NADPH. Incubation volume was 0.5 ml. Blanks, containing microsomes inactivated by addition of HCl solution prior to incubation, were included to quantify non-enzymatic product formation.

Twenty individual human plasma samples were obtained from Bioreclamation, Inc. (Liverpool, NY, USA). Plasma samples were obtained from donors 3 days of age to 43 years. CPF-oxon metabolism by PON1 was measured in both hepatic microsomal and plasma samples by quantifying product formation (TCPy) from *in vitro* incubations with CPF-oxon. Microsome (0.5 mg protein) or plasma (2.5 μL) samples were incubated in 0.1 M Tris-HCl buffer (8.5 pH) containing 2 M NaCl and 2 mM $CaCl_2$ (Furlong *et al.*, 1989; Poet *et al.*, 2003) with 72.3, 173.6, 416.7, 1000, or 2400 μM CPF-oxon. Incubations were conducted at 37º C, initiated with the addition of substrate (CPF-oxon) at 3 min, and terminated with the addition of 0.25 ml of 3 M HCl saturated with NaCl 5 min after the addition of CPF-oxon. Incubation volume was 0.5 ml. Blanks, containing microsomes or plasma inactivated by addition of HCl solution prior to incubation, were included to quantify non-enzymatic product formation. Metabolite levels were determined via GC/MS analysis, using methods comparable to those published previously (Brzak *et al.*, 1998).

Results for in vitro study

The *in vitro* hepatic CYP metabolism, including V_{max} values, K_m values, pseudo first-order rates (V_{max}/K_m), protein concentrations in plasma, and marker substrate activities, was evaluated for age dependence using linear regression models in "R: A language and environment for statistical computing", version 2.9.0 or 2.11.1 (R, 2004). All statistical tests used an α value of 0.05. No age dependence was noted for either pathway (Figure 6). Given the sample size (samples from 30 individuals), linear regression was considered a sufficient test of age dependence. The dearylation V_{max} and K_m were 0.73 ± 0.38 nmol/min/mg microsomal proteins and 81 ± 73 μM, respectively. Neither V_{max} nor

K_m demonstrated age dependence (p = 0.60 and 0.17 respectively). The desulfurylation V_{max} and K_m were 0.35 ± 0.21 nmol/min/mg microsomal protein and 96 ± 62 µM, respectively, and again neither were age dependent (p = 0.90 and 0.16, respectively). Pseudo first-order rates were estimated by dividing the V_{max} by the respective K_m. The mean (± SD) pseudo first-order rates were 5.8 ± 6.4 µL/min/mg and 16 ± 13 µL/min/mg microsomal protein and, again, were not significantly different over age (p = 0.19 and 0.15, respectively, data not shown).

These metabolic rates for CPF are comparable with those published previously by other groups. Previously reported CPF dearylation V_{max} rates (0.70 nmol/min/mg microsomal (Tang *et al.*, 2001) and 0.65 nmol/min/mg microsomal protein (Sams *et al.*, 2004) were also consistent with the mean value determined in this study (0.73 nmol/min/mg microsomal protein), although the K_m values previously reported were, lower than the mean value determined here (12-14 vs. 81 µM, respectively). Tang *et al.*, (2001) and Buratti *et al.*, (2003) reported CPF desulfation V_{max} rates from pooled human microsomes of 0.40 and 0.49 nmol/min/mg microsomal protein, respectively, and Sams *et al.*, (2004) reported a mean V_{max} of 0.35 nmol/min/mg microsomal protein using individual human microsomes. All three values are consistent with the mean value determined here (0.35 nmol/min/mg microsomal protein). Reported K_m values from those studies were lower than those reported here (0.9-30 µM vs. 96 µM, respectively). Since no age-based differences in either of these metabolic rates were observed, the overall mean values are used in the LifeStage model (Section 3) and Variation model (Section 4) to predict hepatic metabolism of CPF in humans.

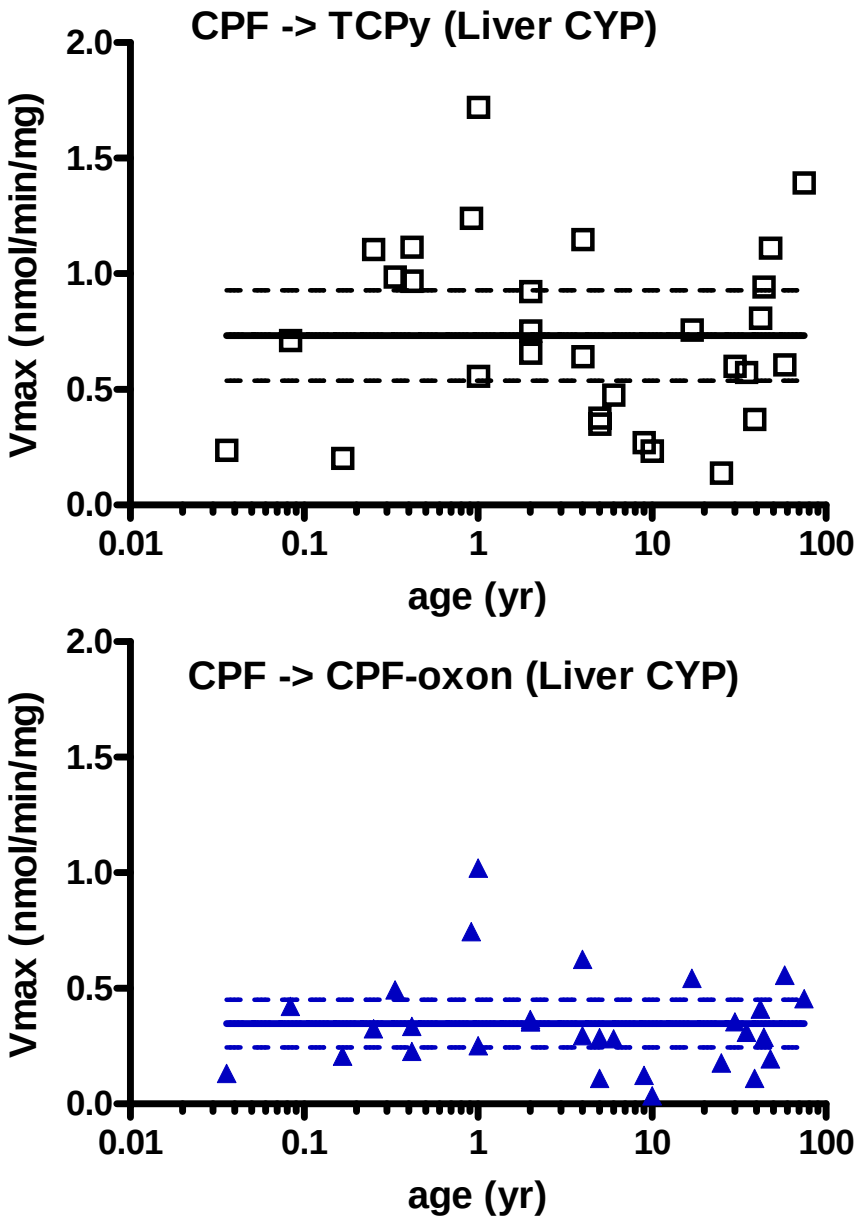

Figure 6. *In vitro* metabolism of CPF to TCPy (top) or CPF-oxon (bottom) in human liver microsomes from individuals from 13 days to 75 years of age. Solid lines show mean values used to extrapolate the rates for the LifeStage model, with 95% confidence intervals (dashed lines) around the data displayed.

Both TCPy and CPF-oxon formation rates were measured simultaneously from each donor liver tissue sample. A comparison of the metabolic rates of TCPy and CPF-oxon

formation was therefore made and shown in Figure 7. Although there is some variability, a fairly good correlation is seen between desulfurylation and dearylation in all of the samples. However, to be conservative, these parameters were varied independently in the Variation model (below).

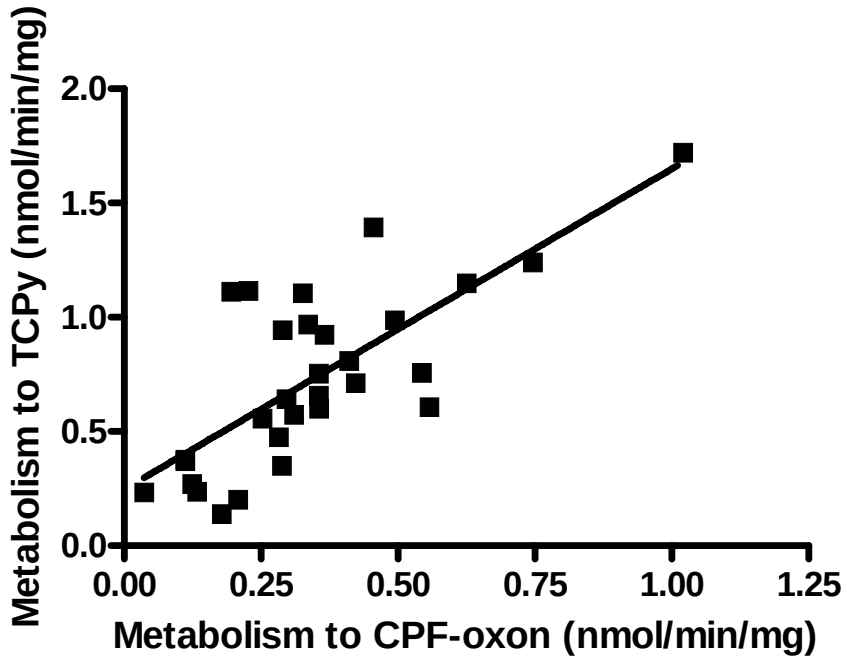

Figure 7. Correlation between CYP-based metabolism of CPF to CPF-oxon and to TCPy in individual human liver samples. Solid line is best fit regression.

Hepatic metabolism rates of CPF-oxon to TCPy are shown in Figure 8. The mean (± SD) V_{max} and K_m values were 78 ± 44 nmol/min/mg microsomal protein and 520 ± 204 μM, respectively. None of the CPF-oxon hepatic metabolism measures changed significantly with age (p = 0.17 and 0.75, for V_{max}, and K_m, respectively). In contrast to hepatic CPF metabolism, there have been fewer studies quantifying *in vitro* hepatic CPF-oxon metabolism to TCPy in humans. Sams *et al.*, (2004) published a mean human hepatic CPF-oxon V_{max} of 233 nmol/min/mg microsomal protein, somewhat higher than the value reported here (78 nmol/min/mg microsomal protein). This difference could potentially be

explained by differing incubation buffers. Sams *et al.*, (2004) used a phosphate buffer (pH 7.4), while a high salt Tris-HCl buffer was utilized in this study (pH 8.5), although others have reported greater PON1 activity with high salt buffers (Costa and Furlong, 2002). Since no age-based differences were observed in CPF-oxon metabolism to TCPy, the overall mean values are used in the LifeStage model to predict hepatic metabolism of CPF in humans.

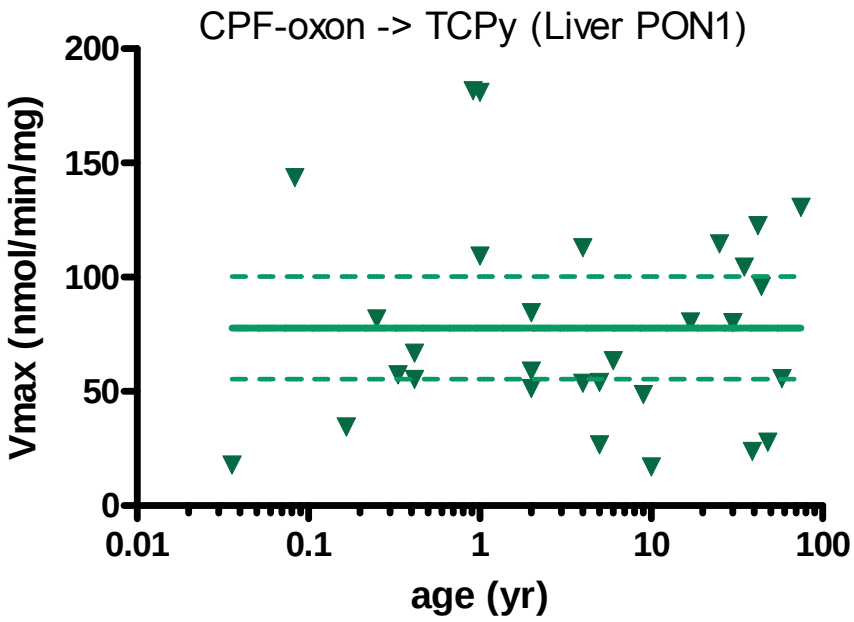

Figure 8. *In vitro* PON1 metabolism of CPF-oxon to TCPy in human liver microsomes from individuals aged 13 days to 75 years. Solid lines show mean value used in LifeStage model, with 95% confidence intervals (dashed lines) around the data displayed.

Rates of both CPF-oxon formation from CPF and subsequent CPF-oxon hydrolysis to TCPy were measured simultaneously from each donor liver sample. A correlation was observed between the metabolic rates of desulfurylation and oxon hydrolysis (Figure 9). However, we could find neither a biological nor a literature basis for this correlation and thus conservatively varied the CYP-based desulfurylation and liver PON1 hydrolysis rates independently in the Variation model.

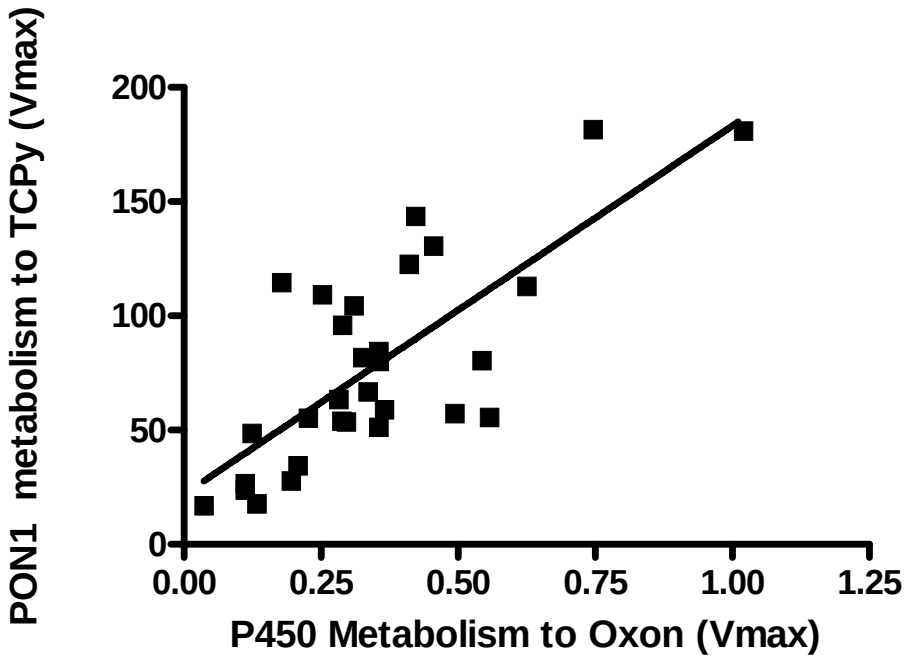

Figure 9. Relationship between hepatic CYP-based metabolism of CPF to CPF-oxon and hepatic PON1 metabolism of CPF-oxon to TCPy in individual human liver samples.

In contrast to PON1 activity in liver microsomes, CPF-oxon metabolism in plasma demonstrated an age-dependent increase in V_{max} rates on a per ml plasma basis ($p = 0.03$, Figure 10). Mean (± SD) V_{max} rates were 1901 ± 663 nmol/min/ml in children < 6 months of age (n=5) and 6828 ± 1614 nmol/min/ml protein in adults (individuals > 12 years of age; n=5). Plasma protein concentration also significantly increased with age ($p = 0.005$). Overall, CPF-oxon metabolism V_{max} rates on a per ml plasma basis demonstrated over a 3.5-fold increase from < 6 months in age to adulthood ($p = 0.01$). With a linear regression analysis, K_m constants did not demonstrate any age-dependence ($p = 0.87$); however, 4 out of the 5 lowest K_m values were measured in children < 6 months of age (data not shown). These age-based changes in plasma PON1 activity are quite consistent with previous reports of ontogeny of this enzyme (Furlong *et al.*, 2005; Huen *et al.*, 2010). This age-dependence in PON1 activity is included in the LifeStage model.

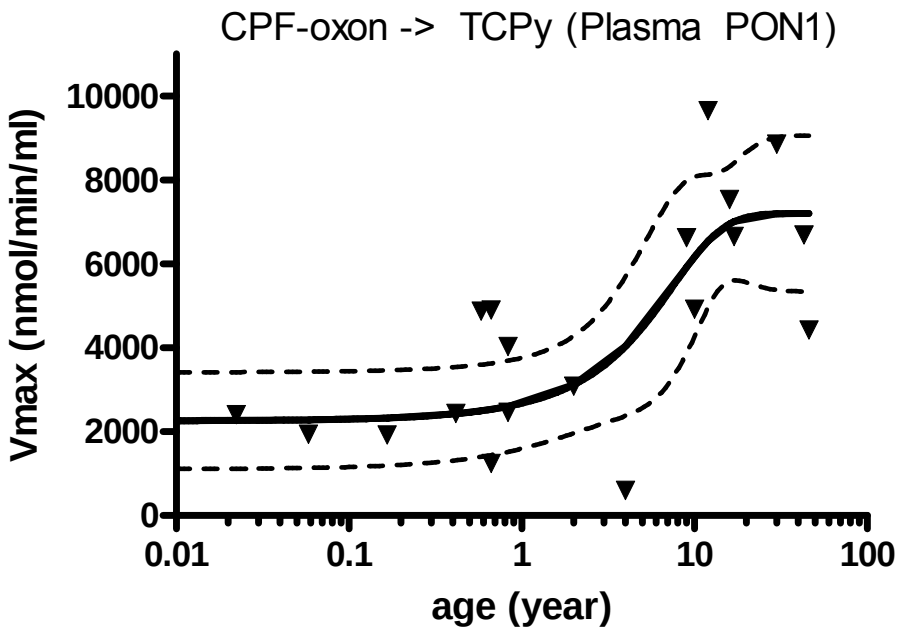

Figure 10. ***In vitro*** **PON1 metabolism of CPF-oxon to TCPy in human plasma samples from individuals aged 3 days to 43 years. Solid lines show mean values used to extrapolate to the LifeStage model with 95% confidence intervals (dashed lines) around the data displayed. Confidence intervals were determined using GraphPad Prism (version 5.03 for Windows, GraphPad Software, San Diego California USA, www.graphpad.com)**

Section summary

The metabolism of CPF and its relationship to the active metabolite CPF-oxon have been the subject of a number of studies. Data on age-related variation in metabolism and variation across individuals at different ages is important to modeling the effects of CPF on AChE. In the studies described in this section, hepatic metabolism of CPF to CPF-oxon and TCPy and CPF-oxon to TCPy did not vary across age on a microsomal protein basis, and CPF-oxon /TCPy ratios were consistent across ages. In contrast, CPF-oxon metabolism to TCPy in plasma demonstrated an age-dependent increase on a per ml plasma basis, increasing over 3.5 times from <6 months in age to adulthood. These results are integrated into the LifeStage model discussed below.

3. PBPK/PD modeling in typical humans of various ages

Section overview

This section presents information on the PBPK/PD modeling of CPF. The chapter begins with a review of the development of the CPF PBPK/PD model over the last 10 years, then discusses the development of the LifeStage model, and concludes with an evaluation of the model and its predictions for adults, children and infants.

The section begins with a description of the original model's (Timchalk *et al.*, 2002b)structure. This structure has remained fundamentally unchanged in all of the subsequent modeling. The sources of data for the model's inputs are also presented. As discussed in the introduction of this paper, the development of the PBPK/PD model occurs in three stages, the modeling of a "typical" adult (the Typical Adult model), the modeling of typical individuals at different ages (the LifeStage model), and the modeling of interindividual variation in populations of a specific age (the Variation model). This section presents a description of the development of the PBPK/PD model as it pertains to the Typical Adult and the LifeStage capabilities. A description of the creation of the Variation model is provided in Section 4. In addition there is an assessment of the changes in estimates between the original model (Timchalk *et al.*, 2002b) and the LifeStage model.

The LifeStage model's predictions and the assumptions on the values of physiological parameters used for the typical individuals of various ages are evaluated by comparing the predictions to observed data. In the case of the predictions of age-related changes in physiology, the values are compared to published data on physiology. The predictions of internal dose and cholinesterases are evaluated by comparisons to data from human volunteers. Finally, the section presents predictions of the dose response curves for RBC and brain AChE inhibitions in typical humans at three different ages, 6 months, 3 years, and 30 years.

3.1 History of PBPK/PD model

The extensive understanding of both the metabolism and biochemical interactions between the oxon metabolite of CPF and acetylcholinesterase has been used to develop a PBPK/PD model for CPF (the Typical Adult model). The procedures for developing and using PBPK models have been extensively reviewed (Andersen, 2003; Clewell *et al.*, 2005; Krishnan and Johanson, 2005; Reddy *et al.*, 2005; Yang *et al.*, 1995). Models have been developed for a broad range of applications including: drug development (Bjorkman, 2005; Blesch *et al.*, 2003; Slikker *et al.*, 2005), biomonitoring and reverse dosimetry (Tan *et al.*, 2006), species extrapolation (Corley *et al.*, 2005; Poet *et al.*, 2002; Reitz *et al.*, 1988; Teeguarden and Barton, 2004; Timchalk *et al.*, 2002b), mechanism of action assessment (Conolly *et al.*, 2004; DeWoskin and Thompson, 2008; Medinsky, 1995; Peters and Hultin, 2008), cancer and non-cancer risk assessments (Andersen, 1995; Andersen *et al.*, 1994; Bois, 1999; Chiu *et al.*, 2007; Dixit *et al.*, 2003; el Masri *et al.*, 1995; Gearhart *et al.*, 1993; Welsch *et al.*, 1995), and estimating human variability and polymorphisms (Licata *et al.*, 2001; Tardif *et al.*, 2002; Timchalk *et al.*, 2002a).

Robust PBPK models that are capable of exploiting large experimentally-derived data for model parameterization and validation offer an elegant solution to determine dosimetry and investigate potential mechanisms of action under a broad range of conditions. PD models are not as common as PBPK models since the mechanism (or mode) of action for many chemicals is not sufficiently well understood to allow the quantitative characterization of toxicological outcomes. The development of such models is challenging in animals, and human data are generally not available.

As described in Section 2, the mechanism of CPF action on AChE is sufficiently well defined to allow the development of a combined PBPK/PD model. The original CPF PBPK model was published in 2002 (Timchalk *et al.*, 2002b). Since then, the model has been applied and expanded to describe research results, test hypotheses, and determine the effects of possible perturbations of the physiological and biochemical system (Busby-Hjerpe *et al.*, 2010; Cole *et al.*, 2005; Garabrant *et al.*, 2009; Lee *et al.*, 2009; Lowe *et al.*, 2009; Lu *et al.*, 2010; Marty *et al.*, 2007; Timchalk and Poet, 2008; Timchalk *et al.*, 2005; Timchalk *et al.*, 2006). The Typical Adult model includes a complete description of the

pharmacokinetics and pharmacodynamics of CPF-oxon, the active metabolite of CPF, and a more simplified submodel that describes the major metabolite, TCPy, which is of importance for biomonitoring (Figure 11). The model contains compartments describing CPF and CPF-oxon concentrations over time in fat, slowly perfused tissue, rapidly perfused tissue, diaphragm, brain, and liver. Model parameterization was achieved most often by extrapolation from *in vitro* studies (animal and human tissues), in some incidences by extrapolation from rat studies, and, for TCPy pharmacokinetics, by fitting to human data. TCPy pharmacokinetics are based on a single compartment with a volume of distribution and first-order urinary elimination of total urinary TCPy.

In the case of CPF and other organophosphorus pesticides, the AChE inhibiting mechanism of action is well understood and biomarkers of exposure, inhibition of plasma cholinesterase, and biomarkers of early effects such as AChE inhibition in RBC, are available (Carr and Nail, 2008; Eaton *et al.*, 2008; Kaushik *et al.*, 2007; Lassiter *et al.*, 1999; Mattsson *et al.*, 2000; Nigg and Knaak, 2000). Pharmacodynamics of AChE inhibition as mediated by CPF-oxon are included in blood (plasma and RBC), diaphragm, brain, and liver compartments. The PBPD model for CPF is a direct extension of the PBPK model and relates the prediction of the formation of CPF-oxon to changes in BuChE (plasma cholinesterase), RBC AChE, and brain AChE. This model has been provided to a number of researchers over the last eight years and has formed the basis of a number of publications on the kinetics of CPF by academics, government, and industry (Cole *et al.*, 2005; Furlong *et al.*, 2005; Garabrant *et al.*, 2009; Lowe *et al.*, 2009; Lu *et al.*, 2010; Marty *et al.*, 2007).

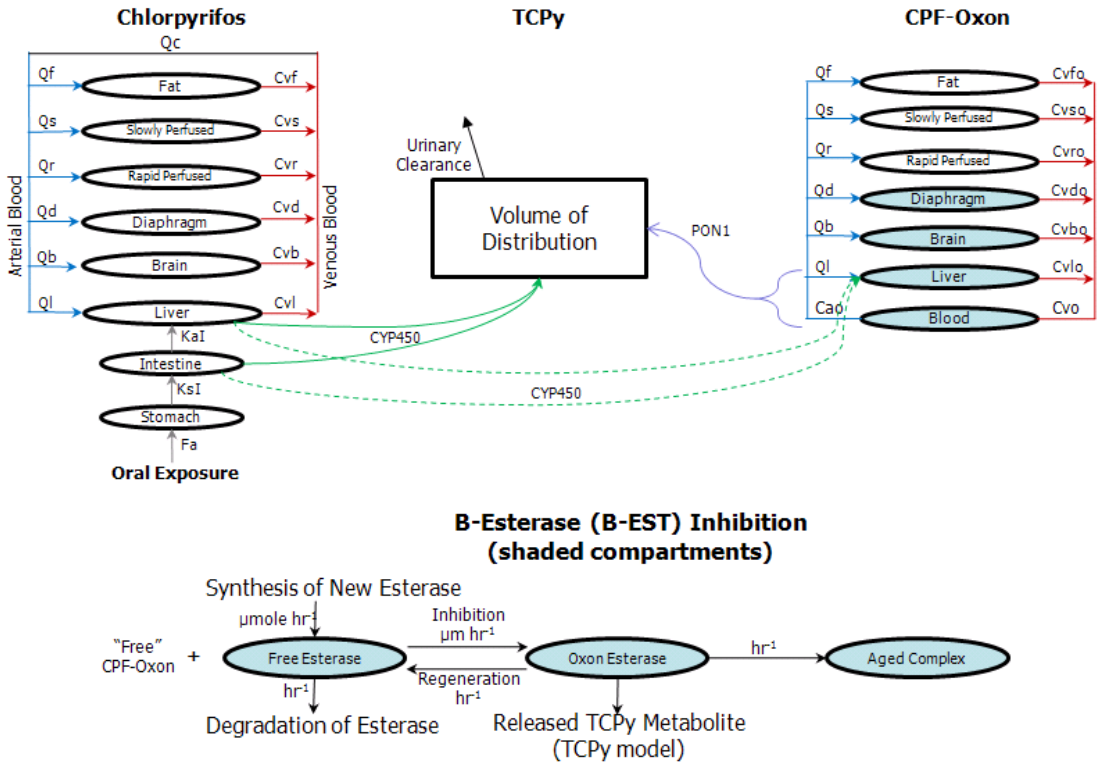

Figure 11 PBPK/PD model (Typical Adult model) structure. The model structure has the same foundation as originally published in 2002 (Timchalk *et al.*, 2002b). The shaded compartments denote tissues which contain B-esterases (bottom panel). Tissue volumes and enzyme activities (V_{max}) change with age based on liver and/or blood compartmental growth (Table 1).

Since 2002, the ongoing development of the CPF PBPK/PD model has been informed by the availability of new environmental, toxicological, and physiological data. Since its original publication (Timchalk *et al.*, 2002b), the model has been further refined with measured *in vivo* and *in vitro* parameters (i.e. cholinesterase inhibition rates and CYP metabolism rates) and has had additional complexity added (i.e. metabolism in the intestines). Specific modifications include:

- Improvement of the modeling of extrahepatic metabolism both at the site of cholinesterase inhibition or presystemically (in the liver). *In vitro* metabolism of CPF was measured in microsomes prepared from rat enterocytes and compared to microsomes prepared from whole liver (Poet *et al.*, 2003).
- Incorporation of *in vitro* measurement of CYP metabolism to TCPy or CPF-oxon and PON1 metabolism of CPF-oxon to TCPy in human liver microsomes from individuals ranging in age from 13 days to 75 years and in the PON1 metabolism in plasma from humans ranging in age from 3 days to 43 years. (Described in more detail in Appendix A.)
- Measurements of partitioning of CPF between plasma and vegetable oil (a fat surrogate) to determine blood:tissue partitioning using a QSAR approach (Lowe *et al.*, 2009)
- Verification of the bimolecular inhibition rate constant by directly determining the AChE and BuChE inhibition dynamics in rat plasma, brain, and saliva (Kousba *et al.*, 2004; Kousba *et al.*, 2007).

3.2 Development of the LifeStage model

The Typical Adult model provides very useful information for purposes like understanding mechanism or for comparison across species. But the model cannot address differences in response in different age groups or gender that arise from differences in physiology or metabolism that occur with growth (ontogeny). To address this issue, gender-specific human growth was incorporated into the LifeStage version of the PBPK/PD model, based on the equations described by Leucke *et al.* (2007) and Young *et al.*, (2009). In this subsection we present the specific equations used in the LifeStage

model. The subsection also presents an evaluation of the predictions using data on age specific body weights and weight - tissue volumes relationships reported in the published literature.

The development of the LifeStage model begins with the development of an age-specific model of body weight. The predictions of body weight for each age are used in turn to predict the volumes of the compartments based on specific ontogeny of each tissue. Once the age-related physiology is defined, it is combined with the age-specific metabolism data discussed in Section 2. Data that are tissue specific are combined with the age-specific tissue volumes to capture changes in metabolism from birth to adulthood. Cholinesterase (A- and B-) are scaled with age-specific tissue volume. Blood flows are likewise scaled based on tissue volume changes with age. This approach provides an excellent means of dynamically modifying PBPK physiological parameters based on age and gender.

A generalized, age- and gender-specific Gompertz function was used to calculate a body weight for modeled individuals (Luecke *et al.*, 2007). A comparison of the model-predicted body weights of men and women to NHANES-reported body weights is shown in Figure 12.

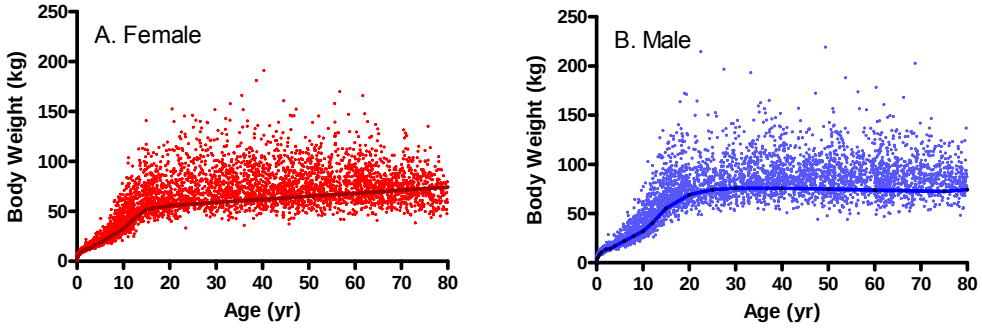

Figure 12. Model prediction for a typical human body weight (lines) compared to NHANES body weight data from 2007-2008 for the U.S. population.

To incorporate linked physiological data into the LifeStage PBPK/PD model, the compartmental volumes, on a fractional body weight basis, are scaled with body weight

dependent polynomial equation. This approach provides a flexible framework that has been used to define and switch among compartments of various species and genders with ease within the framework of the LifeStage model (Luecke *et al.*, 2007; Young *et al.*, 2009). Compartments existing within the LifeStage model are equivalent to the Typical Adult model (Timchalk *et al.*, 2002b), discussed previously) and include brain, blood, diaphragm, fat, liver, rapid, and slow compartments (Tables 1 and 2). The rapidly perfused compartment consists of a summation of kidney, spleen, lung, gastrointestinal tract (GI), and pancreas volumes, and the slowly perfused compartment consists of a summation of muscle, skin, bone marrow, and non-fat adipose tissue volumes.

Figure 13 presents a summary of the compartments and the basis for modeling variation with age that results from the approach outlined above.

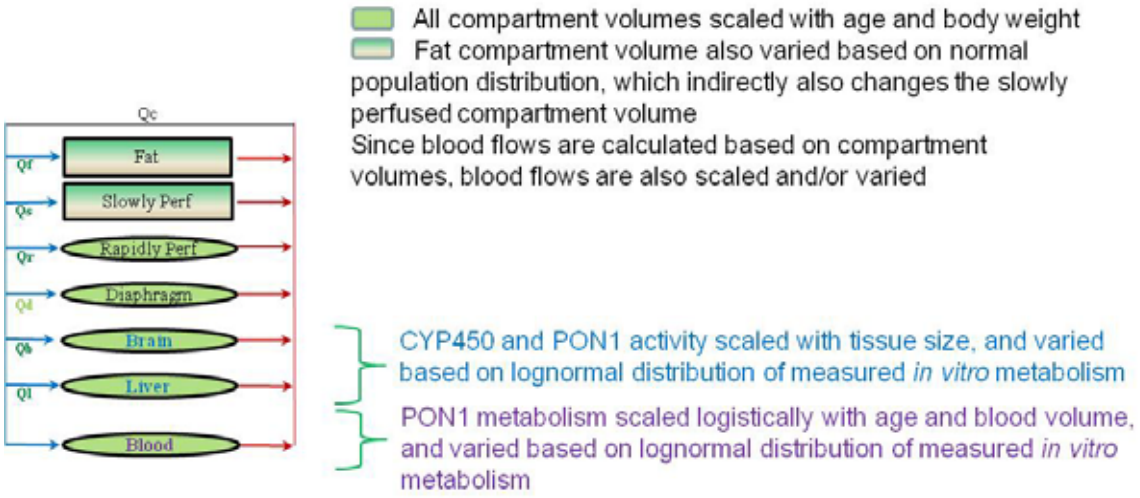

Figure 13. Schematic of age and body weight dependences in the LifeStage model.

All compartment volumes and blood flows vary with age and body weight. *In vivo* metabolic rates are scaled based on tissue size (measured *in vitro* values scaled to describe tissue-specific (brain, blood, and liver) metabolism); in blood, PON1 metabolism of oxon is not only blood volume but also age-dependent.

Table 1. Pharmacokinetic model parameters.

Parameter	Value	Source
Tissue Ontogeny		
All	Scaled by age and body weight	See Table 2
Flows (L/hr/kg tissue volume)		
Cardiac Output	Summed from total tissue flow	See "*Blood flows*" in this section
Brain	30.6	Price *et al.*, 2003
Diaphragm	85.2	Luecke *et al.*, 2007
Fat	1.45	Luecke *et al.*, 2007, Cowles *et al.*, 1971, Price *et al.*, 2003
Liver	50.4	Price *et al.*, 2003
Rapidly Perfused	61.8	Adrenal/Spleen average: Price *et al.*, 2003
Slowly Perfused	1.80	Bone: Price *et al.*, 2003
Partition Coefficients for CPF (tissue:blood)		
Brain	16.5	Lowe *et al.*, 2009
Diaphragm	3.85	Lowe *et al.*, 2009
Fat	250	Lowe *et al.*, 2009
Liver	12.8	Lowe *et al.*, 2009
Rapidly Perfused	16.5	Lowe *et al.*, 2009
Slowly Perfused	3.85	Lowe *et al.*, 2009
Partition Coefficients for CPF-oxon (tissue:blood)		
Brain	5.6	Lowe *et al.*, 2009
Diaphragm	1.8	Lowe *et al.*, 2009
Fat	75	Lowe *et al.*, 2009
Liver	4.5	Lowe *et al.*, 2009
Rapidly Perfused	5.6	Lowe *et al.*, 2009
Slowly Perfused	1.8	Lowe *et al.*, 2009
Hepatic CYP Metabolic Constants (per tissue wt)		
CPF → TCPy Vmax (nmol/hr/kg)	1580	Measured in vitro, Median: See Table 2, Section 2: CPF metabolism/mechanism of action
CPF → TCPy Km (µM)	53.8	Measured in vitro, Median: See Table 2, Section 2: CPF metabolism/mechanism of action
CPF → Oxon Vmax (µmol/hr/kg)	689	Measured in vitro, Median: See Table 2, Section 2: CPF metabolism/mechanism of action
CPF → Oxon Km (µM)	85.8	Measured in vitro, Median: See Table 2, Section 2: CPF metabolism/mechanism of action
Intestinal CYP Metabolic Constants (per tissue wt)		
CPF → TCPy Vmax (µmol/hr/kg)	36.8	Poet *et al.*, 2003
CPF → TCPy Km (µM)	55	Poet *et al.*, 2003
CPF → Oxon Vmax (µmol/hr/kg)	10.0	Poet *et al.*, 2003
CPF → Oxon Km (µM)	8.1	Poet *et al.*, 2003
Brain CYP Metabolic Constants (per tissue wt)		

Parameter	Value	Source
CPF → TCPy Vmax (µmol/hr/kg)	3.85	Extrapolated: See Section 2: CPF metabolism/mechanism of action
CPF → TCPy Km (µM)	5.38	See Section 2: CPF metabolism/mechanism of action
CPF → Oxon Vmax (µmol/hr/kg)	0.91	Extrapolated: See Section 2: CPF metabolism/mechanism of action
CPF → Oxon Km (µM)	8.60	See Section 2: CPF metabolism/mechanism of action
PON1 Metabolic Constants		
Plasma Vmax (µmol/hr/kg)	Logistic Fit	Measured in vitro, Median: See Table 2 and Section 2 of this report
Plasma Km (µM)	192	Measured in vitro, Median: See Table 2 and Section 2 of this report
Liver Vmax (µmol/hr/kg)	3902	Measured in vitro, Median: See Table 2 and Section 2 of this report
Liver Km (µM)	498	Measured in vitro, Median: See Table 2 and Section 2 of this report
Intestine Vmax (µmol/hr/mg)	246	Poet *et al.*, 2003
Intestine Km (µM)	328	Poet *et al.*, 2003
Oral Absorption		
Stomach →Intestine	0.5	Fitted: Nolan *et al.*, Timchalk *et al.*, 2002
Intestinal Absorption	0.2	Fitted: Nolan *et al.*, Timchalk *et al.*, 2002
Plasma Protein Binding (%)		
CPF	99	Lowe *et al.*, 2009
Oxon	99	Lowe *et al.*, 2009
TCPy Compartmental Model		
Vd (L)	$0.2\times BW^{1.117}$	Fitted: Nolan *et al.*, 1984, Timchalk *et al.*, 2003
Ke (/hr)	0.013	Fitted: Nolan *et al.*, 1984, Timchalk *et al.*, 2002
Cholinesterase Degradation Rates (hr-1)		
Butyryl	0.004	Fitted (repeat dose data in rats: DOW unpublished)
Acetyl	0.01	Standardized, Timchalk *et al.*, 2002b
Bimolecular Inhibition Rate (µM hr^{-1})		
Butyryl	2000	Timchalk *et al.*, 2002
Acetyl	220	Kousba *et al.* (Date)
Enzyme Turnover Rate (hr^{-1})		
Butyryl	$1.17x10^{7}$	Maxwell *et al.*, 1987, Timchalk *et al.*, 2002b
Acetyl	$3.66x10^{6}$	Maxwell *et al.*, 1987, Timchalk *et al.*, 2002b
Carboxyl	$1.086x10^{5}$	Maxwell *et al.*, 1987, Timchalk *et al.*, 2002b
Enzyme Turnover Rate (hr-1) Enzyme Turnover Rate (hr-1)		
Butyryl	11700000	Maxwell *et al.*, 1987, Timchalk *et al.*, 2002b
Acetyl	3660000	Maxwell *et al.*, 1987, Timchalk *et al.*, 2002b
Carboxyl	108600	Albers *et al.*, 2009
Enzyme Activity (µmol/kg/hr)		

Parameter	Value	Source
Brain ACHE	440000	Hojring *et al.*, 1976
Diaphragm ACHE	77400	Maxwell *et al.*, 1987, Timchalk *et al.*, 2002b
Liver Carboxyl	1920000	Maxwell *et al.*, 1987, Timchalk *et al.*, 2002b; Pope *et al.*, 2005
Plasma Carboxyl	NA	Li *et al.*, 2005
Brain Butyryl	46800	Maxwell *et al.*, 1987, Timchalk *et al.*, 2002b
Diaphragm Butyryl	26400	Maxwell *et al.*, 1987, Timchalk *et al.*, 2002b
Liver Butyryl	30000	Maxwell *et al.*, 1987, Timchalk *et al.*, 2002b
Plasma Butyryl	263000	Sidell *et al.*, 1975
Enzyme Reactivation Rate (hr^{-1})		
Butyryl	0.0014	Carr and Chambers, 1996, Timchalk *et al.*, 2002b
Acetyl	0.014	Carr and Chambers, 1996, Timchalk *et al.*, 2002b
Carboxyl	0.014	Carr and Chambers, 1996, Timchalk *et al.*, 2002b
Enzyme Aging Rate (hr^{-1})		
Butyryl	0.0113	Carr and Chambers, 1996, Timchalk *et al.*, 2002b
Acetyl	0.0113	Carr and Chambers, 1996, Timchalk *et al.*, 2002b
Carboxyl	0.0113	Carr and Chambers, 1996, Timchalk *et al.*, 2002b

Utilization of the LifeStage model required extrapolation of some compartmental polynomial equations beyond those body weights that were used to fit them by Luecke *et al.* (2007) and Young *et al.* (2009). The equations of Luecke *et al.* (2007) and Young *et al.*, (2009) were fit to individuals less than 100 kg. A goal of the LifeStage model was to also simulate individuals over 100 kg, so additional data including children and larger individuals were used to re-fit the polynomials for the LifeStage model. Compartments existing within the LifeStage model are equivalent to the Typical Adult model (Timchalk *et al.*, 2002b), discussed previously) and include brain, blood, diaphragm, fat, liver, rapid, and slow compartments (Figure 13). The rapidly perfused compartment consists of a summation of kidney, spleen, lung, gastrointestinal tract (GI), and pancreas volumes; and the slowly perfused compartment consists of a summation of muscle, skin, bone marrow, and non-fat adipose tissue volumes. Modified equations include fat (both male and female), adipose, brain, liver, and muscle and were refit with additional data or extrapolations to achieve adequate fits up to a 170 kg individual. For all other compartments, previously published polynomials or constant values were used to define compartmental volumes (Table 2).

Table 2. Compartmental Growth.

Compartment		Fraction of Body Weight Equation[1]							Source for LifeStage Parameters
	Eqn. Format $V0+V1\times BW+V2\times BW^2+V3\times BW^3+V4\times BW^4+V5\times BW^5+V6\times BW^6$								(BW: Body Weight in g)
		V0	V1	V2	V3	V4	V5	V6	
Blood	Leucke	$9.15e^{-2}$	$-8.59e^{-7}$	$1.25e^{-11}$	$-6.46e^{-17}$	-	-	-	Young *et al.* 2009
	Young	$8.97e^{-2}$	$-3.50e^{-7}$	$6.54e^{-13}$					
	LifeStage	$8.970e^{-2}$	$-3.500e^{-7}$	$6.540e^{-13}$	-	-	-	-	
Brain (Figure 14)	Leucke	$1.19e^{-1}$	$-3.51e^{-6}$	$4.28\ e^{-11}$	$-1.82\ e^{-16}$	-	-		Fit to Valentin *et al.* 2002 (bwt≤70) & Young *et al.* 2009 data (body weight>70 kg) and extrapolated values based on Table 4A (Young *et al.* 2009)
	Young	$1.41e^{-1}$	$-5.54e^{-6}$	$9.30\ e^{-11}$	$-6.83e\ e^{-16}$	$1.80e^{-21}$			
	LifeStage	$1.216e^{-1}$	$-3.465e^{-6}$	$4.354e^{-11}$	$2.463e^{-16}$	$5.132e^{-22}$			
Diaphragm	Leucke	$3.000e^{-4}$	-	-	-	-	-	-	Luecke *et al.* 2007
	Young	NA	-	-	-	-	-	-	
	LifeStage	$3.000e^{-4}$	-	-	-	-	-	-	
Fat*									
Female (Figure 16)	Leucke	$5.91e^{-2}$	$1.20e^{-5}$	$-5.80e^{-10}$	$1.12e^{-14}$	$-6.36e^{-20}$	-	-	Fit to Valentin *et al.* 2002 & Lafortuna *et al.* 2005 data and extrapolated data based on equation in Fig 1B (Lafortuna *et al.* 2005)
	Young	$1.84e^{-2}$	$-6.86e^{-6}$	$2.46e^{-10}$	$-2.11e^{-15}$	$7.58e^{-21}$	$-9.94e^{-27}$	-	
	LifeStage	$9.217e^{-02}$	$1.401e^{-05}$	$-6.787e^{-10}$	$1.540e^{-14}$	$-1.558e^{-19}$	$7.249e^{-25}$	$1.273e^{-30}$	

Compartment		Fraction of Body Weight Equation[1]							Source for LifeStage Parameters
	Eqn. Format $V0+V1\times BW+V2\times BW^2+V3\times BW^3+V4\times BW^4+V5\times BW^5+V6\times BW^6$								(BW: Body Weight in g)
		V0	V1	V2	V3	V4	V5	V6	
Male (Figure 16)	Leucke	$3.95e^{-2}$	$1.59e^{-5}$	$-6.99e^{-10}$	$1.09e^{-14}$	$-5.26e^{-20}$	-	-	Fit to Valentin *et al.* 2002 & Lafortuna *et al.* 2005 data and extrapolated data based on equation in Fig 1B (Lafortuna *et al.* 2005)
	Young	$1.61e^{-2}$	$-3.59e^{-6}$	$-8.28e^{-11}$	$-3.57e^{-16}$	$4.73e^{-22}$	-	-	
	LifeStage	$3.484e^{-2}$	$2.803e^{-5}$	$-1.422e^{-9}$	$2.892e^{-14}$	$-2.718e^{-19}$	1.20 $3e^{-24}$	- $2.036e^{-30}$	
Liver (Figure 15)	Leucke	$3.49e^{-2}$	$-3.23e^{-7}$	$2.13e^{-12}$	-	-	-	-	Fit to Valentin *et al.* 2002 (body weight≤ 70) & Young *et al.* 2009 extrapolated values based on Table 4A
	Young	$4.25e^{-2}$	$-1.01e^{-6}$	$1.99e^{-11}$	$-1.66e^{-16}$	$4.83e^{-22}$	-	-	
	LifeStage	$3.917e^{-2}$	$-6.789e^{-7}$	$1.082e^{-11}$	$-7.393e^{-17}$	$1.701e^{-22}$	-	-	
Rapid									
Lung	Leucke	$1.67e^{-2}$	$-9.96e^{-8}$	$-1.09e^{-13}$	$1.13e^{-17}$	-	-	-	Young *et al.* 2009
	Young	$1.860e^{-2}$	$-4.550e^{-8}$	-	-	-	-	-	
	LifeStage	$1.860e^{-2}$	$-4.550e^{-8}$	-	-	-	-	-	
Kidney	Leucke	$7.31e^{-3}$	$-8.29e^{-8}$	$2.13e^{-12}$	-	-	-	-	Young *et al.* 2009
	Young	$7.26e^{-3}$	$-6.69e^{-8}$	$3.33e^{-13}$	-	-	-	-	
	LifeStage	$7.260e^{-3}$	$-6.690e^{-8}$	$3.330e^{-13}$	-	-	-		
Pancreas	Leucke	$1.17e^{-3}$	$-1.18e^{-8}$	$1.81e^{-13}$	-	-	-	-	Brown *et al.* 1997 and Young *et al.* 2009
	Young	$1.48e^{-3}$	-	-	-	-	-	-	
	LifeStage	$1.480e^{-3}$	-	-	-	-	-	-	
Spleen	Leucke	$3.05e^{-3}$	$-2.09e^{-8}$	$1.24e^{-13}$	-	-	-	-	Young *et al.* 2009
	Young	$3.12e^{-3}$	$5.57e^{-9}$	-	-	-	-	-	
	LifeStage	$3.120e^{-3}$	$5.570e^{-9}$	-	-	-	-	-	

Compartment		Fraction of Body Weight Equation[1]							Source for LifeStage Parameters
	Eqn. Format $V0+V1\times BW+V2\times BW^2+V3\times BW^3+V4\times BW^4+V5\times BW^5+V6\times BW^6$								(BW: Body Weight in g)
		V0	V1	V2	V3	V4	V5	V6	
GI	Leucke	$1.93e^{-2}$	$-4.42e^{-7}$	$9.28e^{-12}$	$-4.88e^{-17}$	-	-	-	Brown *et al.* 1997
	Young	NA	-	-	-	-	-	-	
	LifeStage	$1.650e^{-2}$	-	-	-	-	-	-	
Slow									
Non-Fat adipose*	Leucke	NA	NA	NA	NA	NA	NA	NA	Fit to Valentin *et al.* 2002 & Lafortuna *et al.* 2005 fat data/0.8 (Valentin 2002) data and extrapolated data based on equation in Fig 1A (Lafortuna *et al.* 2005)
	Young	NA	NA	NA	NA	NA	NA	NA	
	LifeStage	$2.044e^{-1}$	$2.617e^{-5}$	$-1.542e^{-9}$	$3.268e^{-14}$	$-3.116e^{-19}$	$1.387e^{-24}$	$-2.35e^{-30}$	
Muscle	Leucke	$9.61e^{-2}$	$-4.88e^{-6}$	$3.05e^{-10}$	$-3.62e^{-15}$	$1.22e^{-20}$	-	-	Fit to Valentin *et al.* 2002 & Janssen *et al.* 2000 data and extrapolated values based on Fig 2A (Janssen *et al.* 2000)
	Young	$9.68e^{-1}$	$-3.32e^{-6}$	$1.83e^{-10}$	$-1.24e^{-15}$	-	-	-	
	LifeStage	$1.251e^{-1}$	$1.458e^{-5}$	$-2.927e^{-10}$	$2.114e^{-15}$	$-5.250e^{-21}$	-	-	
Skin	Leucke	$1.07e^{-1}$	$-3.26e^{-6}$	$6.11e^{-11}$	$-5.43e^{-16}$	$1.83e^{-21}$	-	-	Young *et al.* 2009
	Young	$1.03e^{-1}$	$-2.56e^{-6}$	$3.68e^{-11}$	$-2.580e^{-16}$	$8.620e^{-22}$	$-1.100e^{-27}$	-	
	LifeStage	$1.030e^{-1}$	$-2.560e^{-6}$	$3.680e^{-11}$	$-2.580e^{-16}$	$8.620e^{-22}$	$-1.100e^{-27}$	-	
Bone Marrow	Leucke	$5.19e^{-2}$	$8.06e^{-7}$	$-1.96e^{-10}$	$7.63e^{-15}$	$-1.08e^{-19}$	$5.14e^{-25}$	NA	Brown *et al.* 1997 (red only, yellow is in adipose)
	Young	NA	NA	NA	NA	NA	NA	NA	
	LifeStage	$2.100e^{-2}$	-	-	-	-	-	-	

Similar to Luecke *et al.*, (2007) and Young *et al.*, (2009), polynomial models of orders 1-6 were fit to the data ("R: A language and environment for statistical computing", version 2.9.0 or 2.11.1 (R, 2004)), and then the best fit model was chosen based on the Bayesian information criterion (Schwartz, 1978). Bayesian information criterion is very similar to Akaike's information criterion, in that it is a measure of the goodness of fit in terms of both accuracy (positively) and model complexity (negatively), but differs, in that it penalizes for the number of parameters in a model more rigorously than Akaike's information criterion[2].

When selecting data for fitting the polynomials first choice was to use the reference values for various compartments as defined by the International Commission on Radiological Protection (ICRP) Publication 89 (ICRP, 2003), which presents detailed information on age- and gender-related differences in anatomical and physiological characteristics of reference individuals. This source was used for data on body weights from birth to ~70 kg, while other references were used for compartmental data at higher body weights. Data for some compartments were not available up to the desired 170 kg. For those compartments, extrapolations were made with published relationships, extrapolating for body weights 150-175 kg by 5 kg intervals. These compartment refits in addition to the other compartments from various sources provide a total volume of distribution that is ~75-95% of body weight.

[2] In selecting a "best-fit" model for any data set, models with more parameters will always fit the data set better (have a higher likelihood), especially in the case of polynomial models. For example, a polynomial model with (n-1) parameters will connect all data points with a function. However, the usefulness of such a function is usually minimal. Thus for selection of a "best-fit" model that is useful, standard approaches have been developed to quantitatively select the best fit model by balancing goodness-of-fit (by maximum likelihood) and parsimony (penalize by the number of parameters in the model [complexity]) Akaike, H., 1974. A New Look at the Statistical Model Identification. I.E.E.E. Transactions on Automatic Control. AC 19**,** 716-723, Akaike, H., 1976. Canonical Correlation Analysis of Time Series and the Use of an Information Criterion. in: Lainotis, R. K. M. a. D. G., (Ed.), System Identification: Advances and Case Studies. Academic Press, New York, pp. 52-107. In general, these criteria (c) are described mathematically below, where $L_n()$ is the maximum likelihood, k is the number of parameters of a function, n is the sample size of data, $\varphi(n)=2$ for AIC, and $\varphi(n)=\ln(k)$ for BIC.

$$c_n(k)=-2\times\ln(L_n(k))/n+k\times\varphi(n)/n$$

The following sections describe the modeling of the key compartments and tissues for the LifeStage model of CPF. These include, brain, liver, adipose and fat, and muscle. The resulting equations are given in Table 2.

Brain

Luecke *et al.* have published equations for brain compartment growth as a function of body weight (Luecke *et al.*, 2007; Young *et al.*, 2009). The function was refit using data from the ICRP Publication 89 (ICRP, 2003) and Young *et al.* (2009) for body weights greater than 70 kg. Extrapolations of brain volume were made using Table 4A in Young *et al.*, (2009) for both the body weights presented in that table and extrapolated for 150-175 kg body weights. The resulting fit was a 4^{th} order polynomial equation (Figure 14). As Figure 14 demonstrate refitting the equations of Luecke *et al.* (2007) and Young *et al.*, (2009) was required in order to assess individuals with body weights greater than 100 kg. Symbols are published measurements from Valentin, 2002 (blue), or Young *et al.*, 2009 (black). The lines show the implementation of the polynomial equations as published in Young *et al.*, (Green dashed line), Leucke *et al.*, 2007 (green dotted line) or predicted using the LifeStage model (solid black line). The equations of Leucke *et al.*, 2007 and Young *et al.*, 2009, were designed to be used up to 100 kg. BTW is body weight in kg.

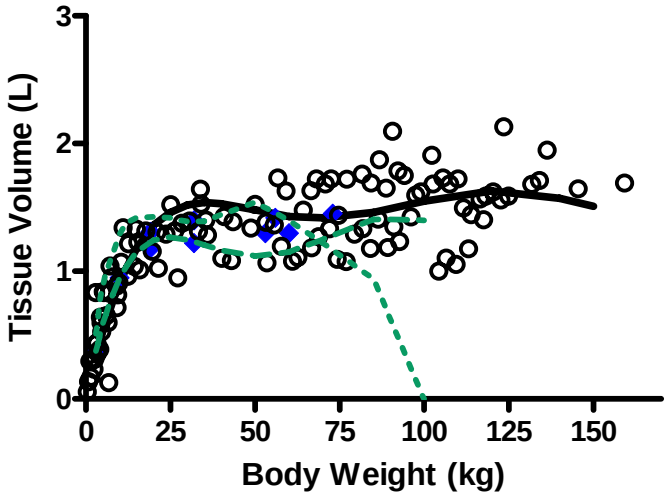

Figure 14. Comparisons of equations to describe ontogeny of brain growth. Symbols are published measurements from Valentin, 2002 (blue), or Young *et al.*, 2009 (black). The lines show the implementation of the polynomial equations as published in Young et al., (Green dashed line) or Leucke et al., 2007 (green dotted line). Brain volume as predicted using the LifeStage model is shown with the black line. The equations of Leucke et al., 2007 and Young et al., 2009, were designed to be used up to 100 kg.

Liver

The function for the liver compartment ontogeny was refitted using the ICRP Publication 89 (ICRP, 2003) and Young *et al.* (Young *et al.*, 2009) data presented in Table 4A of that paper. This refitting allows for the prediction of liver volumes up to 175 kg body weights. Initial attempts in developing the function were based on data from Young *et al.* (2009). These data resulted in fitted equations with undesirably high variation across narrow body weight ranges. Fitting the function to the reference values for liver from Table 4A in Young *et al.* (2009) resulted in a 4^{th} order polynomial that was a much smoother fit (Figure 15, presented with all data).

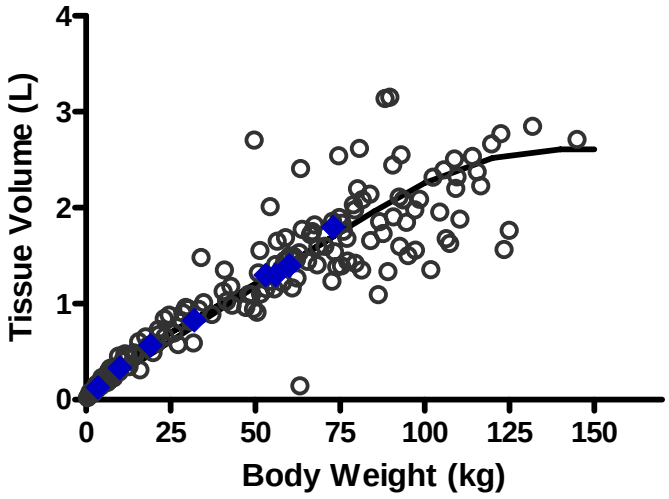

Figure 15. Fit of the LifeStage model-predicted ontogeny of the liver (Black line) to the published measurements from Valentin, 2002 (blue), or Young *et al.*, 2009 (black). BTW is body weight in kg.

Adipose and fat

The ICRP Publication 89 (ICRP, 2003) describes adipose tissue as a combination of fat and connective tissue. Reference fat content of adipose tissue is 40% at birth and increases to ~80% in adults (ICRP, 2003). Failure to account for these differences could lead to inaccurate compartmental volume estimates of fat or fat-partitioning coefficients which are estimated based on chemical makeup of tissue. These potential inaccuracies could have substantial implication on overall pharmacokinetics for lipophilic compounds, like CPF. In the LifeStage model, the fat compartment is defined as the lipid content of adipose tissue. The non-fat adipose tissue (connective tissue and the adipose compartment subtracted from the fat compartment) is included in the slow compartment. Data to fit the fat compartment came from ICRP Publication 89 (ICRP, 2003) and Lafortuna *et al.*, (2005) (Figure 16). Extrapolations were made for 150-175 kg body weights using the respective equations presented in those figures. Data for the adipose tissue came from the ICRP, (2003) and Lafortuna *et al.*, (2005) based on the assumption that 80% of adipose tissue in adults is fat (ICRP, 2003).

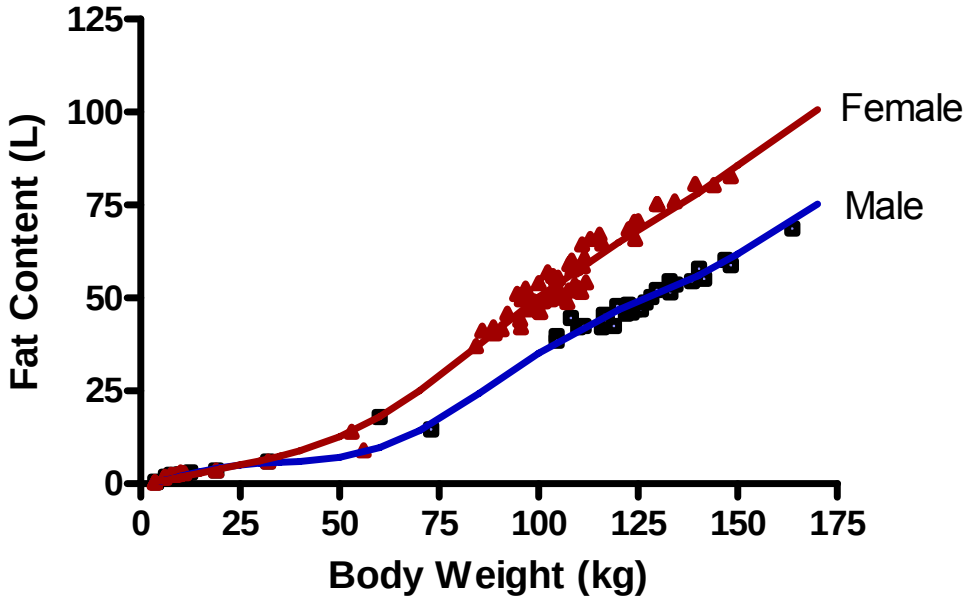

Figure 16. Fit of the LifeStage model-predicted ontogeny of the fat in males and females to the published measurements from Lafortuna, 2005, Butte, 2000; or Valentin, 2002.

Muscle

The function for muscle was based on data obtained from Figure 4 A of ICRP Publication 89 (ICRP, 2003) and from Janssen *et al.*, (2000). The final function was a 4th order equation that is capable of predicting the muscle compartment upto 170 kg. The volume of the muscle is used in the estimate of the volume of the slowly perfused compartment of the individual.

Summary of Tissue Ontogeny

This LifeStage model includes polynomial equations that fit the available tissue growth data from the literature (see Figures 13-16). The ontogeny of the above organs as well as the general PBPK model compartments are shown in Figure 17. The benefit of describing tissue volumes correctly as a function of age and weight, rather than based only on weight (fixed percent of body weight) can be seen for the predictions of the volume of the brain. Brain is a much larger fraction of total body weight in infants than adults and cannot be accurately predicted from body weight alone.

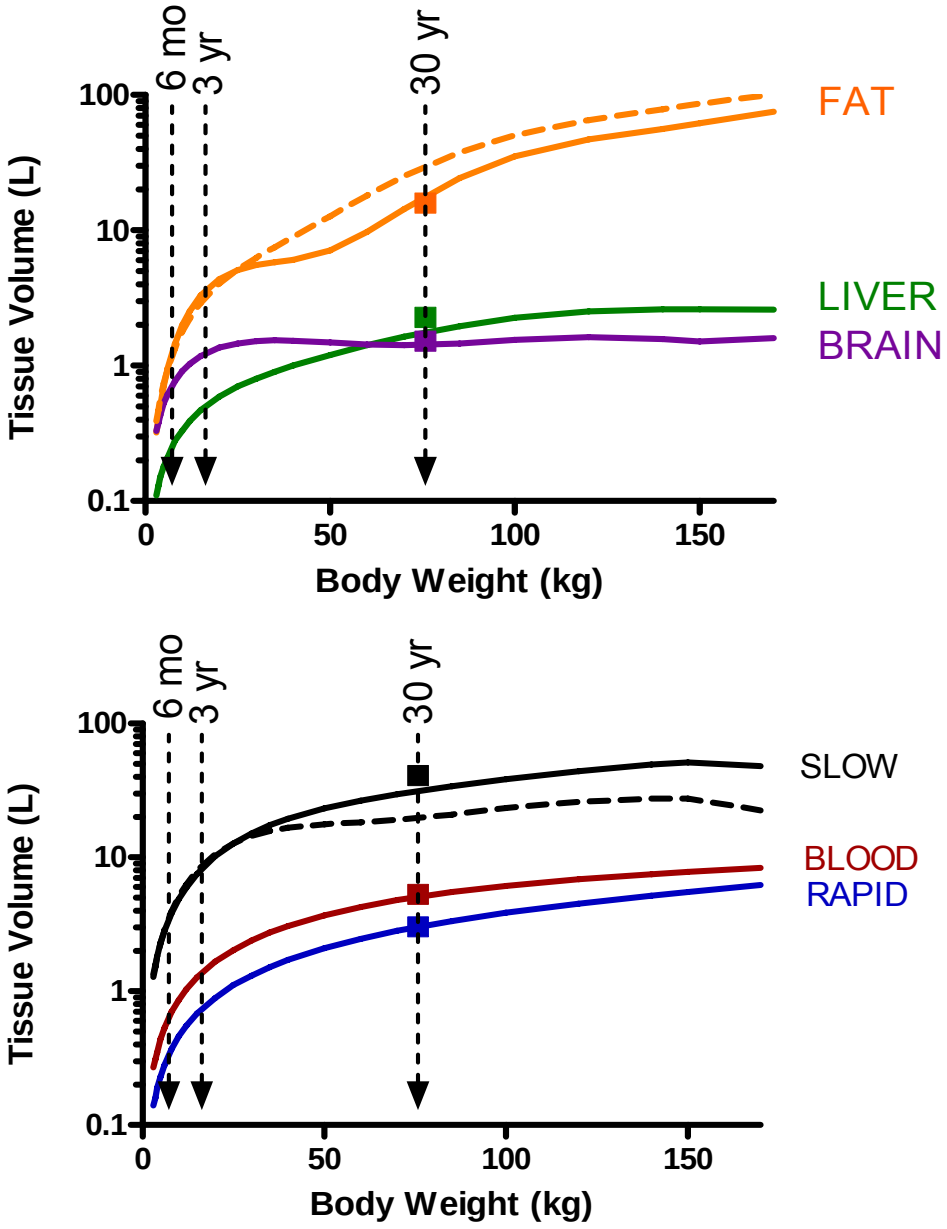

Figure 17. LifeStage model tissue growth. The LifeStage model predictions for typical adult individuals are shown with the lines, the dashed lines show tissue volumes for females, solid lines are males. The symbols represent tissue volumes predicted for at typical male using the original Typical Adult model, and default tissue volumes as a percentage of body weight (Timchalk, *et al.*, 2002; Brown *et al.*, 1997). Arrows indicate typical body weights at each age of interest for this analysis.

Blood flows

Once the volumes of the organs and tissues are defined, tissue-specific perfusion rates are used to define the blood flows for each organ. These values are summed to predict the total cardiac output. Total cardiac output is consistent with predictions of total cardiac output in humans that are based on surface area (Brown, 1997) (Figure 18).

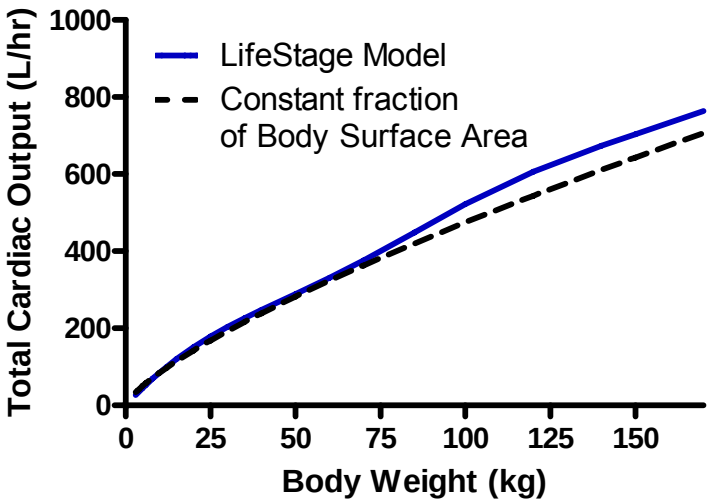

Figure 18. Comparison of the total cardiac output used in the original Adult model (Timchalk, *et al.*, 2002) to the summed tissue-specific perfusion rates from the LifeStage model. The dashed line represents a cardiac output calculated using the formula: Cardiac output =15*(Body wt)$^{0.7}$ (Brown, 1997).

Enzyme activity in individual

The age-dependent enzymatic metabolism of CPF and CPF-oxon was measured *in vitro* using human hepatic microsomes (CYP and PON1) and plasma (PON1), as described previously (Section 2). These *in vitro* V_{max} rates were extrapolated to *in vivo* values for use in the model by multiplying the *in vitro* rates times the levels of microsomal protein per unit volume and times liver (or plasma) volumes (see the following equation).

$$\underset{[\mu mole/hr]}{\text{Enzyme activity in individual}} = \underset{[\mu mole/hr/mg\ protein]}{\text{Enzyme levels in tissue}} * \underset{[mg\ protein/L\ tissue]}{\text{Protein level in organ}} * \underset{[L\ tissue]}{\text{organ volume}}$$

Total V_{max} of human enzymatic metabolism of CPF to TCPy, CPF to CPF-oxon, and CPF-oxon to TCPy in the liver over various ages were scaled to age-dependent volume of the liver (Table 2) and concentration of microsomes in the liver, which is approximately 37 mg/g tissue (Barter *et al.*, 2008).[3]

Thus, even in cases where the enzymatic measures show no *in vitro* age- or physiological-dependences (on a per mg protein basis), the total enzymatic capacity of the individual varies with age. Figure 19 showing the impact of the age-related changes in liver volume. The values in this figure were generated by multiplying the observed Vmax times the age-specific liver volume.

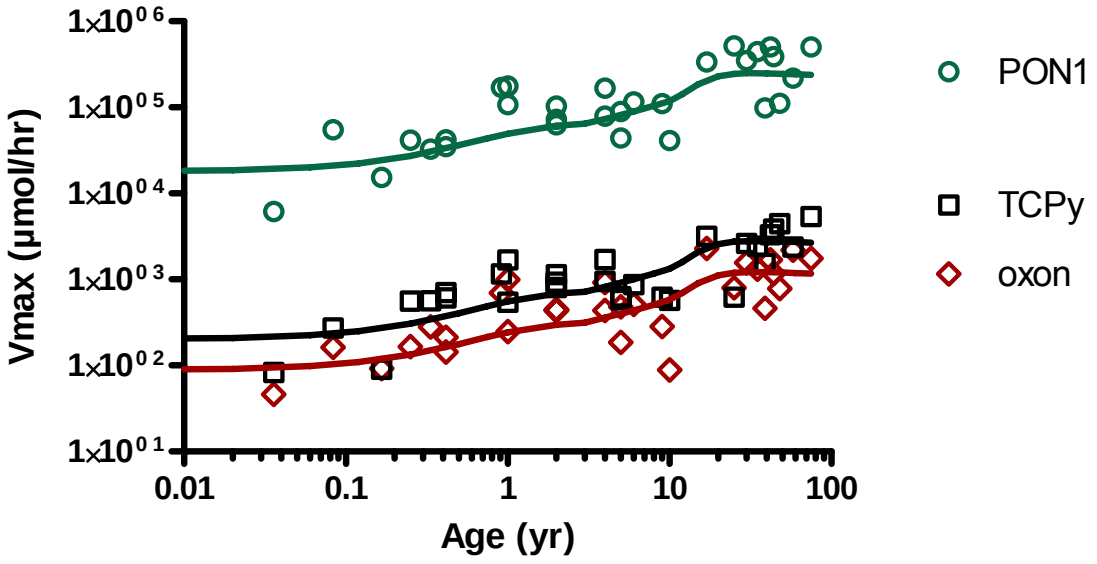

Figure 19. Hepatic metabolism of CPF to TCPy (CYP), CPF-oxon (CYP) and of CPF-oxon to TCPy (PON1) increases with age. Note: total V_{max} is on a logarithmic scale.

3 There is limited evidence that microsomal protein content may change with age Barter, Z. E., et al., 2008. Covariation of Human Microsomal Protein Per Gram of Liver with Age: Absence of Influence of Operator and Sample Storage May Justify Interlaboratory Data Pooling. Drug Metabolism and Disposition. 36**,** 2405-2409.but this study is based on n=4 "pediatric" samples from individuals aged 2, 4, 9 and 13 and uses data from multiple laboratories after "correcting for losses" of microsomal protein during preparation. The adult population from this same study included separate individuals that were as young as 11 years old, overlapping the age of the pediatric samples. In rats, an increase in microsomal protein has been shown from post natal day 1-14, but by day 7 the protein content in the microsomes of neonatal rats were not significantly different than adults, whereas liver weight continued to increase through day 42 Alcorn, J., et al., 2007. Evaluation of the assumptions of an ontogeny model of rat hepatic cytochrome P450 activity. Drug Metab Dispos. 35**,** 2225-31. Overall, the evidence that microsomal protein in human children will vary from adults was not felt to be compelling, but the range in protein content suggested by these data was accounted for in the variability model to address any age- related differences in microsomal protein content (if they exist).

In plasma, however, *in vitro* PON1 metabolism of CPF-oxon to TCPy was age-specific on a per ml plasma volume basis, as described previously (Section 2). Therefore, the age-specific V_{max} was scaled to age-dependent volume of the blood (Table 2), resulting in plasma metabolism varying by nearly 2 orders of magnitude (Figure 20).

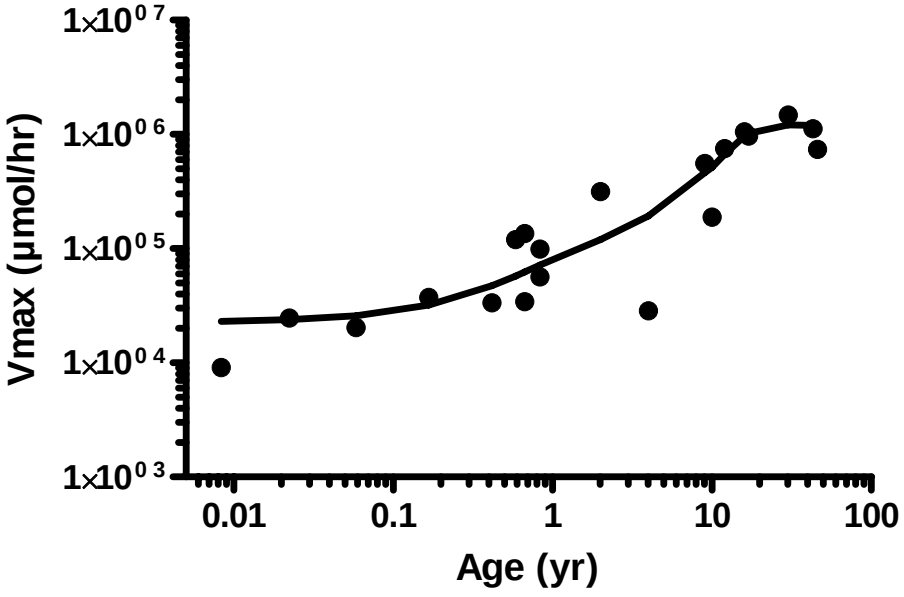

Figure 20. Total V_{max} values of human enzymatic metabolism of CPF-oxon to TCPy in plasma over various ages. Symbols represent *in vivo* rates extrapolated from the *in vitro* data (See Figure 10). The line shows the V*max* used in the model for standard individuals.

Metabolism of CPF in the brain was estimated based on an extrapolation from limited studies in rats. Incubation of brain microsomes with CPF demonstrated metabolism to TCPy 115-fold lower than in liver microsomes. Metabolism to oxon was below the limit of quantification. Based on this assessment, brain metabolism was conservatively estimated to be 115-fold lower than liver on a per mg protein basis for both metabolism to oxon and to TCPy. The microsomal yield in these studies was 5.2 mg/g brain and 35 mg/g liver, so the final *in vivo* metabolic rate constants were estimated to be approximately 760-fold higher in whole liver than whole brain. Because brain size changes much less than

liver size over ontogeny, the difference in predicted V_{max} for the bioactivation of CPF to CPF-oxon in the liver is only 3.7-fold less in newborns compared to adults.

3.3 *Comparison of LifeStage model output to human data*

The estimates of the relationship between oral doses and impacts on blood concentrations of TCPy and cholinesterase inhibition in blood from the LifeStage model can be evaluated by comparing the predictions to the observed values in volunteer human studies. The LifeStage model code includes within it the Typical Adult model (See Figure 2) and is designed such that either a body weight or an age can be put into the model. For these examples, the LifeStage model was employed by assigning body weights instead of ages to the simulated individuals. As indicated in Tables 1 and 2, the majority of the inputs for the LifeStage model are based on measured values and new *in vitro* data (Section 2)[4]. Therefore, results from the human volunteer study can be used to evaluate the predictions of the LifeStage model.

Two controlled human exposure studies are available to compare model output; these studies were evaluated for both scientific and ethical considerations by the EPA Human Studies Review Board (See Attachment B). In the first study (Nolan *et al.*, 1984), human volunteers were administered 0.5 mg/kg CPF, and blood and urinary TCPy and plasma cholinesterase were measured. Plasma cholinesterase inhibition was more than 80% 24 hr after exposure (Figure 21). The *in vitro*-derived metabolic constants were applied to the LifeStage model as described previously and the parameters optimized from the first study were held constant and validated using the results from a second study in which 6 male and 6 female volunteers were administered 0.5, 1 or 2 mg/kg in a capsule (Kisicki *et al.*, 1999; Timchalk *et al.*, 2002b). Based on the urinary output of TCPy from the original study (Nolan *et al.*, 1984), approximately 100% of the dose is expected to be excreted as TCPy. Based on this and TCPy plasma levels in the second study, oral absorption in the Kisicki *et al.* study is believed to be only ~30%.

The LifeStage model's predictions for adults compared well to the human data. The blood and urinary concentrations of TCPy are very good with the prediction following the

4 The one exception to this is the TCPy compartmental parameters.

mean response of the groups at each dose in both studies (Figures 22 and 23). The predictions of the LifeStage PBPK/PD model for BuChE in plasma from the Noland *et al.* study were also very good with the peak inhibition accurately predicted (Figure 21). The LifeStage model's predictions of RBC AChE inhibition are consistent with the finding of Kisicki *et al.* (Figure 24). In this study no statistically significant differences were observed in RBC AChE activity in the volunteers, regardless of dose. The LifeStage predicts a peak inhibition of approximately 7% for the 2 mg/kg exposure and lower inhibition levels for the other groups. This level would not have been detectable given the relatively high day-to-day variation that occurs in humans.

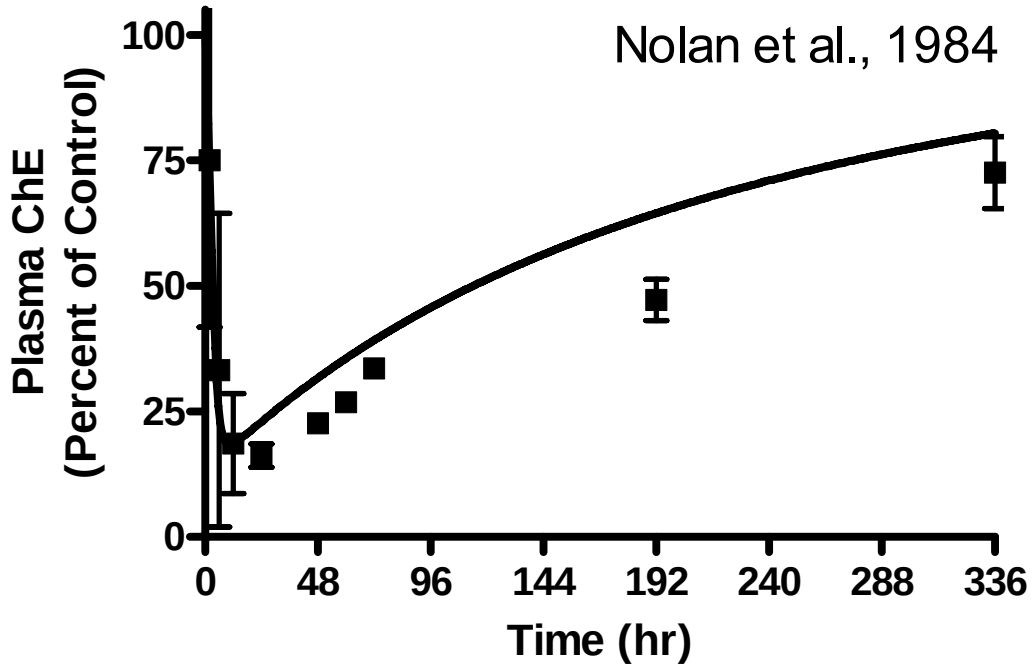

Figure 21. Comparison of the model predictions of plasma cholinesterase inhibition for a typical adult to the data of Nolan *et al.* (1984). Data represent mean ± SD for 11-12 individuals as described in Nolan *et al.* (1984).

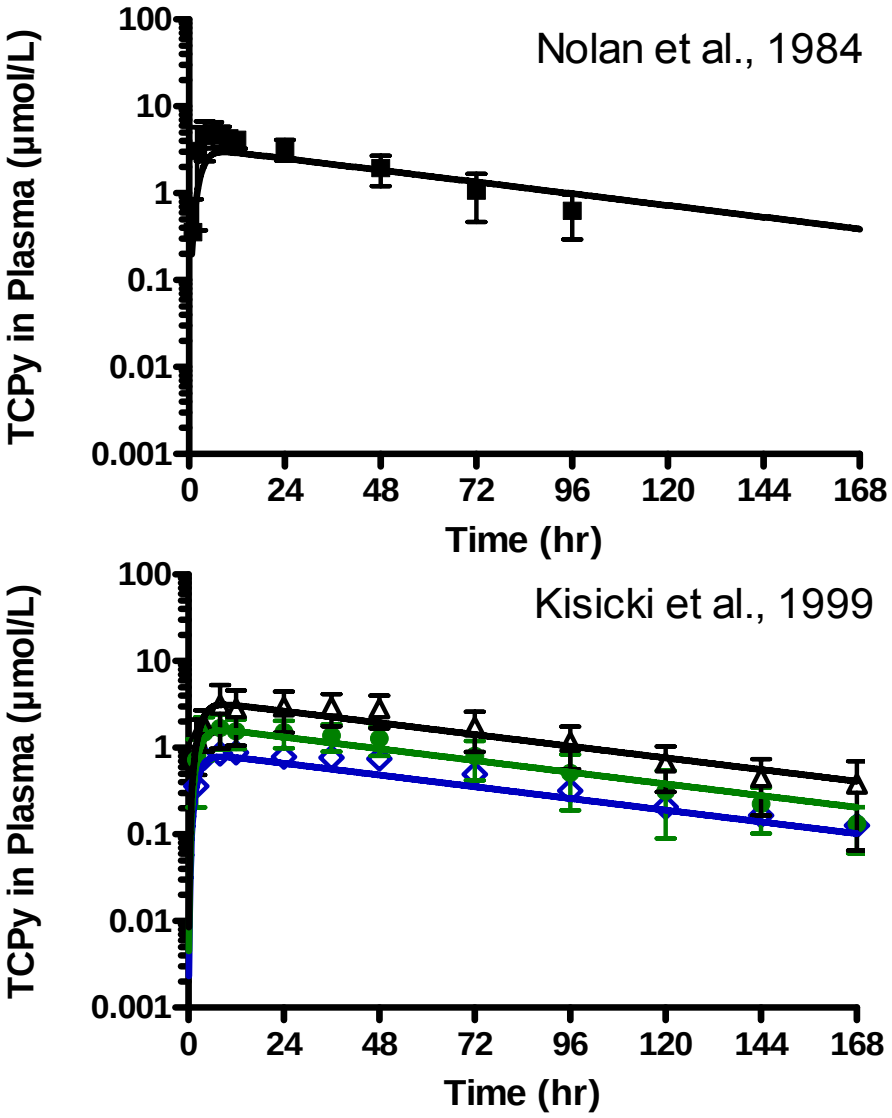

Figure 22. Comparison of the model predictions of plasma TCPy concentration for a typical adult to the data of Nolan *et al.* (1984) and Kisicki *et al.* (1999). Data represent mean ± SD for 5-12 individuals as described in Nolan *et al.* (1984) and Kisicki *et al.*, (1999). In Kisicki et al., data for 0.5 mg/kg dose is given in blue, 1.0 mg/kg in green, and 2 mg/kg in black.

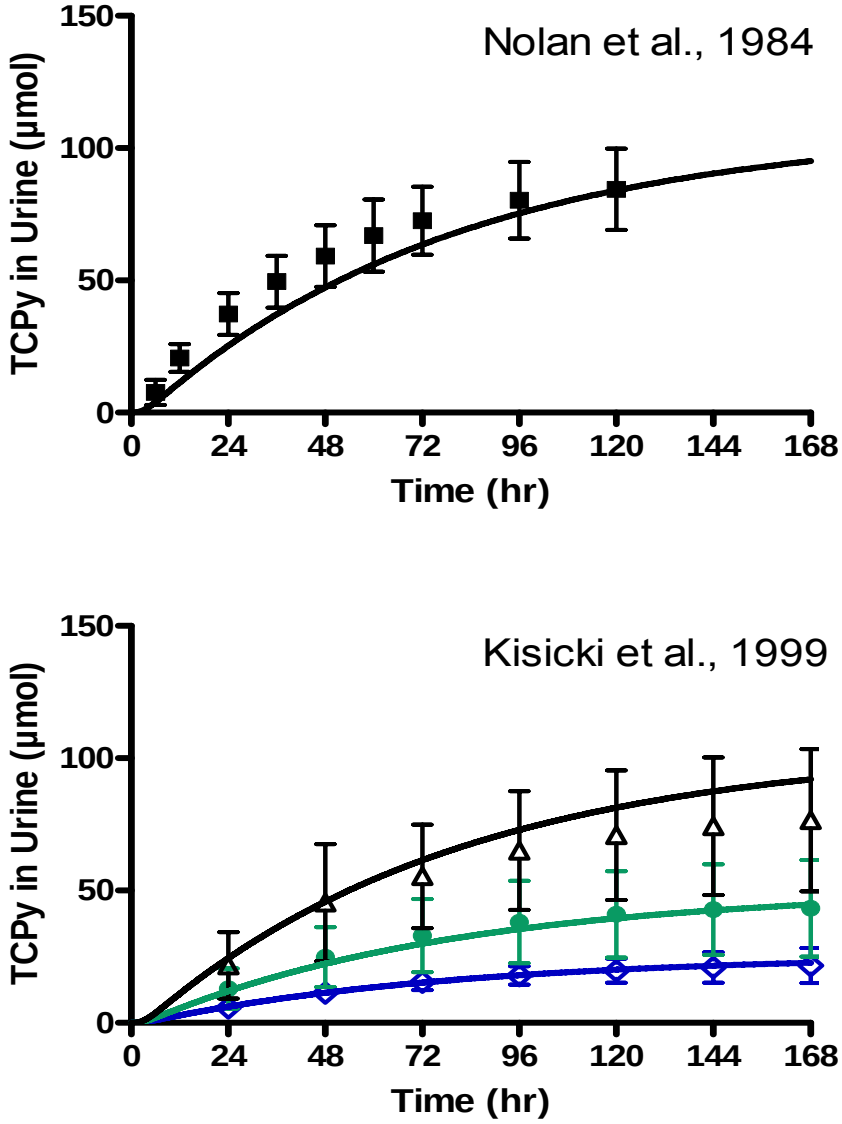

Figure 23. Comparison of the model predictions of urinary TCPy concentrations for a typical adult to the data of Nolan *et al.* (1984) and Kisicki *et al.* (1999). Data represent mean ± SD for 5-12 individuals as described in Nolan *et al.* (1984) and Kisicki *et al.*, (1999). In Kisicki et al., data for 0.5 mg/kg dose is given in blue, 1.0 mg/kg in green, and 2 mg/kg in black. Kisicki *et al.* fits are based on a predicted 30% uptake from the coated pills. Nolan *et al.* is based on 100% uptake, model predictions presented below all assume 100% oral bioavailability.

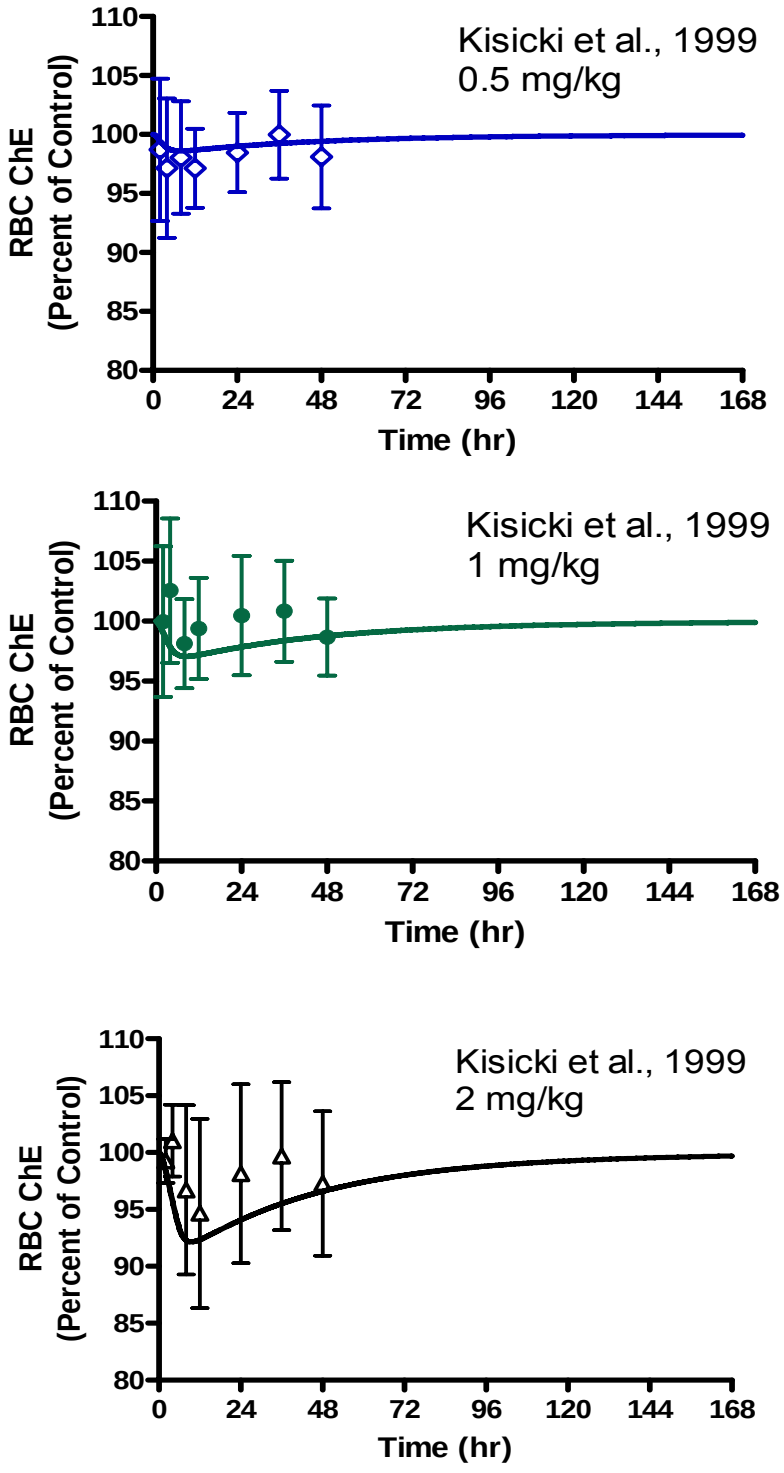

Figure 24. Comparison of the model predictions of RBC cholinesterase inhibition for a typical adult to the data of Kisicki *et al.* (1999). Data represent mean ± SD for 5 individuals as described in Kisicki *et al.*, (1999). Kisicki *et al.* fits are based on a predicted 30% uptake from the coated pills. No statistically significant inhibition was measured after 0.5, 1, or 2 mg/kg dosing: the model predicts about 7 percent inhibition after a 2 mg/kg dose. Model predictions presented in all analyses below all assume 100% oral bioavailability.

3.4 *Comparison of LifeStage model to Timchalk et al. 2002*

The core structure of the LifeStage model is based on the model published in 2002 (Timchalk *et al.*, 2002b), with modifications as described in this Section. In the LifeStage model, more human-specific data have been used to parameterize the model whereas the initial PBPK/PD model used parameters extrapolated from rat data. Thus, our confidence in the parameterization of the human model and its predictive abilities are much greater than in earlier models.

The LifeStage model predictions for adults were compared to those of the original standard adult model and found to be more conservative (Figure 25). In this figure the solid lines represent the predictions from the LifeStage model while the earlier model results are given using dotted lines. While the predictions for plasma BuChE inhibition in the two models are very similar, the predictions of RBC and brain AChE inhibition are approximately 2-3 fold lower. The RBC and brain AChE models have been updated using *in vitro* data for the bimolecular inhibition rate constant for AChE (Ki), PON1 metabolism (liver and blood), and CYP metabolism (brain).

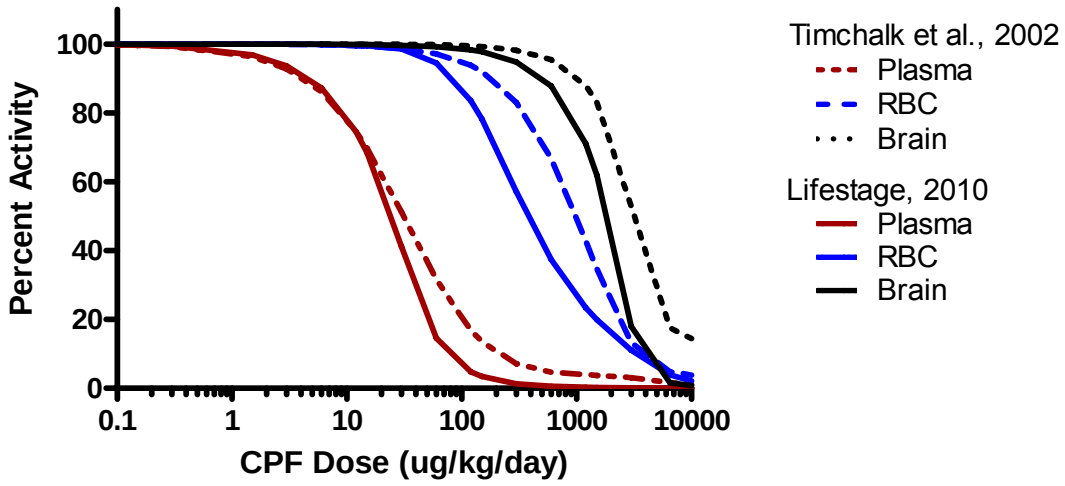

Figure 25. Comparison of 2002 PBPK/PD model output (Timchalk, *et al.*, 2002b) to LifeStage model. Simulations were conducted assuming a zero order (constant) oral uptake.

3.5 Predicted dose response in typical individuals at 6 months, 3 and 30 years.

The LifeStage model was used to determine peak RBC inhibition in adults, 3 year-old children and 6 month-old infants following single dose exposures to CPF (Figure 26). The predictions of the LifeStage model suggest that for a single oral dose at or above 0.5 mg/kg the inhibition of RBC and brain AChE is greater in infants than in adults. Values for children age three fell in between the values for adults and infants. Infants had inhibition rates approximately 2–fold higher than adults. However, at a single oral dose of 0.5 mg/kg and below, the level of inhibition of RBC would not be experimentally quantifiable in any of the age groups.

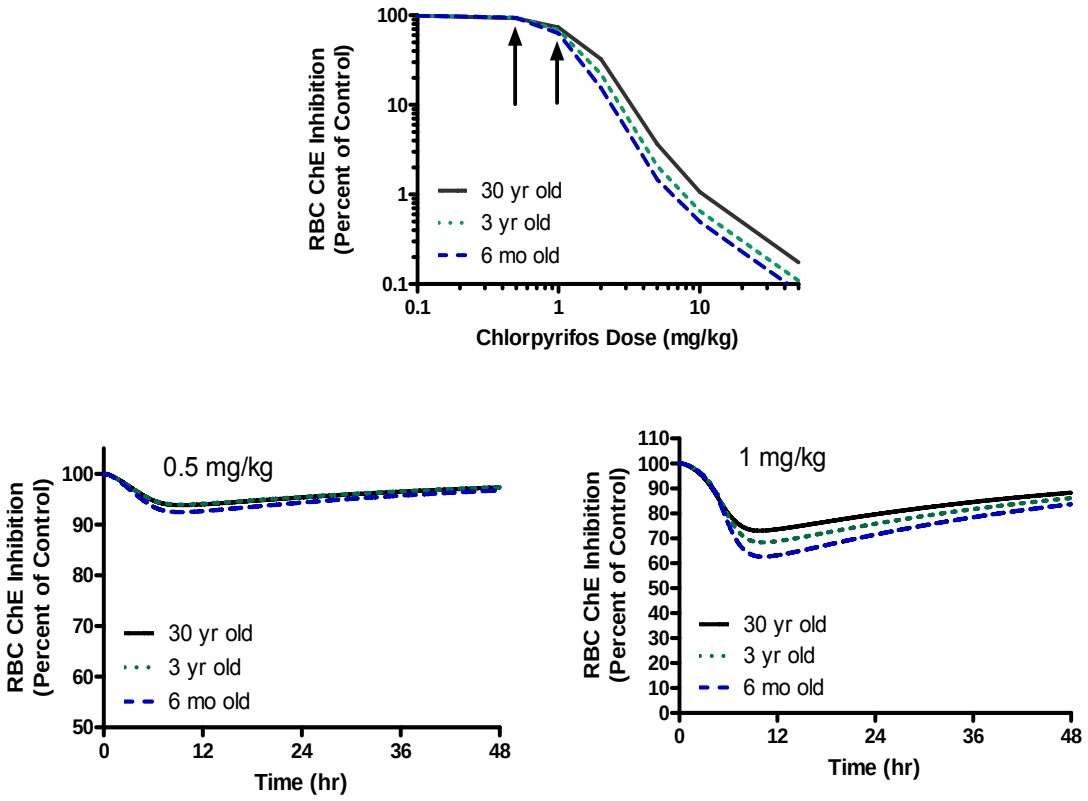

Figure 26. Comparison of the LifeStage model's predictions of RBC inhibition in adults, 3 year-old children and infants. Top) shows a dose response curves for the for peak RBC inhibition for the three ages, the arrows in this plot indicate of 0.5 and 1 mg/kg. Bottom) LifeStage model predictions of time courses of inhibition and recover at 0.5 and 1 mg/kg for the three age groups. Note the different y-axes.

Section summary

This section documents the data and assumptions used in the creation of the LifeStage model. The LifeStage is built on the Typical Adult model which is an update of the original 2002 Timchalk model. The LifeStage model allows the simulation of age-specific dose response curves for humans of any age. The predictions of the LifeStage model reflect a number of improvements over the original 2002 model. In general, the LifeStage model predicts more inhibition in RBC and brain then the original 2002 model (Figure 26). The predictions of the LifeStage model were shown to be consistent with the data from human volunteer studies (Figures 21-24). The predictions of the LifeStage model suggest that for a single oral dose above 0.5 mg/kg, cholinesterase inhibition in the various age groups exhibits the following pattern: infants > children > adults. Infants had inhibition rates approximately 2–fold higher than adults at these doses. However, at a single oral dose of 0.5 mg/kg and below the level of inhibition of RBC would not be experimentally quantifiable in any of the age groups. More detailed comparisons in cholinesterase inhibition are described in Section 4 in conjunction with the development of the Variation PBPK/PD model.

4. Creation of the Variation PBPK/PD model

Section overview

The LifeStage model (Section 3) focused on characterizing the response to CPF in typical individuals of differing age. Once the compartments have been described on a default physiological basis, adding inter-individual variability is the next logical step to determine physiological and enzymatic determinants of pharmacodynamic outputs (Bois, 2010). This section describes the development of models of interindividual variation for each age. The process for deriving the Variation model consists of the following four steps.

Step 1. Use a "sensitivity analysis" to identify parameters in the LifeStage model that drive variation in response;

Step 2. Develop distributions of interindividual variation in values for the parameters that drive response;

Step 3. Define how correlations between input values are addressed;

Step 4. Compare prediction of variability to data from human volunteer studies.

Once the model is created it is used to investigate the factors that drive the increased sensitivity to the effects of CPF. Finally, the Variation model is used to investigate the magnitude of the variation in response in populations of different ages at different doses. Endpoints investigated are measures of internal dose and RBC and brain AChE inhibition.

4.1 Step 1. Determining the relative importance of model parameters using a sensitivity analysis

The sensitivity analysis was conducted using tools provided in the acslXtreme software used to create the model. A local sensitivity analysis was performed using the LifeStage model. In a local sensitivity analysis each parameter was varied individually while the values of all other parameters were held fixed and the impact of the variation on the model's output was determined. A single oral dose of 0.54 mg/kg, was selected since

the Typical Adult model predicted that this dose would cause a 10% RBC inhibition in a typical adult human. The individual was evaluated over time and peak inhibition of RBC and brain AChE were determined.

For each model parameter, sensitivity is measured in terms of a sensitivity coefficient. The sensitivity coefficient of a parameter is defined by the change in peak RBC and brain AChE inhibition divided by the change in the parameter value. In this analysis a small change, 1%, was made in the parameter value and the impact on peak RBC and brain AChE inhibition was determined. A value of 1 indicates that the 1% change in parameter produces a 1% change in either the peak RBC or brain AChE inhibition. Values greater than 1 indicate a greater than 1% change in one of the two target effects. Values close to zero indicate that neither brain nor RBC AChE levels were affected by changes in the parameter.

Model parameters that were varied are those listed in Tables 1 and 2. These parameters include:

- Tissue volumes, blood flows and perfusion rates
- Enzyme activity levels
- Tissue partitioning coefficients
- Binding of cholinesterases, recovery of cholinesterases, and regeneration (turnover) rates
- Rates of transport of CPF from the stomach to the gut or uptake from the gut

As Table 3 indicates, very few of the model parameters impacted the estimates of peak RBC or brain AChE inhibition. Only 8 parameters had sensitivity coefficients greater than 0.1. It is recognized that some parameters that vary widely across a population with coefficients smaller than 0.1 might also contribute to variation in response. However, using a cutoff criterion of 0.1 should capture the major drivers of variation in response.

Table 3. Sensitivity of the model parameters on RBC or brain ChE inhibition

Parameter	Normalized Sensitivity Coefficient	RBC/Brain AChE Basis
Tissue Volume		
Rapidly perfused tissues	0.09	Brain
Slowly perfused tissues	0.20	Brain
Liver	0.74	Brain
Blood	1.77	RBC
Fat	0.19	Brain
Tissue Specific Blood Flows		
Rapidly perfused tissues	<0.01	RBC
Slowly perfused tissues	<0.01	RBC
Liver	0.30	RBC
Fat	<0.01	RBC
Liver Metabolism Cytochrome CYP that converts CPF into:		
Oxon (activation)	0.98	RBC
TCPy (detoxification)	0.92	RBC
Brain Metabolism -Cytochrome CYP that converts CPF into:		
Oxon (activation)	0.32	Brain
TCPy (detoxification)	0.10	Brain
PON1		
Blood	0.26	RBC
Liver	0.47	RBC

Note: The more sensitive endpoint is reported.

Based on the sensitivity analysis, the Variation model includes distributions for the following parameters:

- Brain and liver CYP metabolism and its effect on both the rate of formation of CPF-oxon and the formation of TCPy
- PON1 metabolism in blood and liver
- Compartment volumes and blood flows[5]

The remaining parameters use the mean age-specific values established by the LifeStage model.

5 While only certain compartments were found to be statistically significant, the interrelationship of organ and compartment volumes requires that models of interindividual variation in compartment volume address all of the major compartments of an individual.

4.2 *Step 2. Developing distributions for sensitive parameters*

The critical factors identified in Step 1 can be divided into two categories: physiology (including blood flows) and enzyme activity. The following subsections describe the approach used to develop age-specific distributions for these categories.

Physiology

Modeling variation in physiology is a challenge since physiological parameters are inherently correlated (larger body weight implies larger compartment volumes). Blood flows in an individual are related to organ sizes and variation in one organ affects the other organs. In order to capture these correlations, the modeling of physiology was performed in a systematic manner. The process can be described as follows. First, data on the variation of body weight is taken from the output of the exposure models. As described in Section 5, the exposure models generate estimates of each individual's body weight based on the individual's age and gender. Thus for each individual a body weight, age, and gender is provided as an input.

Second, the volume of each compartment is estimated from the individual's body weight using the equations in Table 2. As discussed above, these equations are polynomial functions that assign volumes to the individual's different compartments and organs. Since each equation for an individual's compartment is based on a common body weight, the volumes are consistent (see Figures 13-18).

The one exception to this process is the method used to assign the volume of the body fat compartment. In the development of the LifeStage model, it was determined that the majority of the variability in the total individual was due to variability in the fat content (Figure 16). For the fat compartment, interindividual variability was added to the predicted compartment volume. The relative variability of height in the NHANES data was determined to be constant across body weight (data not shown). Since no other information was available about the individual variability, the relative variability for the fat compartment volume was thus assumed to be equal to the relative variability of the body height. The LifeStage model then calculates the fat compartment with the equations in the growth model and adjusts the calculated volume by randomly sampling from the normal

distribution of relative variability. The resulting variability in fat volume is shown in Figure 27.

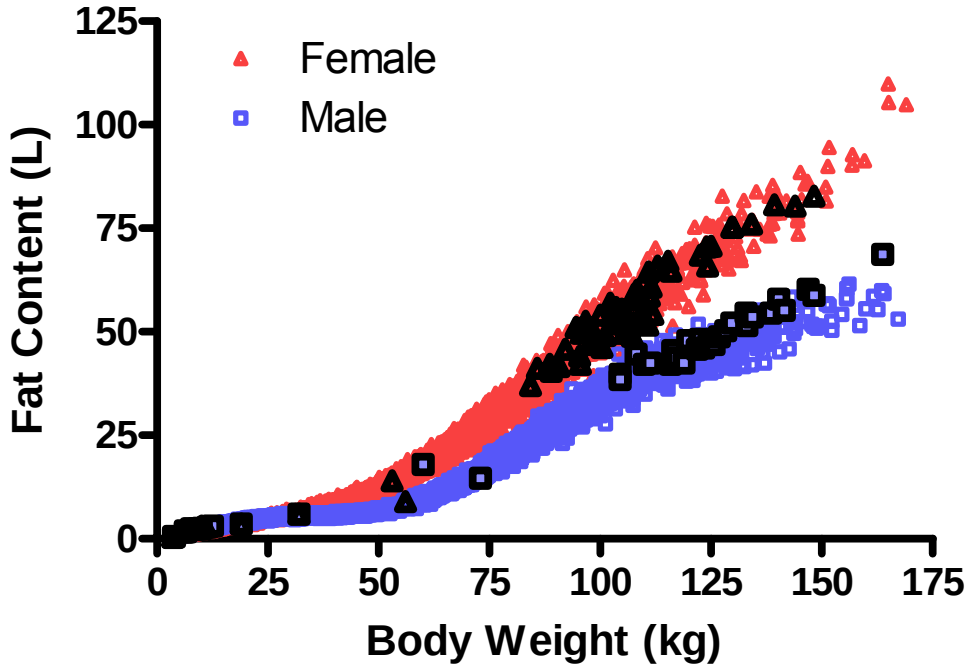

Figure 27. LifeStage model output of fat volumes in simulated individuals (red triangles, blue squares, compared to published measurements (Lafortuna, 2005, Butte, 2000; or Valentin, 2002)

Total Blood flow (Cardiac Output)

As described above, blood flows were defined on a tissue-specific basis and summed to predict total cardiac output (See Figure 18). This approach provides an estimate of the cardiac output and organ-specific blood flow under resting conditions (see Fig 19). In the variability model, inter-individual differences in fat volume and workloads results in total cardiac outputs that have a similar range in values as seen for the volume of fat (data not shown).

Effect of activity on total compartment specific blood flows

Blood flows are affected by an individual's physical activity. Thus, the resting blood flows must be adjusted to reflect interindividual variation in activity levels. Data on interindividual variation in physical activity are available from sources such as the

databases of human activity (Xue, 2010). However, in this project we decided to first test the model to determine the importance of activity before expending the effort to incorporate actual data on human variability in activity levels. This was done by assigning individuals activity levels based on a uniform distribution. Under this approach, individuals were assigned a work level ranging from 0 to 5 Watts. This range of work levels corresponds to a range from a resting state to a level of light exercise (e.g., moderate walking rate). This level of activity is assumed to be constant over the duration of the modeling period. If the variation in activity could be shown to have little or no effect on the predictions of internal doses and impacts on AChE, then there would be no need to assess the impact of actual patterns of human activity.

The role of activity on organ-specific blood flows is not the same for each organ. Increasing levels of activity change the total cardiac output and also redirect the output away from the digestive organs to the muscles and dermis. This redirection is important to capture since it has a critical effect on blood flow through the liver. Standard blood flows (Table 4) were adjusted based on a work to oxygen demand conversion proposed by Jonsson *et al.* (2001) in the following equation.

$$Q_i0\ (L/hr) = \text{Perfusion Rate}_i\ (L/hr/L\ tissue) * \text{Tissue Volume}_i\ (L) + \text{Work Change}_i\ (L/hr/W) * \text{Work}\ (W)$$

Table 4. Impact of work on Organ-Specific Perfusion Rates

Model Compartment	Change in Perfusion rate /Change in work level [a] (L/hr/W)
Fat	0.00017
Liver	-0.0019
Brain	0
Slowly perfused [b]	0.075
Richly perfused [c]	-0.0019

[a] Adapted from work rates from (Jonsson *et al.* 2001)
[b] Skin and Muscle
[c] Red Marrow, GI Organs, Pancreas, Thyroid, Spleen, Kidney

As Table 4 indicates, richly perfused tissues including the liver are relatively unchanged by increases in activity levels. In addition, the perfusion rates actually decrease

with activity. This suggests that individuals are most sensitive to CPF at lower activity levels.

Modeling enzyme activity levels

The activities of CYP and PON1 in plasma and liver have been investigated using a number of substrates. The catalytic efficiency of hepatic and plasma PON1 is believed to be an important factor in modulating CPF neurotoxicity (Albers *et al.*, 2010; Costa *et al.*, 2005). There are two polymorphisms of PON1 that have been discovered, a leucine (L) to methionine (M) substitution at position 55, and a glycine (Q) to arginine (R) substitution at position 192 (Furlong et al., 1988; Adkins et al., 1993; Costa et al., 2003; Richter et al., 2009). The first polymorphism has little impact on the catalytic activity of PON1; however, the polymorphism at position 192 has been demonstrated to have a substrate-dependent functional impact on PON1 mediated esterase activity (Furlong et al., 1988; Adkins et al., 1993; Costa et al., 2003; Richter et al., 2009). These different phenotypes of PON1 have been reported to demonstrate different age-dependent maturation patterns as well (Huen et al., 2009; Huen et al., 2010). Genetic variation in the PON1 gene results in polymorphisms that alter the catalytic efficiency toward organophosphorous compounds (Albers *et al.*, 2010; Costa *et al.*, 2005; Furlong *et al.*, 2000). The ability of each form of PON1 to hydrolyze different oxon substrates depends on the specific substrate (Davis *et al.*, 2009; Richter and Furlong, 1999). To address this issue, variation in enzyme activity was determined in liver and plasma using CPF as a substrate (See Figures 8 and 10 in Section 2).

As described in Section 2, plasma samples were obtained from individuals ranging from 3 days to 43 years of age. Rates of diazoxon and paraoxon hydrolysis were used to resolve the plasma samples into three functional genotypes. Frequencies of functional genotypes were 0.5, 0.4, and 0.1 for QQ, QR, and RR phenotypes, respectively (Figure 28). The ability of these plasma samples to hydrolyze CPF-oxon was compared to their polymorphic identification. When CPF-oxon V_{max} values were paired with paraoxonase activities, QQ and QR functional phenotypes were clearly resolved, but RR was not

resolved from the QR phenotypes (Figure 28). These results are consistent with those presented by Albers *et al.*, (2010), who showed that changes in BuChE activity in workers following exposure to CPF are not dependent upon PON1 phenotype or CPF-oxonase activity.

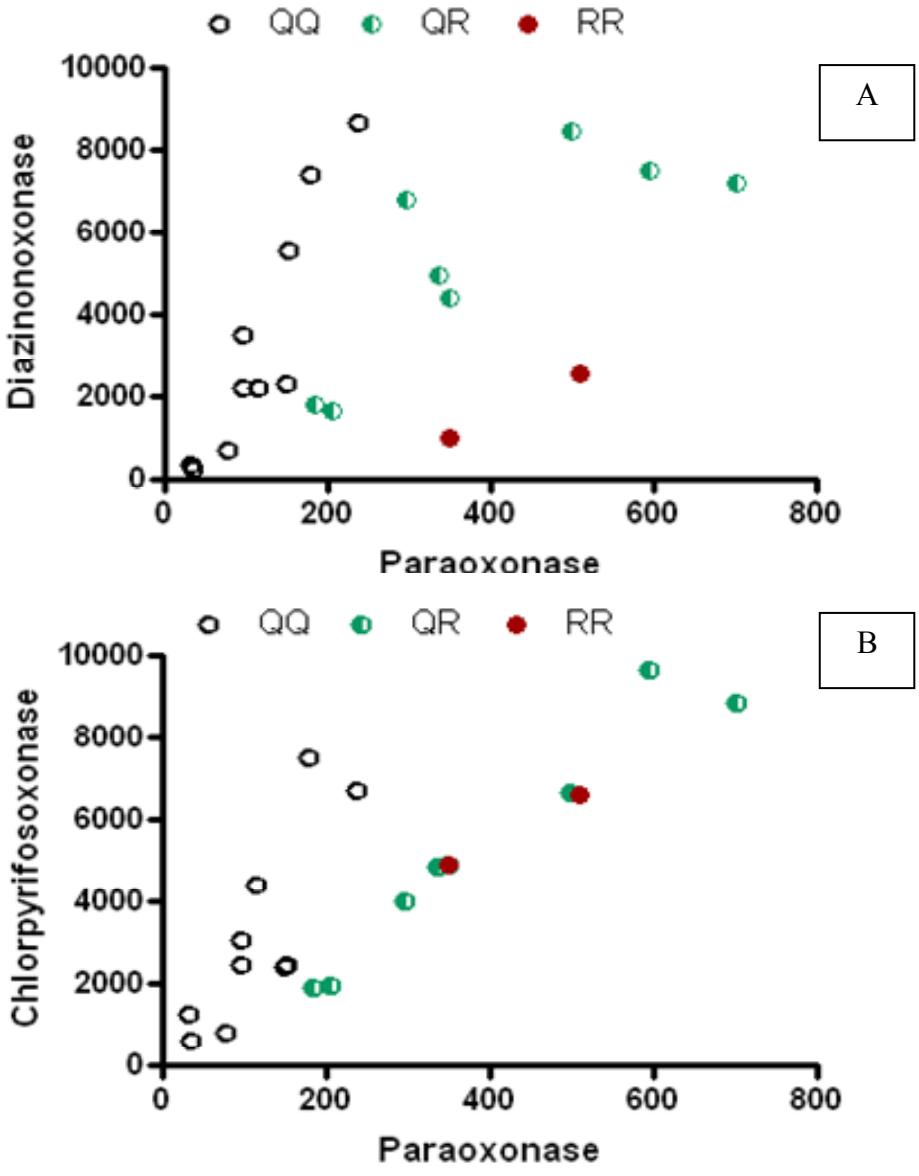

Figure 28. (A) PON1 phenotypes in human plasma samples from individuals aged 3 days to 43 years. (B) PON1 phenotypes (QQ, QR, RR) comparing CPF-oxonase vs. Paraoxonase in human plasma samples from individuals aged 3 days to 43 years.

Modeling variation in enzyme activity in liver

As discussed above, there is no indication of age-related differences in metabolic activity in the liver on a per mg protein basis, suggesting that ontogeny of enzymes that metabolize CPF occurs at a young age. The variations in activity levels of the three enzymes are modest, varying by approximately an order of magnitude (See Figures 6 and 8 in Section 2). The cumulative distribution of the observed levels of activity, presented as the Z-score of the V_{max} for the three enzymes are given in Figure 29. The lognormal distributions used in the Variation model to characterize the enzymes are also presented in Figure 29 (the three solid lines).

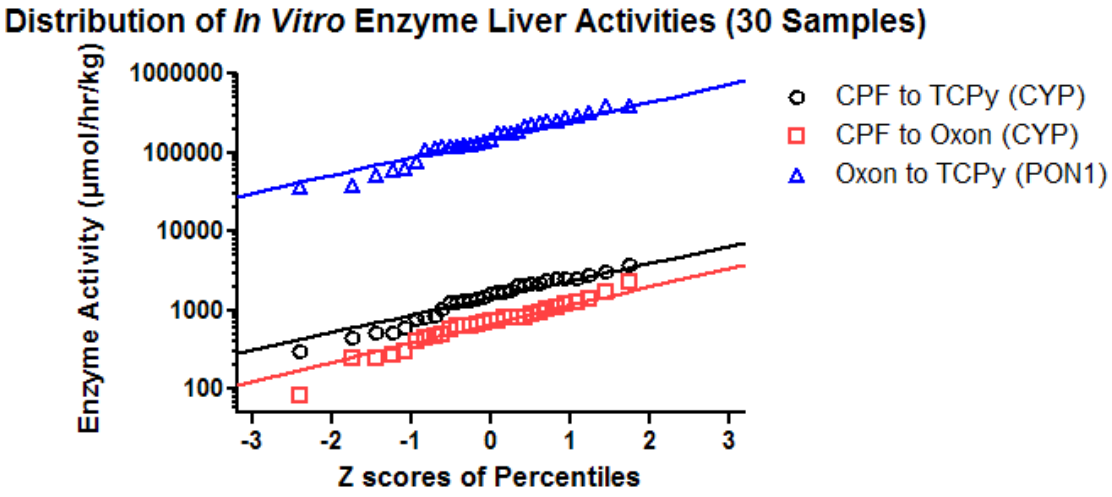

Figure 29. Distribution of *in vitro* enzyme liver activities for CYP (CPF to Oxon and TCPy) and PON1 (Oxon to TCPy). Data points represent measured *in vitro* values scaled to the standard adult. Lines represent the fitted lognormal distribution used in the Variation model. Note that the distribution is allowed to extend beyond the limits of the measured data.

There were a limited number of microsomal samples available from younger individuals. To address this limitation, the distributions of rates are allowed to exceed the observed range. For computational implementation, the lognormal mean and standard distribution are entered into the distribution functions in acslXtreme and used to calculate the tissue-based V_{max} for each individual. The values of Vmax are then multiplied by the tissue volumes (as is standard) to derive the *in vivo* rates (as previously described).

Modeling variation in plasma

The variation in the plasma PON1 is handled slightly differently than metabolic variability in the liver and brain. Since the plasma PON1 is produced in the liver and released into the plasma, the variability in the plasma PON1 can reasonably be expected to be correlated with the variability in the liver PON1 (i.e., individuals with high or low liver PON1 will have similarly high or low plasma PON1[6]). For the Variation model, the value of PON1 in plasma was rank correlated with the value in plasma for each individual[7]; The end result is that in the Variation model no simulated individual will be assigned a low PON 1 activity in liver (or plasma) and high activity level in the plasma. Thus an individual with low plasma PON1 will not be masked by having a high liver activity.

Figure 30 shows the range (mean ± 95% CI) for model output for plasma PON1 for three ages six months, three years, and 30 years. There three ranges are super-imposed over the PON1 data from the 20 plasma samples discussed in Section 2. The *in vitro* values in the original study (See Figure 10 in Section 2*)* have been converted to *in vivo* equivalents by multiplying them times average age specific protein levels and plasma volumes. As Figure 30 shows, the current ranges of plasma PON1 are consistent with, or exceed the range of the measured data.

6 While actual data on PON1 activity levels was measured in both plasma and liver the tissue samples did not come from the same individuals; therefore, it was not possible to directly determine correlation between the levels in the tissues.

7 A small additional variability was included in the plasma PON1 to allow for some interindividual variation in liver/plasma ratios. This additional variation was set to 5% of the mean value for the individual's age.

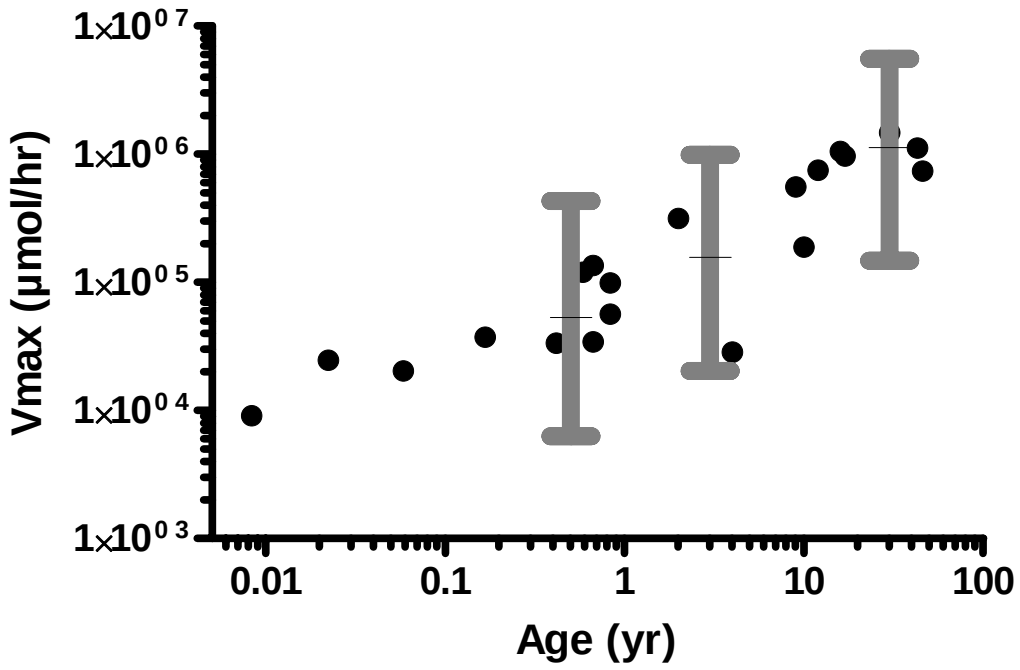

Figure 30. Total V_{max} of human enzymatic PON1 metabolism of CPF-oxon to TCPy in the plasma over various ages. Symbols represent *in vivo* rates extrapolated from the *in vitro* data (See Figure 10). Error bars show the 95% CI of Vmax values used in the model.

Modeling variation in the brain

There are no experimental data available to estimate the enzymatic variation in the brain. The variation in brain CYP450 levels was therefore assumed to have the same size of distribution as the corresponding liver CYP450s. The liver and brain CYP450 levels are not, however, correlated to each other in the simulated individuals.

Combination of enzyme and tissue volumes

As discussed in the LifeStage model development (Section 3), the final variability in the metabolic capacity of a simulated individual is a combination of the varied *in vitro* metabolic rate scaled with the individual's compartment volumes. In this manner, the ranges of the final metabolic capacity can be quite large (Figure 31). Infants (6 months old) have lower plasma PON1 than adults. In addition, the variation in metabolism in infants is

smaller than in adults (roughly 30-fold vs. 100-fold) due to the small interindividual variation in physiology (compartment volumes).

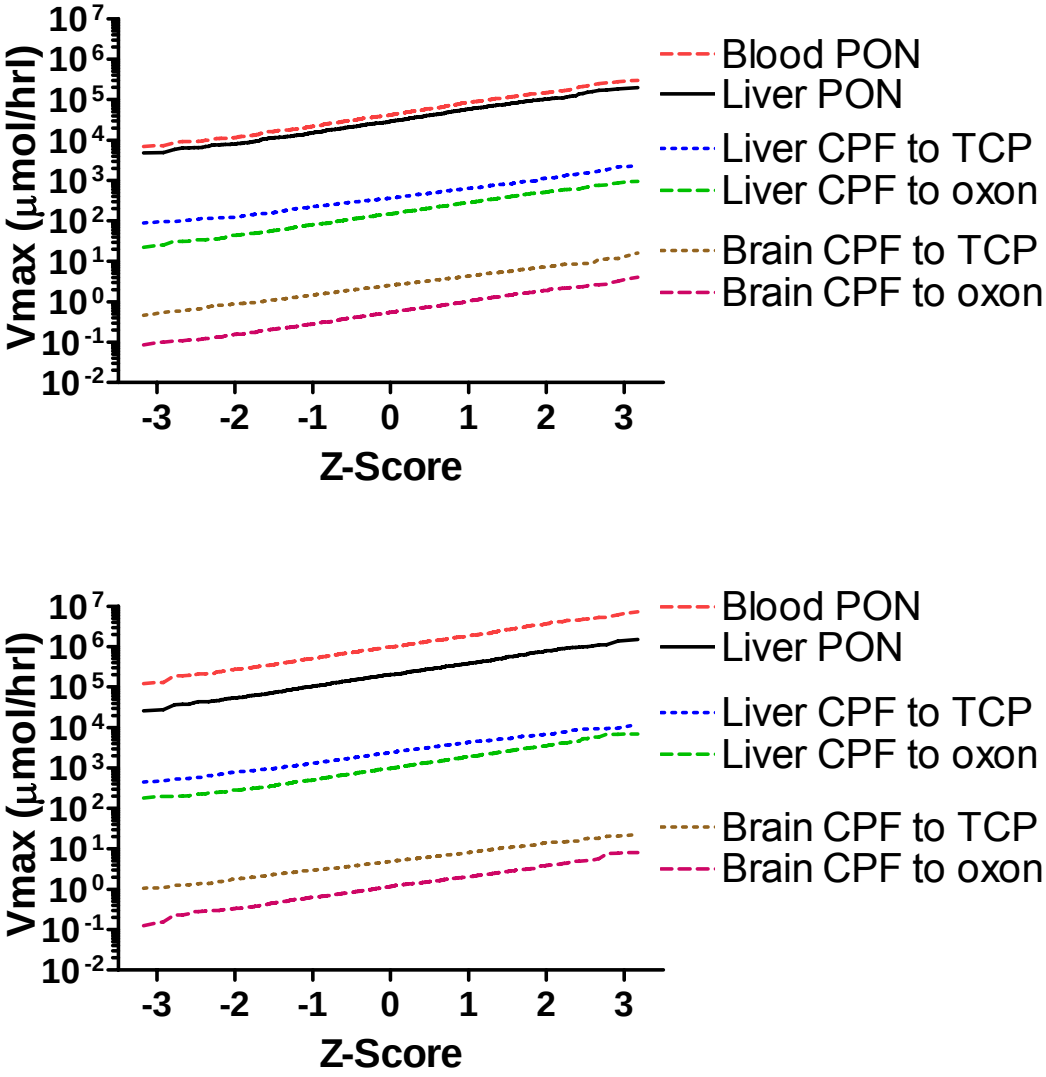

Figure 31. Variation *in vivo* metabolic rates in children (top) and adults (bottom). The range of the variation in metabolism can be inferred by comparing the ranges of the curves for the various enzymes.

Variation in Response to CPF and Ethnicity

Certain investigators have raised the issue of potential for ethnic variation in response (Davis et al., 2009; Ginsberg, 2010). This concern has been based on the

observation that the PON1 phenotypes exhibit differential distributions in different ethnic groups. The functional phenotype ratios reported for a Caucasian population was 0.6 for QQ, 0.31 for QR, and 0.07 for RR. The ratios for an African American population were; and 0.15 for QQ, 0.34 for QR, and 0.44 for RR (Davis et al., 2009). Ratios for Hispanics are 0.24 for QQ, 0.52 for QR, and 0.24 for RR (Huen et al., 2009; Huen et al., 2010). Although the distribution of each polymorphic expression may be different, this variation has limited impact on the variation in metabolism of CPF oxon. As shown in Figure 26 individuals in each of the three phenotypes have similar abilities to metabolize CPF-oxon. This finding is compound specific. As shown by (Ginsberg, 2010), polymorphic expression may be important for other compounds. Thus the issue of ethnic variation in metabolism should be evaluated when constructing source-to-outcome models for other compounds.

4.3 Step 3. Accounting for correlation

Based on body weight, the volume of each compartment is estimated using the equations in Table 2. As discussed above, these equations are polynomial functions that assign volumes to multiple compartments and organs. Since each equation for an individual is defined by a common body weight, the volumes are internally consistent (See Figures 13-18). This produces compartment volumes which are physiologically consistent.

The potential for correlation is also addressed when assigning metabolism rates. As was discussed in Step 2, plasma PON1 originates in the liver so it is modeled as rank correlated with the levels in the liver. Variations in CYPs are assumed to be genetically determined and activities in the brain are likely correlated to the levels in the liver. There are no experimental data available to estimate the enzymatic variation in the brain. The variation in the brain CYP450 levels was therefore assumed to have the same size of distribution as the corresponding liver CYP450s. The liver and brain CYP450 levels are not, however, correlated to each other in the simulated individuals.

Rates of CPF-oxon formation from CPF and its subsequent hydrolysis to TCPy were measured simultaneously from each donor liver sample. A correlation was observed between the metabolic rates of desulfurylation and oxon hydrolysis (Figure 9). However,

we could find neither a biological nor a literature basis for this correlation and thus conservatively varied the CYP-based desulfurylation and liver PON1 hydrolysis rates independently. This assumption is conservative because it allows combinations of enzyme levels that allow for high formation of the CPF-oxon and low removal rates.

4.4 *Step 4. Comparison of variation model's predictions to observed variation in human volunteer studies*

As discussed in Section 3, the LifeStage model predictions were compared to the mean responses in human volunteer studies (Figure 24). In this section we compare the *range* in responses predicted using the Variation model to the range of values reported in the (Kisicki *et al.*, 1999) study.

In the Kisicki *et al.* study, groups of healthy 12 adult volunteers were given single dietary exposures of 2.0, 1.0 and 0.5 mg/kg of chlorpyrifos. Figure 32 presents the ranges of the measured values using the black triangles and error bars determined in (Timchalk *et al.*, 2002a).

The Variation model was used to predict the range of the values of the blood measurements that would occur in each of the individuals in each group. Variation in the test individuals was simulated by modeling each individual in each dose group separately using data on the individuals' physiology and gender. To capture enzyme variability, each individual was simulated 100 times each time varying the levels of enzyme activities. The median values from each simulation for each time point over the five days are shown as the solid line in Figure 32 and the ranges of the 5-95th percentiles are presented in gray. As the figure shows, the simulations closely match the experimental data for blood levels of TCPy for all three doses. The model also predicts RBC AChE levels for doses of 0.5 and 1 mg/kg. The model overestimates the impact of CPF on RBC AChE by a factor of 2 to 3 for individuals exposed to 2 mg/kg.

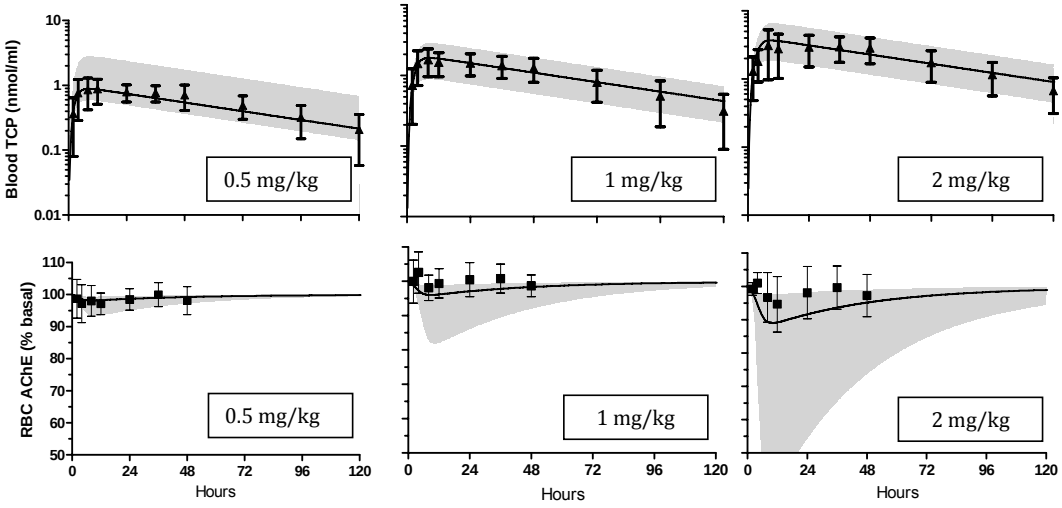

Figure 32. AChE inhibition and TCPy in blood in volunteers (Kisicki *et al.*, 1999) over time following a single oral dose of CPF. Triangles and error bars reflect actual data. Black line is mean predictions and gray area presents the 5th and 95 percentiles of predicted range of response for individuals over time from the Variation model.

4.5 Description of the Variation model

The LifeStage model produces a single estimate of response to one dose at any given age. The Variation model produces a range of responses to a single dose that reflect differences in physiology, metabolism, and activity levels. The Variation model requires that the modeler provide a series of inputs for each individual including age of the individual, gender, body weight, and doses on consecutive days. These inputs are described in Sections 5 and 6. Based on the age and gender, values are selected for each of the parameters described in Table 2 using the distributions and procedures described above. The Variation model then predicts the time course of blood concentrations of CPF and CPF-oxon, the inhibition of RBC and brain AChE inhibition, and plasma BChE inhibition (other tissue concentrations may be simulated but are not discussed here). If the same inputs are repeated, different values and different estimates of the output values are generated reflecting the range of responses associated with individuals of that age, gender, and body weight.

A copy of the Variation model is attached to this report (Attachment C).

4.6 *Applying the Variation model to the assessment of the toxicity of CPF*

In this section we have described the development of the Variation model and the evaluation of the model by comparison to the Kisicki *et al.* study. In the next two sections we use the model to investigate the toxicological properties of CPF in humans. This is done in two ways. First, the different sources of interindividual variation are systematically turned on and off, to identify those factors which drive variation in human sensitivity. Second, the Variation model is used to generate dose response relationships for different age groups that include human variation. The purpose of these assessments is to gain insight on human response to that would inform an actual risk assessment.

4.7 *Evaluating the contribution of the different sources of variation on human response to CPF*

One of the major interests in toxicology is human variation and its impact on the ability to tolerate chemical exposure. This section uses the Variation model to investigate the relationship between variation in physiology, enzymes, and level of physical activity. The goal is to determine which of these characteristics of humans has the greatest impact on the relative sensitivity of individuals.

Methodology

The relative importance of each source of variation was investigated by running the Variation model for a population of individuals of a specific age exposed to a single dose of CPF. The result is an age-specific measure of variation in human sensitivity. This approach is used to investigate the impact of different sources of variation on different endpoints, different doses, and for individuals of different ages. The approach was to systematically introduce distributions for the various characteristics in populations of different ages. The sources of variation were grouped as follows:

- Variation in level of physical activity;
- Variation in physiology;
- Variation in CYP enzymes in the liver and brain; and
- Variation of PON1 in the liver and the blood.

Preliminary work demonstrated that the relative contribution of the four groups of characteristics to the variation in RBC AChE increased in the following order for the four groups: PON1>CYP>Physiology>Physical Activity. The following six combinations of sources of variation were run for populations of 1,000 individuals:

1. Vary physical activity only
2. Vary physical activity plus physiological differences
3. Vary physical activity, physiology, and CYP enzymes
4. Vary physical activity, physiology, and CYP enzymes and PON1

Because PON1 was found to be the major source of variation in sensitivity for RBC inhibition, two additional analyses were performed; one where only liver PON1 was varied and a second where only liver and plasma PON1 are varied.

5. Vary PON1 in liver only
6. Vary PON1 in liver and plasma only

These six assessments were run at a number of doses including 1 mg/kg, 0.5 mg/kg, 0.1, and 0.001 mg/kg. Separate assessments were modeled for infants (six months), young children (ages 3 years) and adults (30 years). Variation in body weight and gender was determined by using data from the population generator in the CARES model (for additional information see the discussion in the section of this report on dietary modeling). When physiology was turned off (simulation run number 1) the mean body weight for females of each age group was used and the individual was assumed to be female.

The results of the simulations were analyzed as follows. First, the levels of either RBC or brain inhibition in each of the 1,000 individuals in each of the six simulations were ranked from smallest to largest. Second, the rank of each individual was used to assign a Z-score for that individual. Third, the relative impact of the dose on each individual compared to the impact on a "typical" individual in their age group was determined by dividing each individual's inhibition level by the inhibition observed in the median individual. These ratios represent a measure of relative sensitivity across the population. Finally, the cumulative distributions of the ratios were plotted against the Z-scores of the individuals. The results are six curves that show the impact of variation in different

characteristics on the relative sensitivity of a population of humans of a specific age to a specific dose of CPF.

Factors that drive variation in RBC AChE inhibition

The relative contributions of the variation in the four characteristics on relative sensitivity to CPF as measured by peak inhibition of RBC for the three age groups were examined at the point of the largest interindividual variation, using an oral dose of 0.5 mg/kg. Figure 33 present the curves for the six analyses. Note that the relative sensitivity is shown on log scale. At 0.5 mg/kg when all sources of variation are included, the range of peak inhibitions across the simulated individuals (from the most sensitive to the least sensitive of the 1,000 simulated adults) is about 100-fold. However, the most sensitive of the 1,000 individuals has an inhibition rate that is approximately 12-fold higher than the inhibition rate for the typical individual.

The contributions to variation in sensitivity from the different characteristics of the individuals are not the same. Variation in physical activity does not significantly contribute to variation in RBC inhibition. This is shown by the fact that the curve for physical activity alone is virtually flat. Adding variations in physiology and CYPs explains about one third of the variation in sensitivity. The largest change in sensitivity comes from the introduction of variation in PON1 levels in liver and plasma. This can be seen when variation in PON1 in liver and plasma are run alone (physiology, CYPs, and physical activity are held constant). As Figure 33 shows, the interindividual variation in RBC from the variation in PON1 in the liver and blood is almost as large as the variation observed when all sources are considered.

Finally, variations in plasma PON1 levels do not appear to drive variation in RBC response. Evidence of this lack of impact is shown in the fact that the results for varying "liver PON1 enzyme levels" and "liver PON1 plus plasma PON1 enzyme levels" are virtually identical.

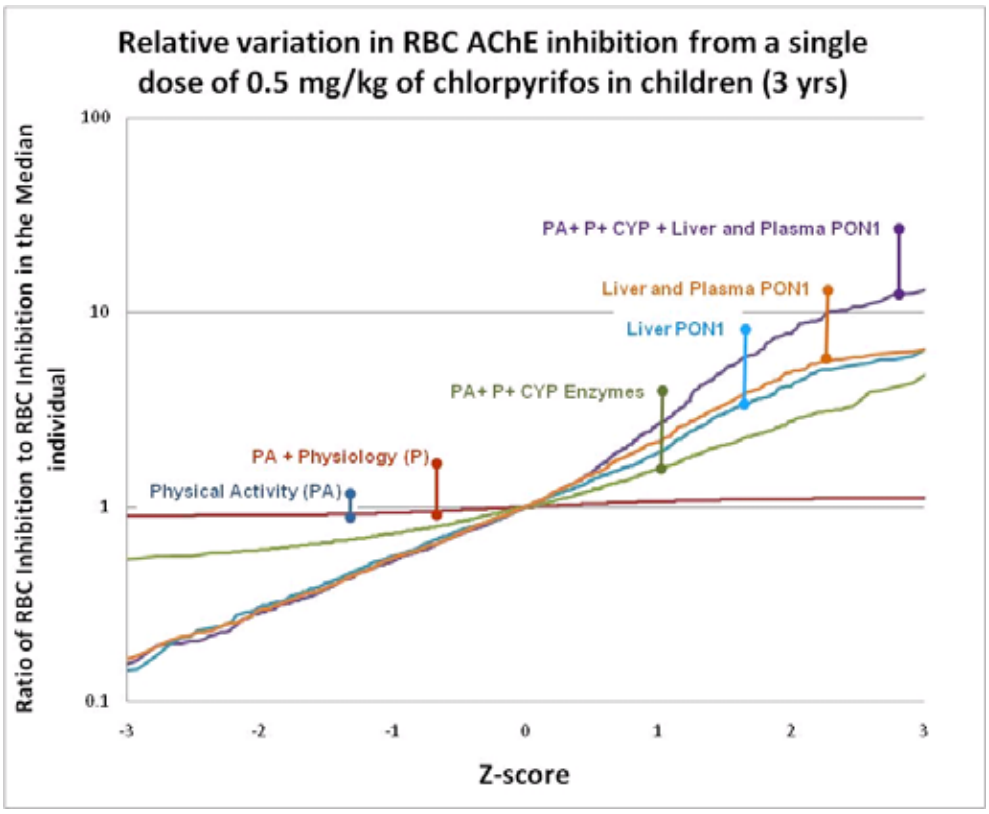

Figure 33. Six cumulative distributions of RBC Inhibition (relative to the median inhibition rate) in adults exposed to 0.5 mg/kg where variation in Physical Activity (PA), Physiology (P), liver and brain CYP Enzymes (CYP), and Liver and Plasma PON1 are "turned on" either alone or in combinations.

A review of the two younger ages shows a similar pattern (Figures 34 and 35). CYPs appear to play a slightly larger role and physiological variation a smaller role than in adults. However, liver PON1 variation is still the dominant source of variation in response.

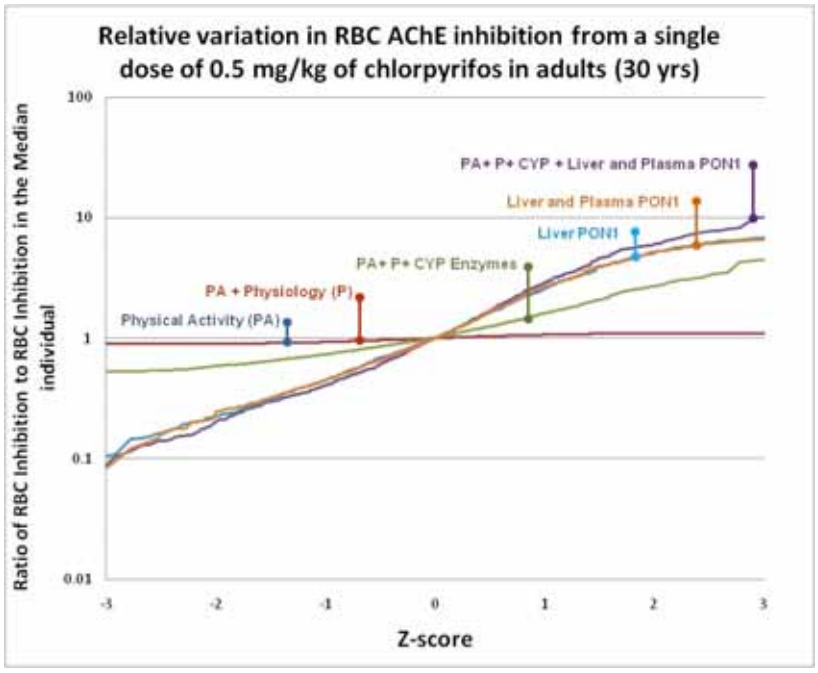

Figures 34. Six cumulative distributions of RBC Inhibition (relative to the median inhibition rate) in young children exposed to 0.5 mg/kg where variation in Physical Activity (PA), Physiology (P), liver and brain CYP Enzymes (CYP), and Liver and Plasma PON1 are "turned on" either alone or in combinations.

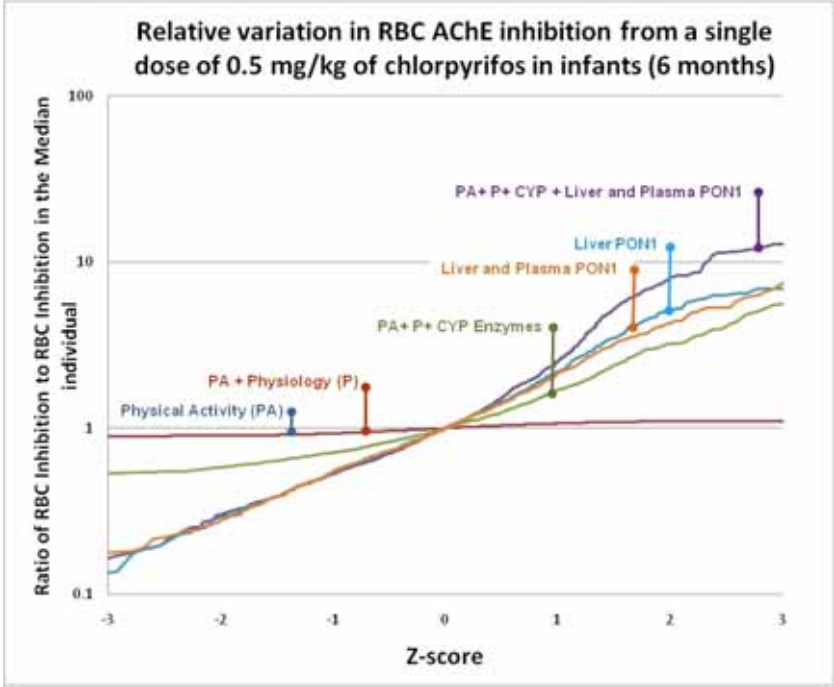

Figure 35. Six cumulative distributions of RBC Inhibition (relative to the median inhibition rate) in infants exposed to 0.5 mg/kg where variation in Physical Activity (PA), Physiology (P), liver and brain CYP Enzymes (CYP), and Liver and Plasma PON1 are "turned on" either alone or in combinations.

The impact of variation in an individual's characteristics at doses above 0.5 mg/kg were evaluated and found to be similar to those at 0.5 mg/kg (data not shown).

The contribution of variation in individual's characteristics on RBC AChE inhibition was investigated at lower doses, Figures 36, 37, and 38. Note these three figures are in arithmetic-scale (not-log scale as in Figures 33, 34, and 35). At a dose of 0.1 mg/kg per day, the level of variation was found to be significantly smaller than at 0.5 mg/kg. The total range in response (most sensitive to lease sensitive of the 1,000 individuals) when variation in all four groups of characteristics are considered dropped from 100 fold to 10 fold. The difference between the typical and the most sensitive of the simulated individuals when all sources of variation are considered dropped from 12 fold to 2-fold. The driver for the variation at these lower doses was the same, PON1 levels in liver. The same pattern of variation was observed for all three age groups. Finally this pattern of sensitivity remained constant at all lower doses evaluated including doses as low as 0.0001 mg/kg (data not shown).

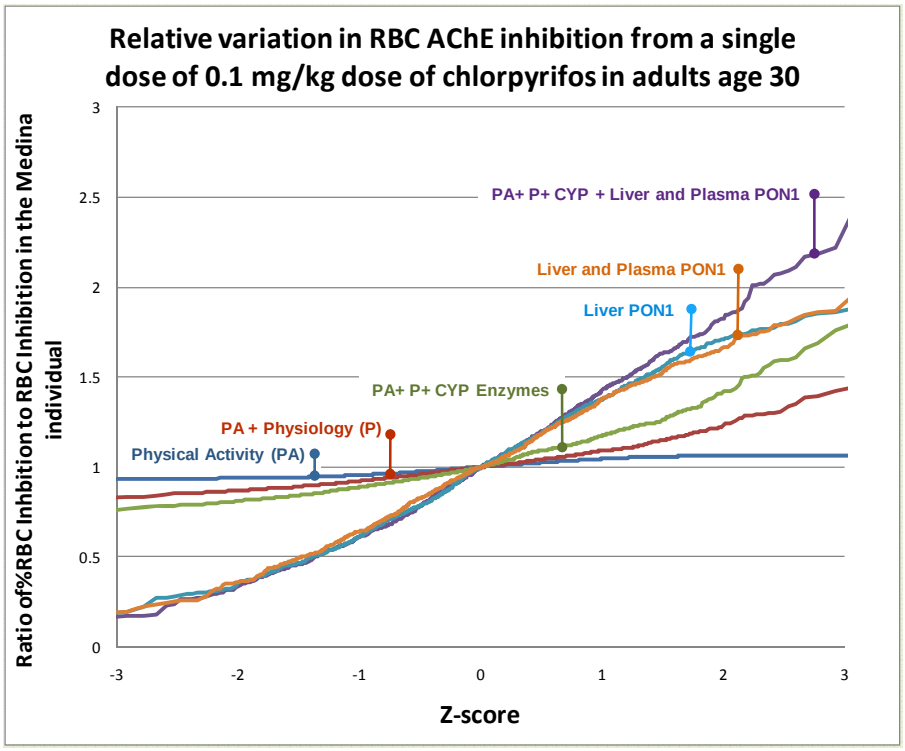

Figure 36. Six cumulative distributions of RBC Inhibition (relative to the median inhibition rate) in adults exposed to 0.1 mg/kg where variation in Physical Activity (PA), Physiology (P), liver and brain CYP Enzymes (CYP), and Liver and Plasma PON1 are either "turned on" alone or in combinations.

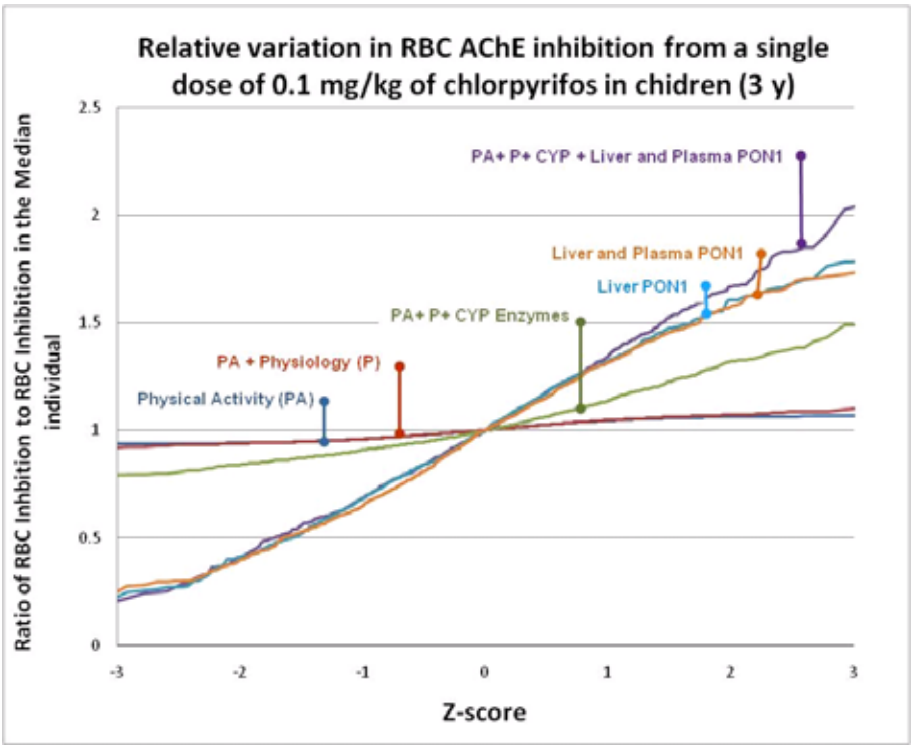

Figure 37. Six cumulative distributions of RBC Inhibition (relative to the median inhibition rate) in young children exposed to 0.1 mg/kg where variation in Physical Activity (PA), Physiology (P), liver and brain CYP Enzymes (CYP), and Liver and Plasma PON1 are either "turned on" alone or in combinations.

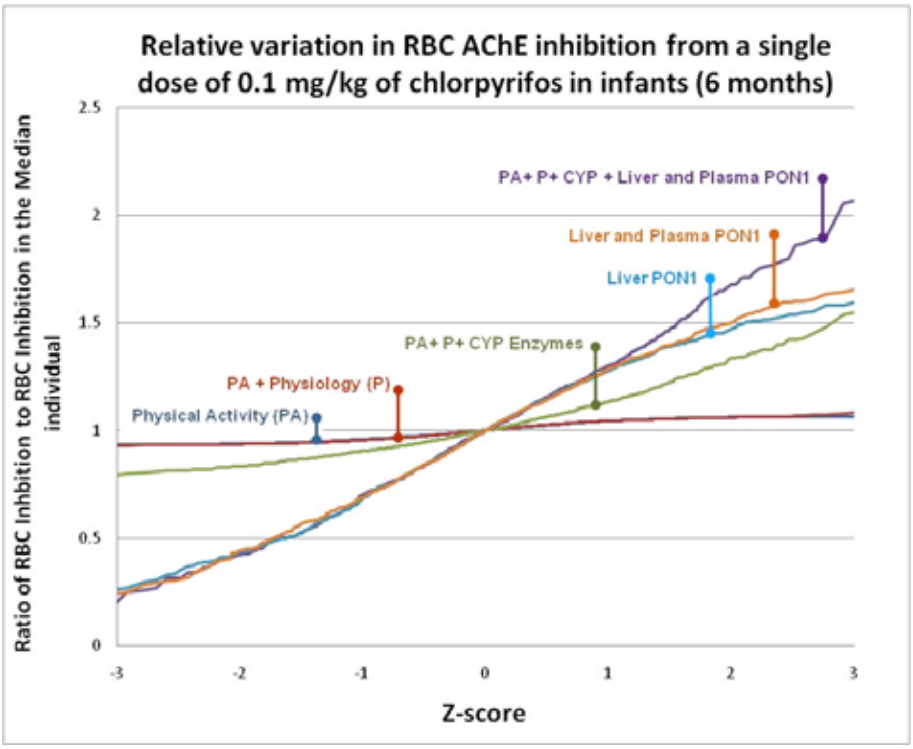

Figure 38. Six cumulative distributions of RBC Inhibition (relative to the median inhibition rate) in infants exposed to 0.1 mg/kg where variation in Physical Activity (PA), Physiology (P), liver and brain CYP Enzymes (CYP), and Liver and Plasma PON1 are either "turned on" alone or in combinations.

Evaluation of the factors that drive variation in the level of brain AChE inhibition

For brain AChE inhibition, the same ages and grouping of sources of variation were used. In general, the range of variation was similar to that of RBC AChE inhibition at 0.5 mg/kg, with the most sensitive individual having about an 8-fold increase in response compared to the median individual. However, the driver for the variation was different. The variation in brain inhibition across populations at all ages and at doses of 0.1, 0.5, and 1.0 mg/kg doses was driven entirely by variation in CYPs in the liver and the brain (Figure 39). Future work should focus on the relative impact of the different CYPs in the different organs.

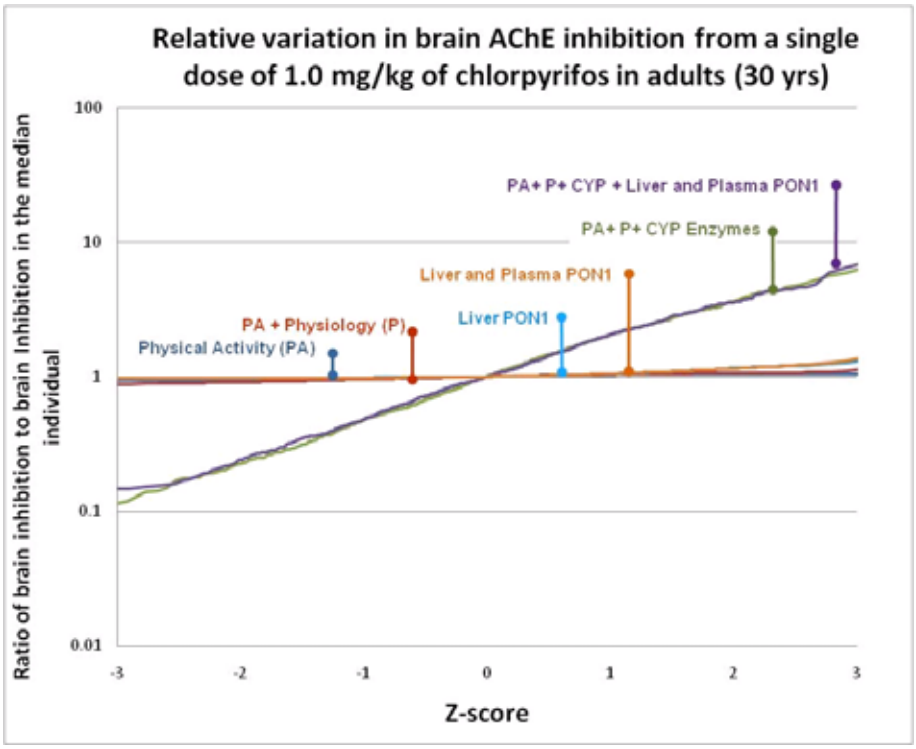

Figure 39. Six cumulative distributions of brain inhibition (relative to the median inhibition rate) in adults where variation in Physical Activity (PA), Physiology (P), liver and brain CYP Enzymes (CYP), and Liver and Plasma PON1 are either "turned on" alone or in combinations. The figures for the other ages and doses are similar (data not shown).

These analyses are not meant to be exhaustive investigations into CPF. Rather they demonstrate how the Variation model and future versions for other compounds could be used to identify those factors that are most important to investigate when modeling interindividual uncertainty in response. Based on these findings for CPF, interindividual variation in response to CPF is driven by variation in metabolism and is only slightly affected by differences in physiology and level of physical activity. Thus, future work on refining estimates of outcome should focus on the improvement of estimates of interindividual variation in metabolism rather than attempting to refine estimates of variation in physical activity levels or physiology.

These finding can also be used to determine the reasonableness of the behavior of the Variation model. The impact of variation in physiology is predicted to be smaller for

infants than adults. This appears reasonable since adults have higher variations in weight than infants and thus physiology would be more important for adults. The fact that the level of physical activity had little or no effect on sensitivity appears to be reasonable given the finding that blood flow to the liver and brain are relatively unaffected by increase levels of physical activity (see Table 4).

4.8 Interindividual variation in response- predictions by the Variation model

The Variation model created using the previously described distributions can generate dose response predictions for any of the model outputs such as blood concentrations of CPF and CPF-oxon and RBC or brain AChE inhibition. Separate predictions can also be made for groups of various ages. Unlike the single curve produced by the Lifestage model, the Variation model produces a fuzzy "band" or "cloud" that reflects the interindividual variation in response to a given dose. The size of the variation at a specific dose is determined by a vertical distance across the cloud at that dose.

To examine the model's predictions of peak CPF and peak CPF-oxon blood concentrations, populations of 5,000 individual adults (30 years) and infants (6 months) with varying body weights and similar numbers of both genders were modeled as receiving a single oral dose where the dose rate ranged between 0.01 and 10 mg/kg (Figure 40)[8].

8 Data for children age three were also calculated and fell between the infants and adults. These data were not included in the figure for clarity.

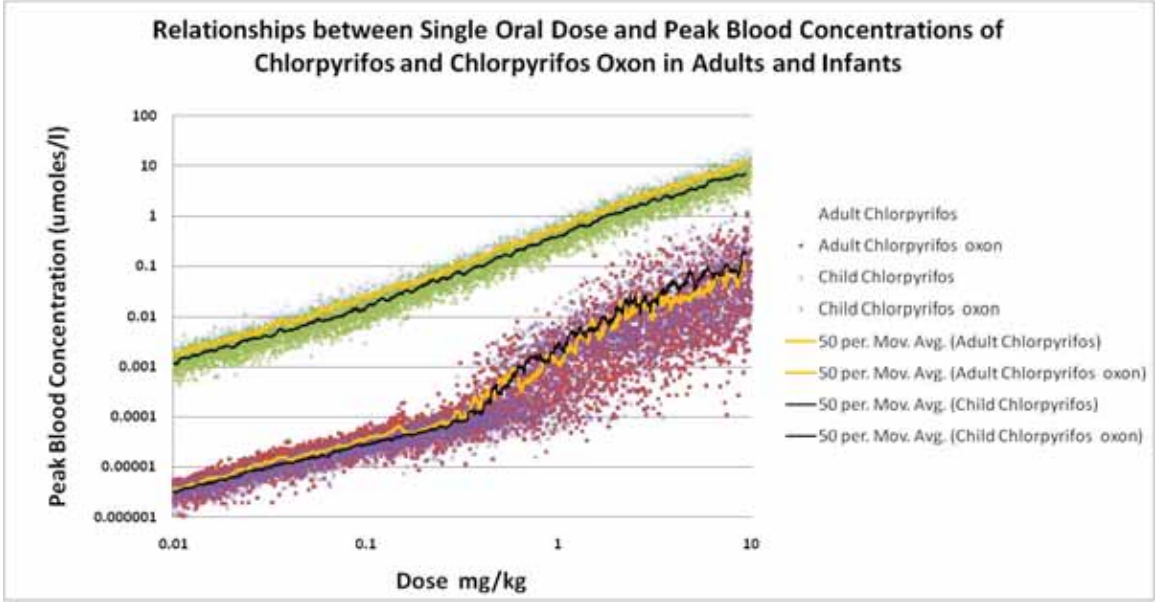

Figure 40. Peak blood concentrations of CPF and CPF-oxon following single oral doses that range between 0.01 and 10 mg/kg (log-log plot). 5,000 individual adults (30 years) and infants (6 months) with varying body weights and similar numbers of both genders are modeled.

The relationship between oral dose and the peak blood concentration of CPF increases in a consistent, but non-linear fashion over this range of doses[9]. The constant width of the cloud around CPF suggests that the processes that drive interindividual variation in levels of CPF in blood are not dose-dependent for this dose range. Finally, the predicted peak doses of CPF are slightly higher for adults than children as seen by comparing the moving averages for the two age groups (Figure 40).

The results for the peak CPF-oxon are different from CPF. A visual inspection of Figure 40 indicates that at doses below 0.3 mg/kg, the oxon appears to be a consistent fraction of the CPF peak concentrations. Interindividual variations at doses below 0.3 mg/kg have a consistent width that is similar to, but slightly larger than, the width of the CPF blood concentration cloud. Above 0.3 mg/kg, the ratio of peak concentrations to oral dose become more variable and the ratios increase by a factor of 20 for adults and 40 for

9 The slope appears to be linear due to the log-log plot but actually indicates a sub-linear relationship between the peak levels and the dose. This can be seen from the approximately 4 orders of magnitude decline in peak levels of blood CPF over the 3 orders of magnitude change in dose.

infants. In addition, at doses above 0.3 mg/kg, infants have higher peak levels of oxon than adults at the same doses.

This suggests that the balance of CPF metabolism changes above doses of 0.3 mg/kg for both adults and infants and that variation PON1 and CYP in the liver activity becomes more important above this dose. Additional evidence for this point is given in the discussions of the importance of PON1 variation on AChE inhibition in Section 2. Additionally, while the data are not shown, the pattern of interindividual variations in CPF and CPF-oxon between 0.3 and 0.01 mg/kg were found to apply to doses below 0.01 mg/kg. This includes the range of doses that result from current dietary exposures (see Sections 5 and 9). Finally, the fraction of the oral dose of CPF converted to CPF-oxon is predicted to increase slightly in an age-related manner.

A comparison of the dose-response predictions for peak RBC and brain AChE inhibition for adults and infants for the Variation and LifeStage models shows behavior similar to the predictions of peak levels of oxon in blood (Figure 41). The same increase in variability occurs at 0.3 mg/kg and infants become more sensitive at that dose. This is not surprising since the oxon directly complexes with RBC AChE.

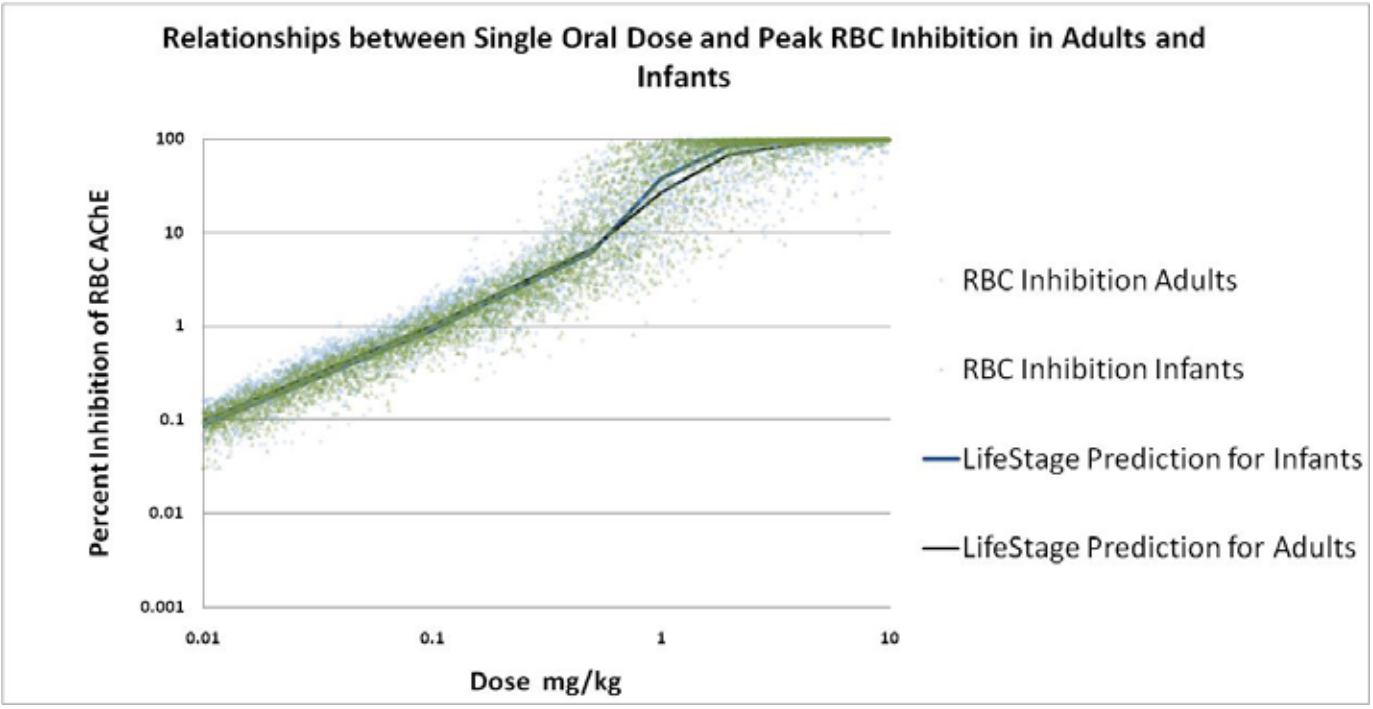

Figure 41. Peak blood RBC AChE inhibition following single oral doses that range between 0.01 and 10 mg/kg (log-log plot). 5,000 individual adults (30 years) and infants (6 months) with varying body weights and similar numbers of both genders are modeled with the Variation model. The lines represent the typical 30 year-old and 6 month-old from the LifeStage model.

In contrast, the variation in prediction of the inhibition of brain AChE is similar to the predictions of peak CPF concentrations (Figure 42). There is no sharp change in interindividual variation at 0.3 mg/kg, with adults always appearing to be slightly more sensitive than infants. One difference is that width of the cloud is larger than the width of the peak CPF.

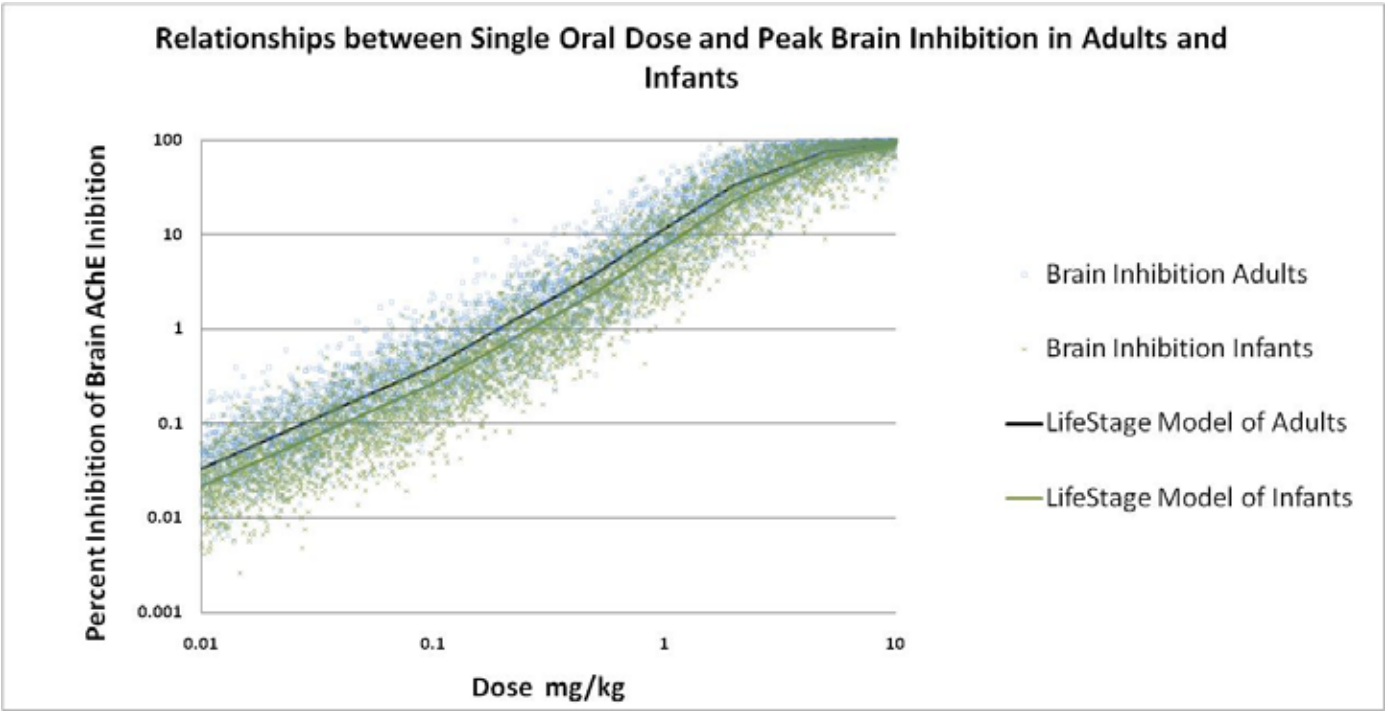

Figure 42. Peak blood brain AChE inhibition following single oral doses that range between 0.01 and 10 mg/kg (log-log plot). 5,000 individual adults (30 years) and infants (6 months) with varying body weights and similar numbers of both genders are modeled with the Variation model. The lines represent the typical 30 year-old and 6 month-old from the LifeStage model.

Section summary

This section has presented the development of the Variation model and its evaluation by comparison to the results of the human volunteer studies. The model's predictions of interindividual variation were either consistent or over estimated the observed variations in small groups of healthy volunteers.

This section provides two examples by which a Variation model of PBPK/PD can be used in the assessment of a pesticide and possible responses to exposure. The section demonstrated how a model can be used to identify the drivers of a populations' relative sensitivity to a chemical's effects. For example, RBC and brain AChE inhibition by CPF were driven by variation in metabolism and not physiology or levels of physical activity. Variation in RBC inhibition was driven by variation in liver but not plasma PON1 activity.

Variation in brain inhibition was not affected by PON1 but was affected by variation in CYP activities in the liver and the brain. Such findings could help researchers identify issues where additional research is warranted. The Variation model also indicates that variation in RBC inhibition is strongly dose dependent. Variation across individuals ranges from 100-fold at doses above 0.3 mg/kg but drops to 4-fold for dose at below 0.3 mg/kg. This finding allows a better understanding of differences in sensitivity at low doses. In contrast, the variation in brain inhibition was not dose dependent.

5. Modeling variation in dietary exposure for different age groups

Section overview

This section presents a review of the current approaches to assess dietary exposures. The section describes the collection and organization of residue data and the software used to characterize dietary exposures. The issue of longitudinal dietary exposure is investigated and estimates of correlations between an individual's doses of CPF on two consecutive days are determined using three different methods of simulating longitudinal dietary exposures.

5.1 Dietary exposure assessments

The Agency uses a probabilistic approach to characterize interindividual variation in dietary exposures. The dietary exposure software programs originally focused on estimating interindividual variation in doses that occurred on a single day. Over the last 10 years, however, program developers have sought to assess longitudinal dietary exposures as well. There are a number of dietary exposure programs available or currently under development (CARES, LifeLine, DEEM^{TM}, and SHEDS). All of these programs use similar approaches for estimating dietary exposures. Software comparison exercises have shown that dietary exposure software programs (CARES, LifeLine and DEEM^{TM} (U.S. EPA, 2004) and DEEM^{TM} and SHEDS (Xue, 2010)) produce similar estimates of the distribution of single-day doses in various age groups.

This assessment uses the CARES software for the exposure portion of the source-to-outcome model. CARES is a software program designed to conduct complex exposure and risk assessments for pesticides. Scientific and technical contributions to the program's development came from a broad team of experts, including scientists from Crop Life America member companies and staff, consulting companies, and the Environmental Protection Agency and Department of Agriculture. CARES is available without charge

from the ILSI Research Foundation.[10] CARES, has been reviewed by the Science Advisory Panel (U.S. EPA 2002[11]) and is used in regulatory decisions by the Agency.

The CARES dietary software was used a number of ways in this project. The program was used to produce estimates of daily doses over multiple consecutive days that form the basis for the predictions of the impact of the current dietary exposures on levels of cholinesterase inhibition (Section 9). The program also was used to produce longer exposure histories (365 days) that are used in the analysis of the upper peak exposures in the general population (Section 8). Finally the program was used to assign gender and body weights to the populations of individuals assessed using the Variation PBPK/PD model (Section 4).

Dietary exposure software programs depend on input estimates of residues of CPF on different foods as a result of crop protection. The values used in this demonstration were developed using general EPA policies for use of residue data in dietary risk assessments and regulation of pesticides. The input files were built up from EPA's reregistration-era (1999 – 2002) dietary assessments for chlorpyrifos as well as the comprehensive listing of tolerances announced by EPA *via* the CFR Final Rule in 2008 and include new monitoring data through 2008 as posted by USDA in late 2009 and updated percent crop treated (PCT) data. USFDA monitoring data for a few commodities are also incorporated. A parsing of the dietary exposure between imports and domestic observations was made for several key crops. The dietary files were built using the recent DEEM software version 2.16. Over 70 individual residue files (RDF) were built; most were created from the newer monitoring data, although a few were reused from the reregistration-era assessment conducted by EPA in 2000. Decisions for the inclusion or exclusion of specific information reflect general guidance for a higher tiered regulatory exposure assessment. Attachment D provides a detailed description of the data used in developing these inputs and the specific assumptions used to analyze the data.

10 Electronic copies of the program and support documentation are publicly available at no charge at HTTP://www.ilsi.org/ResearchFoundation/Pages/CARES.aspx.

11 http://www.epa.gov/oscpmont/sap/meetings/2002/april/agenda.htm

The residue data was entered into three dietary exposure software programs, CARES, DEEM™ version 2.16 (Durango Software, 2010) and LifeLine version 4.40 (LifeLine, 2006). Electronic copies of the input files for the three software programs are provided in Attachment E.

5.2 *Results of the dietary exposure modeling prediction of daily doses*

The cumulative distributions of daily doses of CPF created using CARES for 1,000 adults, three year-old children, and six month-old infants are given in Figure 43. The dietary doses (on a body weight basis) are larger for the three years-olds than either adults or infants. The data in Figure 43 are plotted on a dose versus Z-score. The Z-scores reflect that portion of the population from the 3rd to 97th percentile. None of the individuals is predicted to have a one day dose greater than 0.0002 mg/kg.

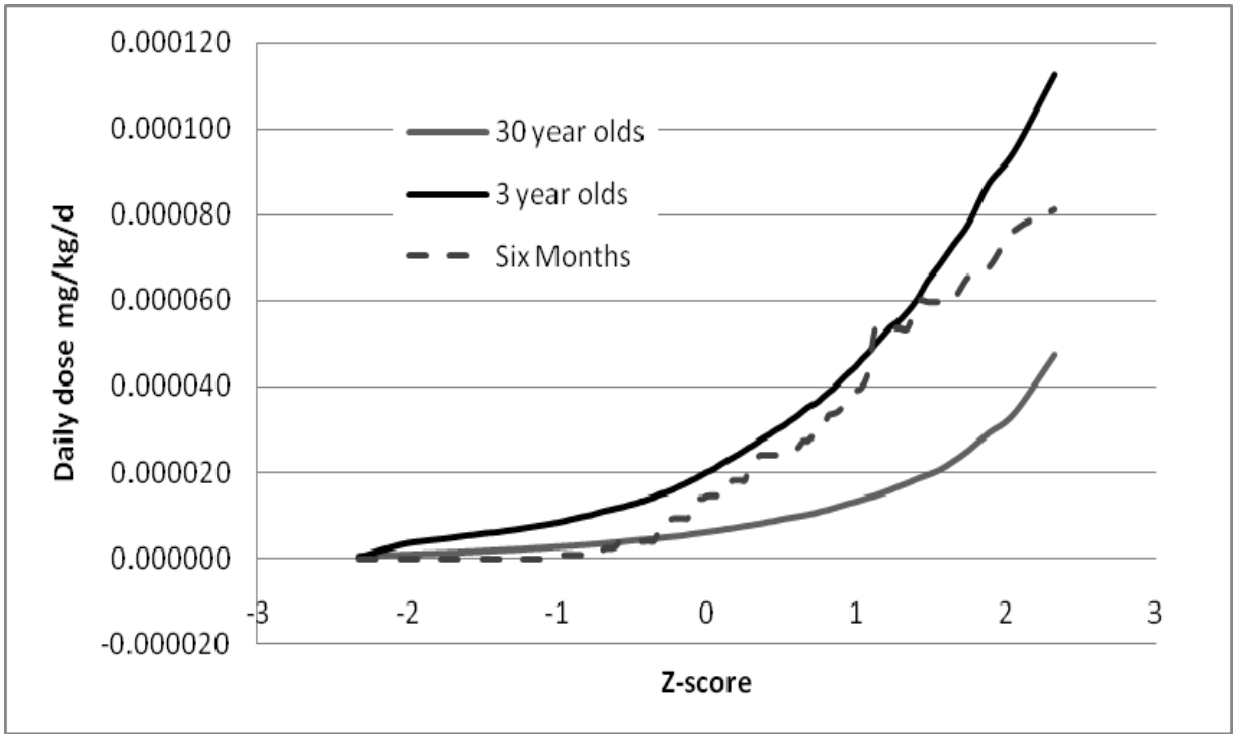

Figure 43. Predicted distribution of daily dietary doses of CPF in 1,000 adults, 3 year-old children, and six month old infants from the CARES program using the assessment of dietary residues given in Attachment D

The predictions of dietary exposure produced by CARES were compared with the predictions of DEEM™ version 2.16 (Durango Software, 2010) and LifeLine version 4.40 (LifeLine, 2006)(Table 5). The predictions of the variation in daily doses in the top 10 percent of the U.S. population of adults, children, and infants are similar for all three programs. The findings increase the confidence that the data have been entered into the CARES program correctly and indicate that the predictions reflect the current data on residues and U.S. diets.

Table 5. Estimates of CPF Daily Dietary Intake for Three Percentiles of the Cumulative Distributions of Three age groups in the U.S. Population (mg/kg)

	DEEM ™(Version 2.16)	LifeLine (Version 4.1)	CARES (Version 3.0)
Adults			
90th Percentile	0.000010	0.000010	0.000017
99th Percentile	0.000034	0.000026	0.000047
99.9th Percentile	0.00015	0.000045	0.00012
Children 3 year-olds			
90th Percentile	0.000033	0.000031	0.000055
99th Percentile	0.000093	0.000083	0.000113
99.9th Percentile	0.00022	0.00014	0.00021
Infants (6 months)			
90th Percentile	0.000043	0.000027	0.000054
99th Percentile	0.000086	0.000075	0.000081
99.9th Percentile	0.00021	0.00011	0.00020

CARES is also used to generate estimates of body weight for different ages. Table 6 presents the values of body weight generated by the CARES and LifeLine dietary exposure programs. As the table indicates, both programs predict values that are consistent with the results from the NHANES 1999-2000 survey.

Table 6. Body weight predictions from dietary programs and national survey results

	Infant Body weights Age 6 Month (kg)			Children Body weights Age 3 yr (kg)			Adults Body Weights Age 30 yr (kg)		
Percentile	**10th**	**50th**	**90th**	**10th**	**50th**	**90th**	**10th**	**50th**	**90th**
NHANES (1999-2000) [1]	7	8	10	13	16	18	59	80	107
LifeLine	7	8	9	13	15	17	44	62	91
CARES	6	7	9	13	16	19	54	76	100

[1](McDowell, 2005)

5.3 Simulating longitudinal exposures

Longitudinal dietary exposure is an issue for source-to-outcome models since the effects of one day's exposures carry across to subsequent days. However, current surveys of dietary intake do not collect data on food consumption on contiguous days. As a result, dietary programs are required to make assumptions on how to simulate temporal relationships between dietary intakes in an individual. Multiple approaches have been proposed for constructing longitudinal dietary histories for individuals based on the available data (Crop Life America, 2002; LifeLine, 2006; Xue, 2010). There is no consensus on which of these approaches should be preferred or the level of uncertainty that is introduced by the use of such approaches.

For this project we investigated the impact of the use of different simulation approaches for characterizing longitudinal exposures. Both the CARES and LifeLine dietary exposures software produce longitudinal estimates of dietary doses for individuals. LifeLine estimates an individual's dietary doses for up to 5 sequential days using two options for simulating longitudinal exposures - a daily and a seasonal approach. The daily approach selects a separate dietary record from multiple individuals to create a longitudinal record of a person. The seasonal approach selects two records for each of the four seasons. The records are selected from individuals of a similar age and from the same season of the year. The records are repeated, the first one for 2 days (representing the week end days) and the second for 5 days (representing the week days). This pattern is repeated multiple times to complete a season, and new records are selected for the next season. This approach was later adopted by SHEDs as one of its options (the eight record approach) (Xue, 2010). The seasonal approach results in a smaller longitudinal variation in dose than

the LifeLine daily model since the same records are often repeated for multiple consecutive days. CARES produces sequential daily estimates for periods of up to one year. CARES uses a statistical technique for identifying demographic and anthropometric records that come from individuals with statistically similar characteristics. Using this technique, the creators of CARES constructed 365 day dietary histories for a set of simulated individuals (Crop Life America, 2002).

Longitudinal dietary exposures were created for each of the three approaches. Estimates of doses on two consecutive days were determined for 1,000 adults. The correlation between the doses of CPF received on two consecutive days under each approach was evaluated. Figure 44 presents a scatter plot of individual's doses on day one versus their dose on day two. The doses are plotted on a log-log scale. A simple trend line was created in Excel using a power function. The slope and R^2 of the trend line are also given on the plots.

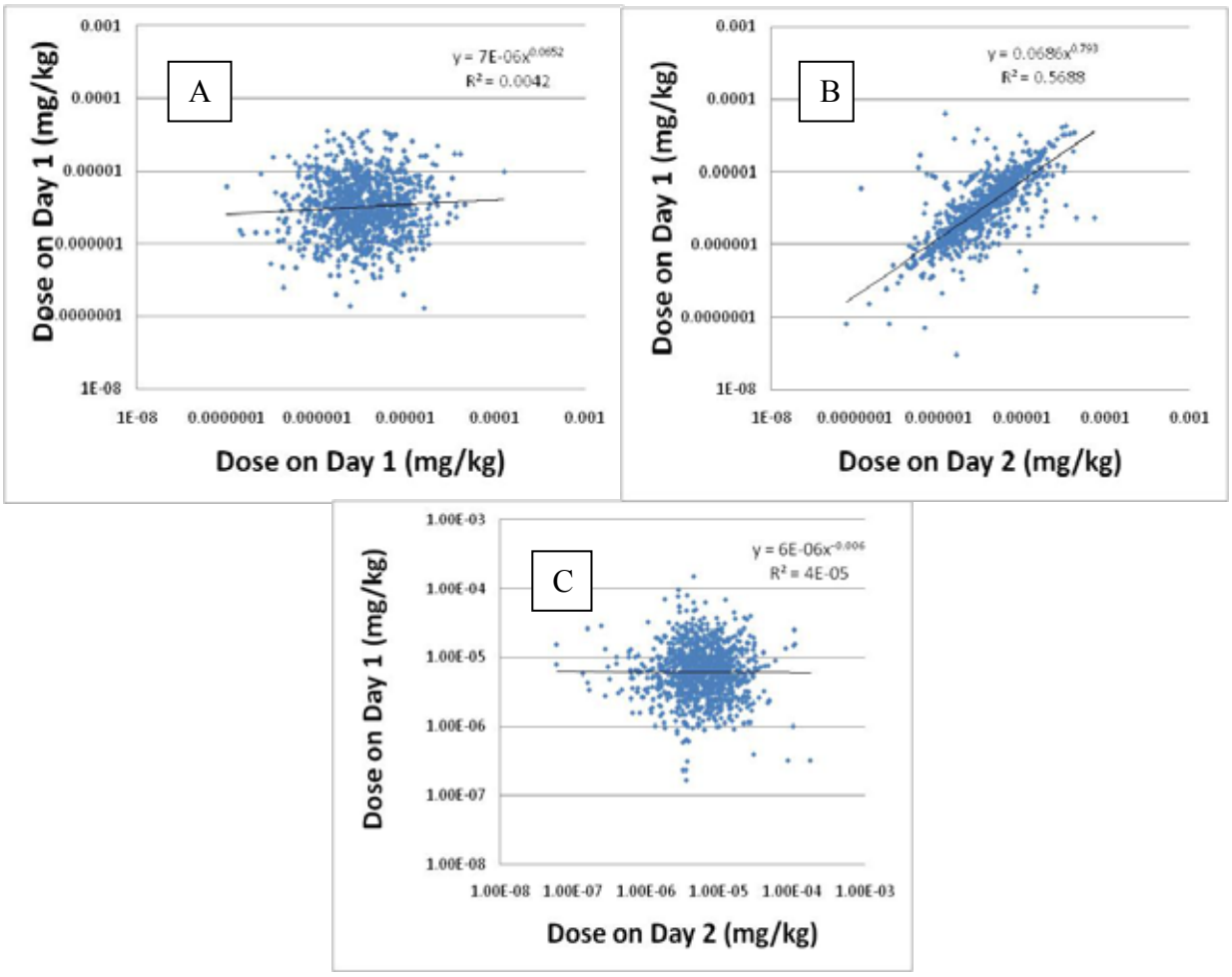

Figure. 44 Correlation between daily doses on consecutive days under A- LifeLine Daily approach, B- LifeLine Seasonal approach, and C- CARES approach.

As Figure 44 indicates, the three approaches of longitudinal exposures produce different correlations between consecutive days. The Lifeline daily approach (A) and the CARES (C) approach essentially make each day's dose independent of the prior day. The LifeLine seasonal approach produces estimates of dose with a moderate correlation between days (R^2 of 0.57). This correlation occurs because in the LifeLine seasonal approach, the majority of individuals are assumed to eat the same foods in the same amounts on consecutive days. Because none of the approaches correlate residues from one day to the next (the concentration of the residue on an apple consumed on one day is assumed to be independent of the residue on an apple consumed the following day), none of the approaches predict the occurrence of identical doses on consecutive days. The impacts of the three sets of longitudinal data are presented in Section 7 of this document.

Section summary

Dietary exposures for CPF are defined by the residue data and the software programs available for dietary exposure assessment. The estimates of daily dose predicted by multiple software programs produce similar results. However, different longitudinal approaches predict different correlations between doses on consecutive days.

6. Connection of exposure and PBPK/PD models

Section overview

Up to this point we have described the development of the two components of the source-to-outcome model, a dietary exposure software program (Section 5) and the Variation PBPK/PD model (Section 4). This section now addresses the linking of the two components. The linkage of the two components raises technical issues on the definition of the individual's characteristics and the definition of dose. Specifically, the components need to have consistent definitions of the individual and establish a clear process for converting the oral doses from the dietary exposure model into the dose information used by the PBPK model (LifeLine, 2004). This process must account for the absorption and uptake process.

6.1 Assigning characteristics to each individual

The approach used to link the two components' definition of 'individual' was to use an individual's demographic and anthropometric characteristics as defined by the CARES model and incorporate that data into the PBPK model. As discussed in Section 5, the CARES model defines the age, gender and bodyweight of each individual (ILSI, 2009). These data are taken from the 2000 Public Use Microdata Sample released by the U.S. Census Bureau (Crop Life America, 2002). The Variation model used this information to develop the detailed physiology required by the PBPK/PD simulations. This detailed physiology includes definition of the volumes of the key compartments, including liver and adipose tissues, compartment and organ specific blood flows, and total cardiac output (see Sections 3 and 4). This approach leverages the fact that the CARES model determines the individual's characteristics by taking data from one individual. As shown in Section 5, the predictions are representative of the U.S. population on a national basis. This approach gives a statistically representative set of internally consistent physiological data for each of the simulated individuals.

6.2 *Definition of dose in the source-to-outcome model*

The output of the dietary models has historically been an estimate of the total daily dose received from all foods consumed in a day. The reason for this is that the modeling results were compared to measures of toxicity, such as Reference Doses, that are expressed in units of daily dose per kg body weight (mg/kg). The oral uptake portion of the PBPK model converts the daily dose per kg body weight into a rate of CPF uptake from the gut over time in units of mass per time (μmoles/sec, see Figure 11 in Section 3). The development of the oral uptake portion of the model was performed using the following assumptions.

1. PBPK models have the ability to address doses that are consumed over the course of a day. Considerable effort has been made to capture this variation in dose over a day in dietary models. Recent versions of CARES[12] and SHEDS (Xue, 2010) include the ability to assign times of the day for different eating events (eating occasions). The source-to-outcome model for CPF, however, has not attempted to account for the impact of the daily doses being spread over multiple eating events. Instead the source-to-outcome model assumes that an entire day's dose occurs during a single meal. The reasons for this assumption are threefold.

   First, we investigated the fraction of the daily dose that comes from various foods. This analysis suggests that daily exposures are not evenly spread across eating events (meals and snacks) of a day. Instead, most, or all, of a day's intake of CPF occurs from the consumption of a specific type of food (e.g. a fruit or vegetable). Specifically, the analysis of the CARES model outputs suggest that on average 43% of an individual's daily dose comes from the consumption of a single food. For those individuals with daily doses in the top 2% of the population, this fraction increases to 75%. Thus, the assumption that the entire dose occurs at one meal does not appear to be unreasonable for CPF. This may not be true for other chemicals.

12 http://www.ilsi.org/ResearchFoundation/Pages/CARES.aspx

Second, use of a single daily dose greatly simplifies size and complexity of the information that is passed to the PBPK/PD model.

Finally the assumption is conservative. Assuming that the entire days' dose occurs in one dose increases the estimate of peak blood concentrations of CPF and peak inhibition since the dose is not spread over multiple eating events in a day.

2. Digestion of foods during a meal is a well-understood process. Solid foods consumed during a meal are held in the stomach for digestion. This digestion involves secretion of gastric fluids and the conversion of the food into a liquid (chyme) that then passes at a controlled rate (gastric emptying rate) into the gut on a continual basis until the stomach is empty. The gastric emptying rate decreases over time and has been described based on the "time to empty the first half" of the stomach's content ($t_{1/2}$). Values for $t_{1/2}$ in individuals range from 30 to 120 minutes (Hellmig S, 2006).

3. The CPF uptake parameters are determined by fitting data from human volunteers (Nolan *et al.*, 1984) into the PBPK model. The parameterization is consistent with the gastric emptying rates identified in step 2.

4. The gut compartment of the PBPK model also contains metabolism of CPF to both CPF-oxon and TCPy (via CYP) as discussed in Section 3 (see Table 1).

5. As discussed in Section 4, the sensitivity analysis of model parameters evaluated the rate of CPF entering the gut. The peak levels of RBC and brain AChE inhibition were not sensitive to the gut parameters. The sensitivity coefficient for the first order rate uptake was less than 0.1.

Based on these assumptions, the daily dose of CPF entering the PBPK model is treated as a single event that occurs over several hours at the beginning of each day. The total mass of CPF entering the gut during this process is equal to the total daily dose as estimated by the dietary exposure models. The uptake parameterization is not age-dependent.

6.3 *Design of the source-to-outcome model*

The final model consists of the following. The CARES (or other appropriate dietary software model) is used to convert a pesticide's residue data into estimates of daily dietary exposures in populations of individuals of a specific age. The output from CARES is used to create a table containing each individual's daily doses for the number of consecutive days of interest to the risk assessor. The format used for storing this table is "Comma-separated values" format (.csv). This format can be specified for programs running on SAS or can be created using Excel.

The .csv file has the following format. Data on each individual is provided in one row. The values in the first columns 1 through 3 define the individual's age, weight and gender. The daily doses for each day of each individual's longitudinal dietary exposure history are placed in the columns 4 and above. Any number of days up to 50 days[13] can be modeled by placing the daily doses in the appropriate columns. The following is an example of a table for two individuals having five consecutive days of exposure.

Table 7. Example table for five days of exposure for two infants

Age (y)	Sex (0=male, 1=female)	Weight (kg)	Dose Day 1 (mg/kg)	Dose Day 2 (mg/kg)	Dose Day 3 (mg/kg)	Dose Day 4 (mg/kg)	Dose Day 5 (mg/kg)
0.5	1	6.8	3.97E-06	4.39E-07	1.12E-05	1.04E-05	1.65E-06
0.5	1	6.4	3.31E-06	9.61E-07	1.12E-05	6.78E-05	1.65E-06

Copies of the .csv files used in the simulations describe in the following sections are included as Attachment F.

As described in Section 3, the Variation model reads the .csv file and uses the age, sex and weight data to predict the physiology of the individual. The model assumes that the meals occur once every 24 hours. The gut uptake rate assumed in the model results in approximately one half of the dose entering the gut within the first 90 minutes and three quarters in the first 180 minutes.

13 The model currently only accepts 50 daily doses but can easily be modified to accept more..

In the final source-to-outcome model, the PBPK/PD model reports:

- The blood concentration of CPF
- The blood concentration of CPF-oxon
- The inhibition of RBC AChE
- The inhibition of brain AChE
- The inhibition of plasma BuChE
- The mass of TCPy removed from the blood stream

The model provides a continual simulation of all modeled compartments, including the metrics above. By default, the model reports every 15 minutes for each 24 hour period following a dietary dose and saves an individual output file for each of the six metrics above. Attachment C provides additional information on the program.

Section summary

This section has presented a description of the approaches used to link the output from the dietary model to the PBPK/PD Variation model. Data on the characteristics and the exposure history of the simulated individuals is prepared by the user from the output of one of the dietary exposure software programs. This file is read by the Variation model and the predictions of the time course of the outputs are produced.

7. *Predictions of one and multiple day (longitudinal) dietary exposures on internal doses and cholinesterase inhibition*

Section overview

This section presents the use of the source-to-outcome model to investigate and ultimately characterize the impacts of longitudinal dietary exposures to CPF on body burdens and inhibition of blood and brain AChE. Longitudinal exposures are of interest because neither the pharmacokinetic nor pharmacodynamic effects of a dose may return to normal 24 hours after an intake of CPF. The body retains CPF for periods of time longer than 24 hours. In addition, at high doses the effects on cholinesterase are not fully reversed within 24 hours. However, as discussed in Section 5, there is considerable uncertainty in modeling longitudinal exposures. Therefore in this section we will examine how the impacts of longitudinal exposures relate to the impact of a single day's exposure.

This section begins by using the Variation model to investigate the impact of longitudinal exposures to constant dietary doses on internal metrics of exposure and RBC and brain AChE inhibition. This is followed by an analysis of the impact of the variable dietary exposures over multiple days using the complete source-to-outcome model. The impacts of the three different models of longitudinal dietary exposures discussed in Section 5 (CARES, LifeLine daily and LifeLine seasonal) on predictions of the impact of five days of dietary exposures are then investigated using the complete source-to-outcome model. Finally an analysis of responses at or above the 99.9th percentile of daily dietary exposures is presented. This analysis measures the impact of doses on the days prior or subsequent to the days when an individual receives a dose at or above the 99.9th percentile dose.

7.1 Model predictions of the impacts of identical daily exposures over time

The Variation model was used to investigate the cumulative effects of consistent dietary exposures to CPF. The model was used to predict the progressive impact of constant exposures in a typical adult and infant over a thirty day period. Parameters were

assessed include: blood concentrations of CPF and CPF-oxon, percent inhibition of RBC AChE, and percent inhibition of brain AChE. Five doses are modeled ranging from 0.0001 to 0.5 mg/kg. The lowest of these doses, 0.0001 mg/kg falls in the upper end of the range of currently estimated acute dietary exposures (see Attachment D).

Figure 45 presents the predicted time courses of the blood concentrations of CPF and CPF-oxon. These two plots only present data for the first 10 days. This was done to make the changes in the first few days clearer in the figure. (The patterns of daily changes in these two parameters do not vary for days 11 through 30.) The CPF plot indicates at all five doses there was little carryover of CPF from one day to the next for either adults or infants. The peak concentrations of the two compounds are only 5% higher on day 30 than day 1 for infants and 16% higher for adults.

In contrast, the second plot indicates that CPF-oxon levels increase over time. At doses of 0.5 mg/kg the peak oxon level on day 30 was 18-fold (1,800 %) higher than on day 1 for infants and 9 (900 %) fold higher for adults. Most of this increase occurs in the first 5 days of exposure. However this increase is dose dependent and decreases with dose. At the lowest dose modeled, 0.0001 mg/kg, only a 1% increase in peak oxon levels was observed over the 30 day period.

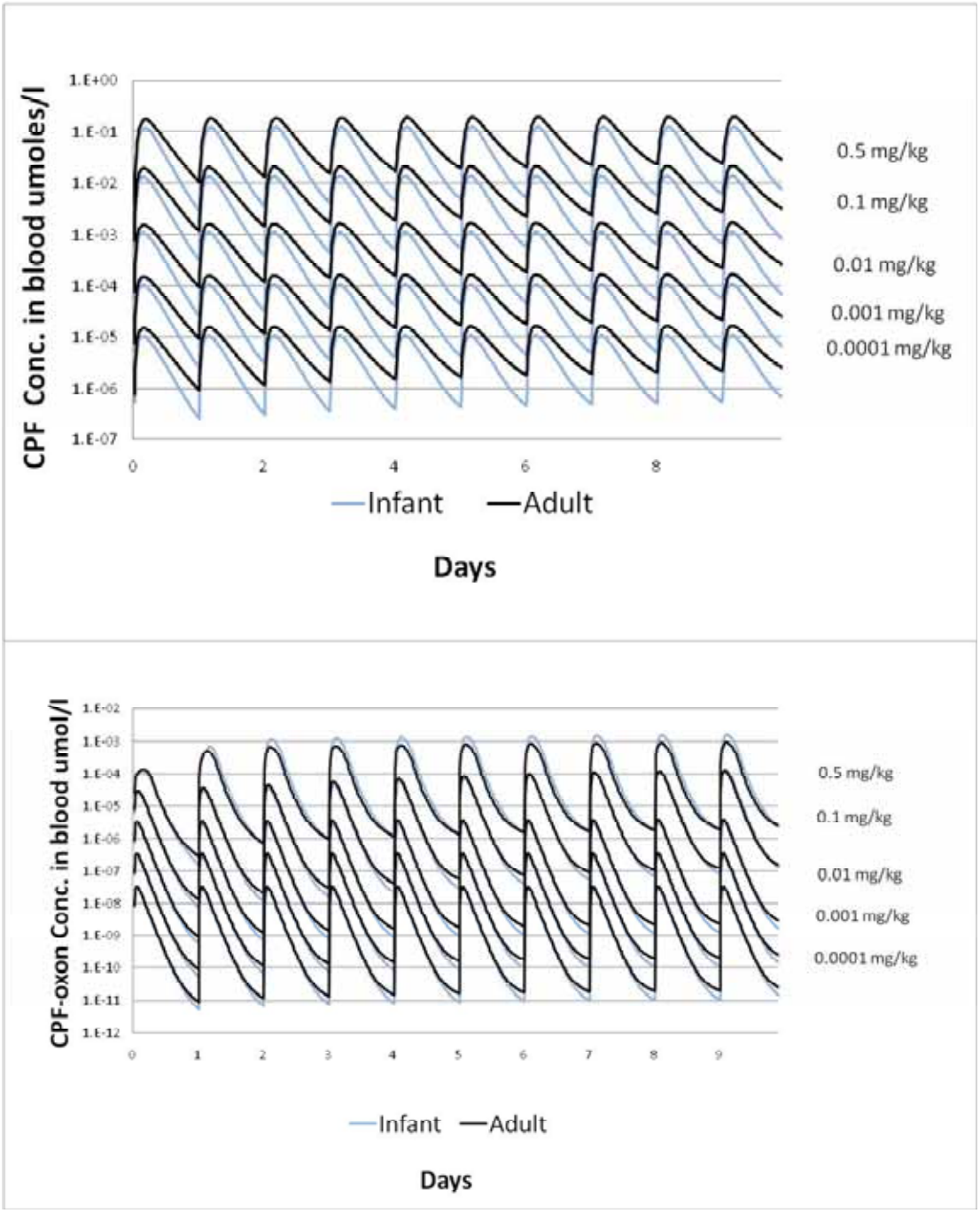

Figure 45. Predicted time course of CPF and CPF-oxon in blood (umoles/l) for a typical adult and child exposed to 10 consecutive daily oral doses of CPF for one of five modeled dose rate ranging from 0.5 to 0.0001 mg/kg.

Figure 46 presents the time course of inhibition of RBC and brain AChE in a typical adult and child. The two plots indicate that at constant doses, the peak inhibitions increase over time in a tissue and dose-dependent manner.

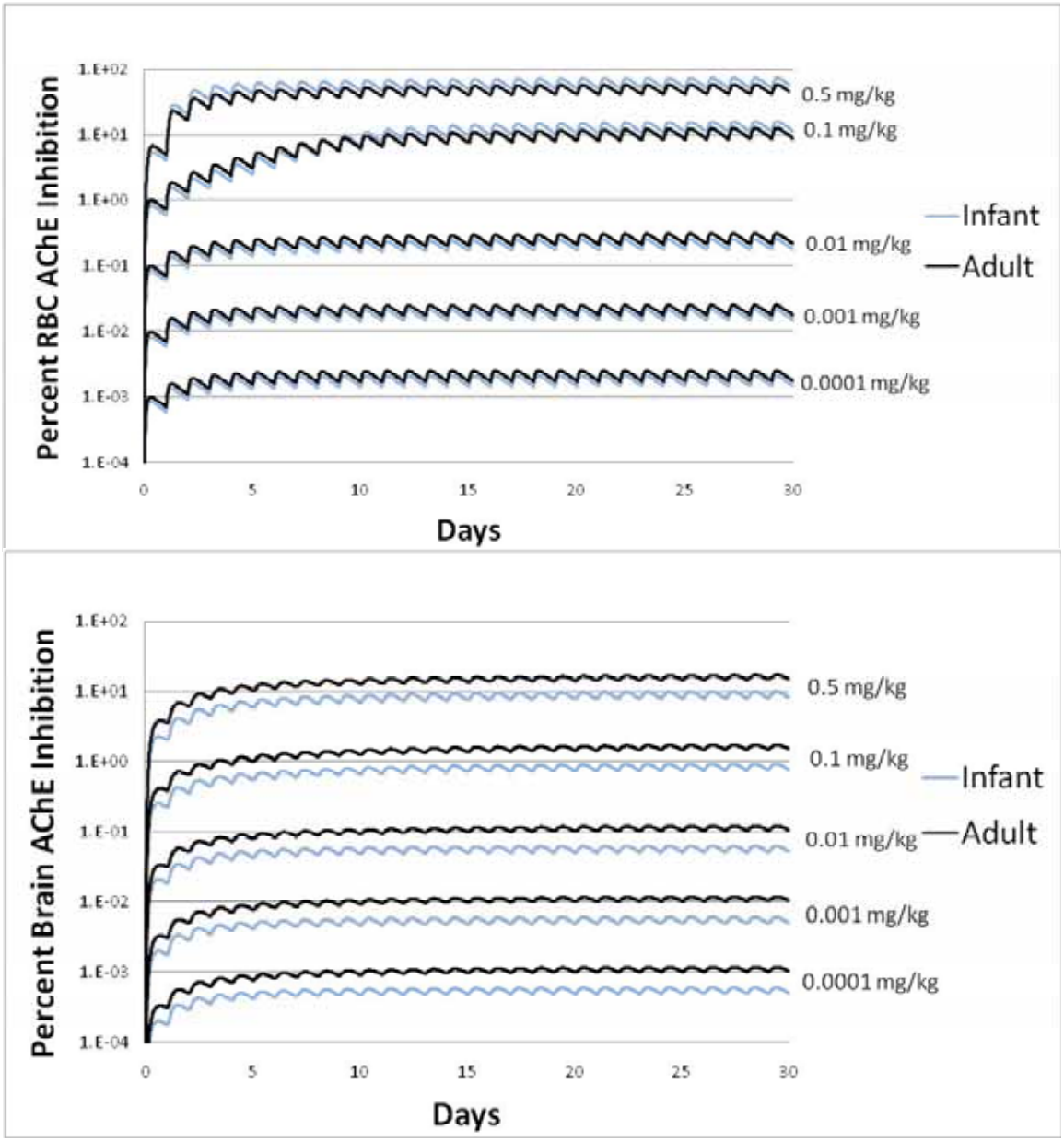

Figure 46. Prediction of RBC and brain inhibition from thirty days of constant exposures to five modeled doses in typical adults and infants.

As indicated in Figure 47, at all of the doses, the majority of the decreases in RBC AChE activity occur in the first 10 days. However, at lower doses the decreases occur sooner and 90% of 30 day inhibition is achieved by day 5. For RBC AChE in infants, there is a 20-fold difference between the day 1 peak inhibition and the day 30 peak inhibition at doses of 0.1 mg/kg. The difference between day 1 and day 10 levels of inhibition is smaller for adults (12-fold increase). At lower doses the difference between day 1 and day 30 is less for both adults and infants. At the lowest dose tested the difference for both adults and infants was 2.5-fold.

The time required to reach steady state is less for brain inhibition and is not strongly dose dependent. At both ages, 80% of the inhibition occurs by day 5 and 90% by day 10. At the lowest dose tested, the increase over the thirty days is 3-fold for infants and 3.5-fold for adults.

7.2 *Modeling the impacts of time varying dietary exposures –determining when a population reaches quasi-steady state conditions*

Dietary doses of pesticides vary from day to day. As a result, no individual ever reaches true steady state with respect to their dietary intakes. Rather the blood levels and levels of AChE inhibition constantly fluctuate over time. However, if the distribution of doses received by a population remains relatively constant, the distribution of peak levels of the CPF and CPF-oxon in the blood and AChE inhibition in RBC and brain across a population stabilizes over time. Under this quasi-steady state condition, the peak values can be specified for different fractions of the population. The time necessary for a population to reach quasi-steady state can be empirically measured by determining the cumulative distribution of peak levels across the population for each day in a model simulation.

In this analysis the peak concentrations and peak inhibition levels that occur at any point in time during the day are determined for each individual in two age groups, adults age 30 years and infants age 6 months. The cumulative distributions of the peak values for each of the 1,000 individual in the age groups for each day can then be used to determine if and when the populations have reached a quasi-steady state.

Figures 47 and 48 present the cumulative distribution of peak blood concentrations of CPF and CPF-oxon across the populations of adults and children for each of the five days. As the figures indicate, there is no change from day 1 to day 5. This suggests that peak blood concentrations of CPF and oxon across the population have reached quasi-steady state by day 1. This finding is consistent with the results in Figure 46 that showed that at the doses currently received from diet, neither CPF nor CPF-oxon increased over time. This implies that dietary exposures from prior days have little or no effect on blood levels of CPF or CPF-oxon.

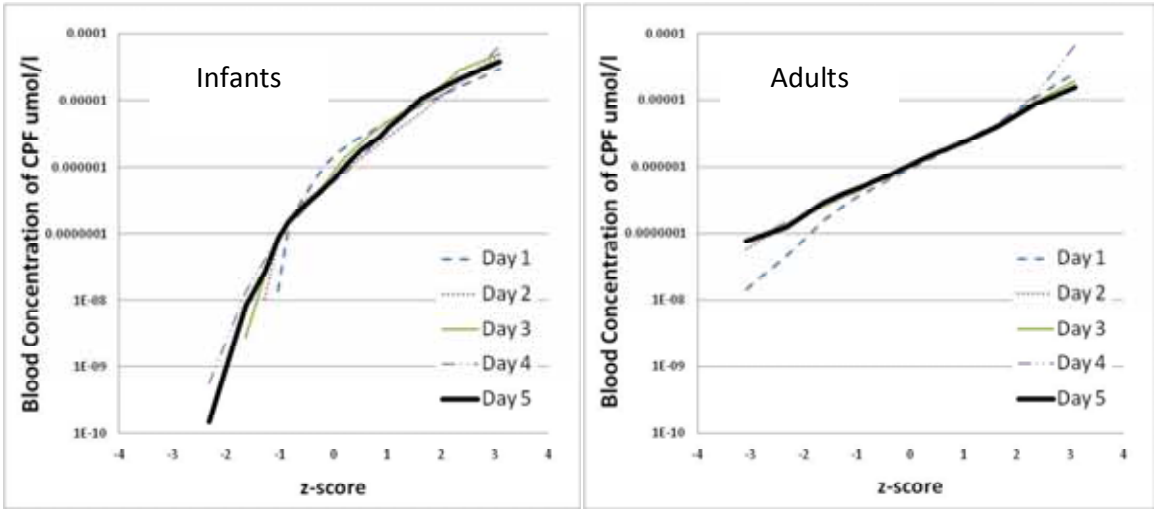

Figure 47. Cumulative distributions of peak CPF across populations of adults and infant on days 1 through 5 of a simulation of five days of dietary exposures.

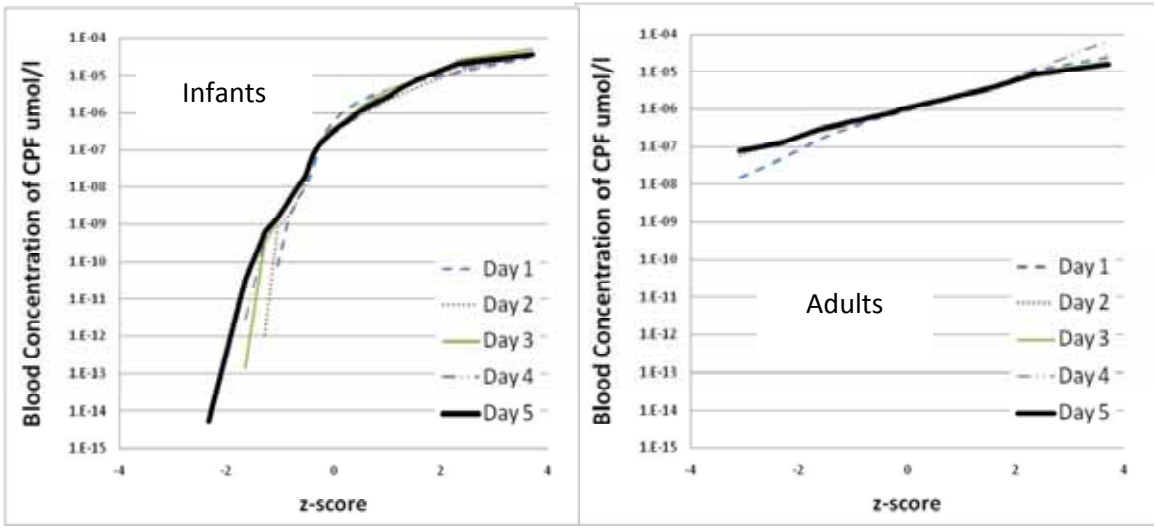

Figure 48. Cumulative distributions of peak CPF-oxon across populations of adults and infant on days 1 through 5 of a simulation of five days of dietary exposures.

Figures 49 and 50 present plots of the cumulative distributions of the peak levels of RBC and brain AChE for each of the 5 days. In contrast to the CPF and CPF-oxon, the plots in these two figures show that there is a small increase in the distribution of peak RBC and brain inhibition over the five days. However, the distributions for day 3 through day 5 are essentially identical. This suggests that by day 3 the population has reached quasi-steady state and that modeling individuals for longer durations of time would not result in different predictions of the distribution of body burdens or levels of AChE inhibition. In addition, for the highest percentiles the differences between day 1 and day 5 are less than a factor of 2. However, with only a thousand individuals, estimates above the 99^{th} percentile (Z-score >2.3) are unstable (values are driven by the last few outliers). The data on infants at low Z-scores is affected by the number of individuals who are breast fed and whose intakes are not evaluated by the dietary exposure models.

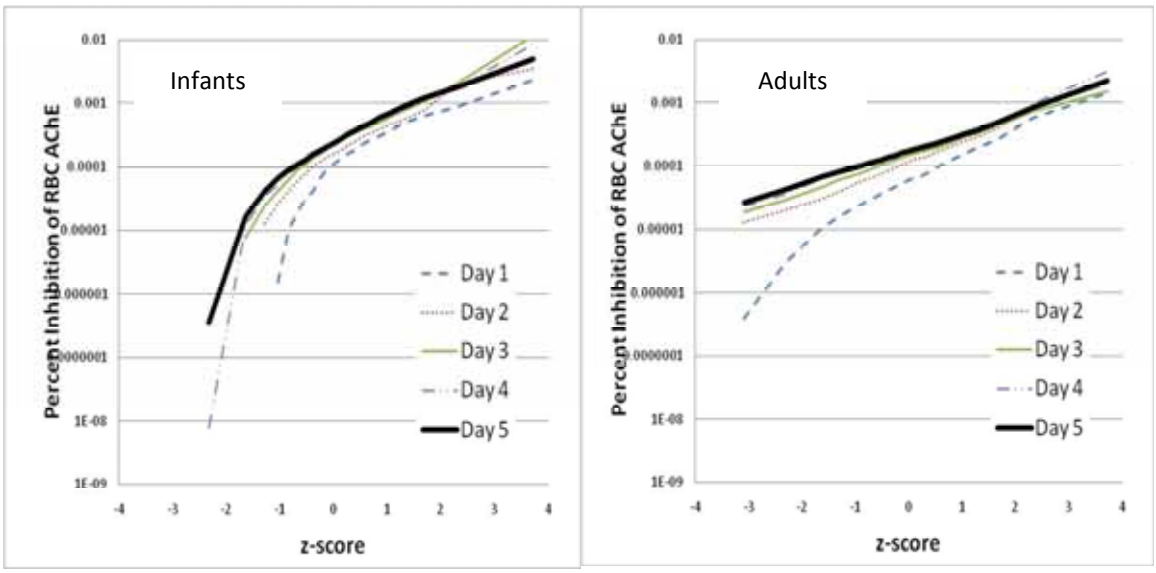

Figures 49. Cumulative distributions of peak RBC AChE inhibition on days 1 through 5 of a simulation of five days of dietary exposures to CPF in adults and infants.

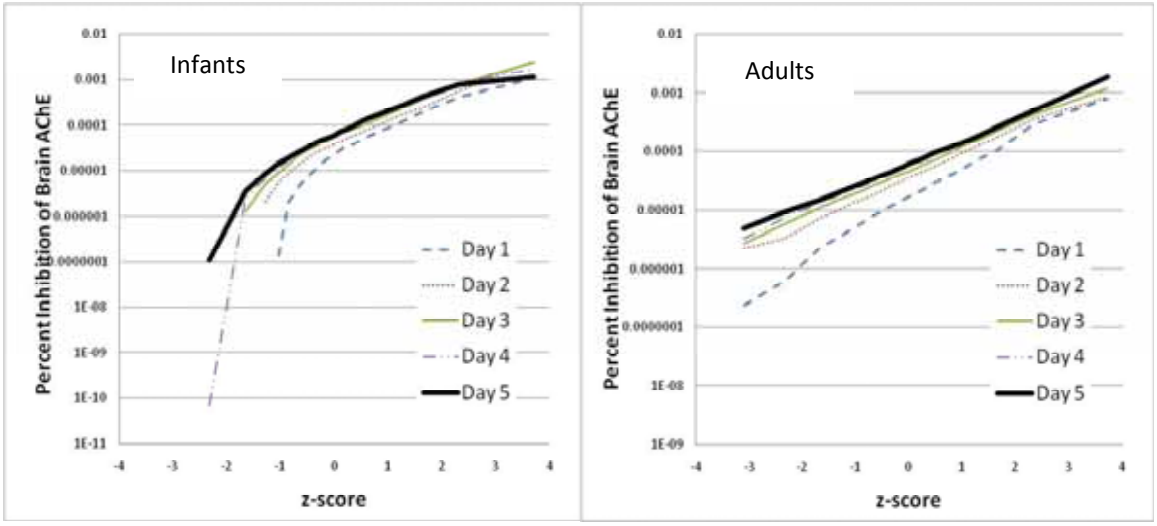

Figures 50. Cumulative distributions of peak RBC AChE inhibition on days 1 through 5 of a simulation of five days of dietary exposures to CPF.

In summary, Figures 49 and 50 confirm that CPF and CPF-oxon do not accumulate over time. The inhibition of RBC and brain AChE do increase but the impact is minimal for individuals in the upper portion of the population. By day 2, the portion of the population with above average doses has reached quasi equilibrium and the distribution of values for this portion of the population do not appear to change over longer periods of time.

7.3 Impact of three different longitudinal approaches of dietary exposure

The three longitudinal approaches of dietary exposure CARES, LifeLine daily, and LifeLine seasons were used in the source-to-outcome model. LifeLine is limited to modeling five consecutive days. Therefore, to be consistent, in this exercise the CARES program was also limited to 5 consecutive days. At the doses that currently occur from dietary exposure 80 to 90% of the cumulative impact on cholinesterases occurs in the first 5 days. Two age groups were investigated, adults and three year-olds. One thousand individuals were investigated in each age group.

Figure 51 presents the cumulative distribution of peak blood concentrations of CPF and CPF-oxon across populations of adults and children for each of the three approaches of longitudinal dietary exposures. The data presented are from the fifth day of the five-day simulation. These data reflect the contribution of day 5 and the prior days and thus should reflect the differences between the three longitudinal approaches. The data are plotted on a log dose versus Z-score. In general, the distributions of peak levels were found to be approximately log normal. This format has the advantage of expressing data that are log-normally distributed as straight lines. This facilitates the visual evaluation of the predictions of the three approaches.

As Figure 51 indicates, all three approaches produce very similar estimates of the distribution of peak levels of CPF and CPF-oxon. This suggests that any of the three approaches can be used to predict the impact of longitudinal dietary exposures on internal

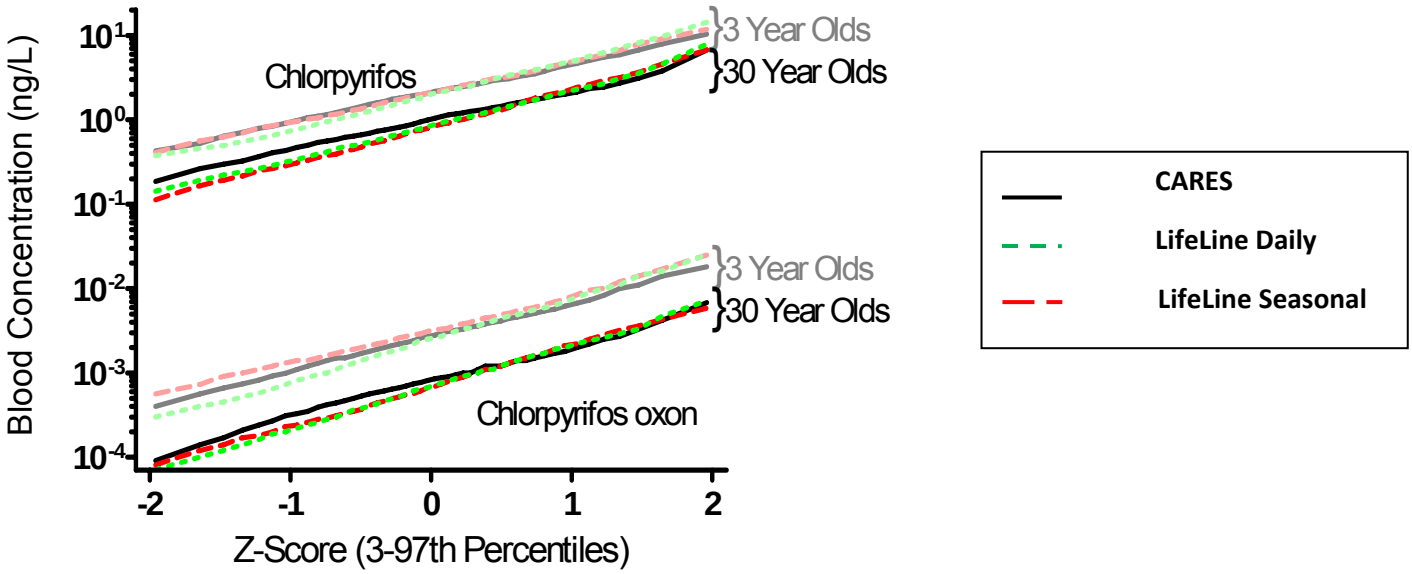

doses.

Figure 51. Predictions of the distribution of blood levels of CPF and CPF-oxon AChE on day 5 of a 5 day simulation in two age groups in three approaches of longitudinal exposures.

In Figure 52, two plots present the distributions of the three approaches for RBC and brain AChE. In contrast to CPF and CPF-oxon, the choice of dietary software does have an impact on the predictions of cholinesterase inhibition. CARES and LifeLine daily approaches produce similar values. However, the LifeLine seasonal approach results in predictions of less inhibition for individuals in the lower half of the population. This finding is consistent with analysis of day to day correlation presented in the three plots that comprise Figure 45. Those plots indicates that LifeLine daily and the CARES approaches produced little or no correlation between doses of CPF on consecutive days and that LifeLine seasonal produced moderate levels of correlations.

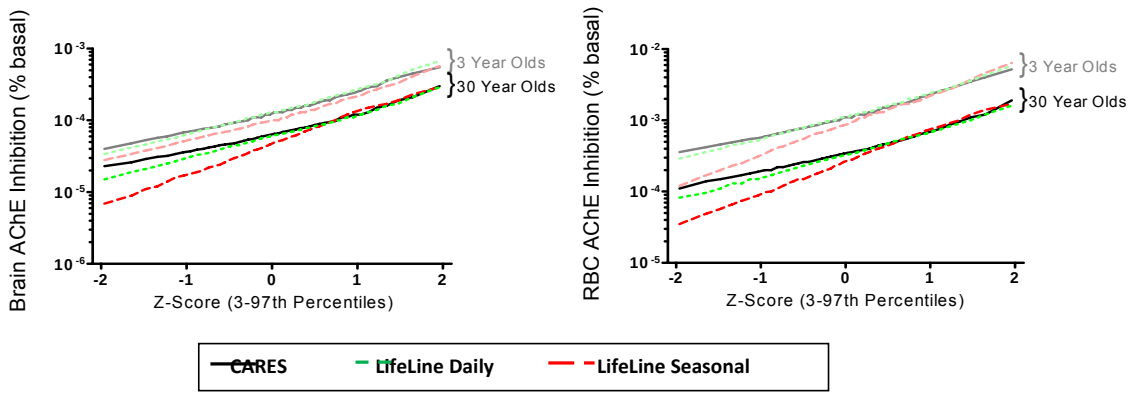

Figure 52. Predictions of the distribution of blood RBC and brain AChE on day 5 of a 5 day simulation in two age groups in three approaches of longitudinal exposures.

In summary, the three approaches to modeling longitudinal dietary exposures produced similar values for the blood levels of CPF and CPF-oxon. The three models predictions of AChE inhibitions were essentially identical for the portion of the population with the highest exposures. This suggests that any of the three approaches can be used to characterize the impacts of dietary exposure of CPF on individuals with above average exposures. Further, it suggests that predictions of internal doses and impacts on AChE from dietary exposures in the top half of the population are not substantively affected by the uncertainty introduced by the absence of longitudinal data on dietary intakes. Based on this finding, the CARES model of longitudinal variation is used in the remaining analyses in this report.

7.4 *Determining the impact of longitudinal exposures on the impacts of high level dietary exposures (the 99.9th percentile dose) on RBC and brain AChE inhibition*

The above analyses of quasi-steady state and multiple longitudinal models provide evidence that the impact of prior exposures on blood levels and AChE inhibition is different for individuals with relatively low exposures than for individuals with high exposures. This difference causes the distributions on days 1 through 5 and the differences in the three longitudinal models to "fan out" at lower Z-score values (See Figures 49, 50,

and 52). The explanation for the "fanning" is the asymmetry of the effect of dose from prior days on the blood levels of CPF and CPF-oxon and the AChE inhibition. Specifically, high doses on one day affect the four parameters on subsequent low dose days but low doses do not affect subsequent days with high doses. For example, when day 1 produces an exposure that is 100-fold larger than an exposure on day 2, it has a large impact on the four parameters on day 2 (and possibly later days). However, if day 2 exposures are 100 times day 1 exposures, there is little or no effect on day 2 from day 1. Individuals with low Z-scores have received lower doses on a given day and thus are more sensitive to the impact of the prior day's exposure. As a result, the values for the four parameters in this portion of the population are most affected by prior exposures. Thus this portion of the distribution of doses takes longer to reach equilibrium than individuals with above average exposures.

This finding suggests that individuals receiving the highest exposures (>the 99.9^{th} percentile) in a population will be least affected by exposures from prior days. This hypothesis was investigated using the source-to-outcome model.

In this analysis, the CARES dietary model was used to simulate year-long exposure histories for each of 4,000 adults. Figure 53 presents the year-long exposure history of three adults randomly selected from 4,000 individuals. The adults' highest daily exposures for the year are identified by the ovals.

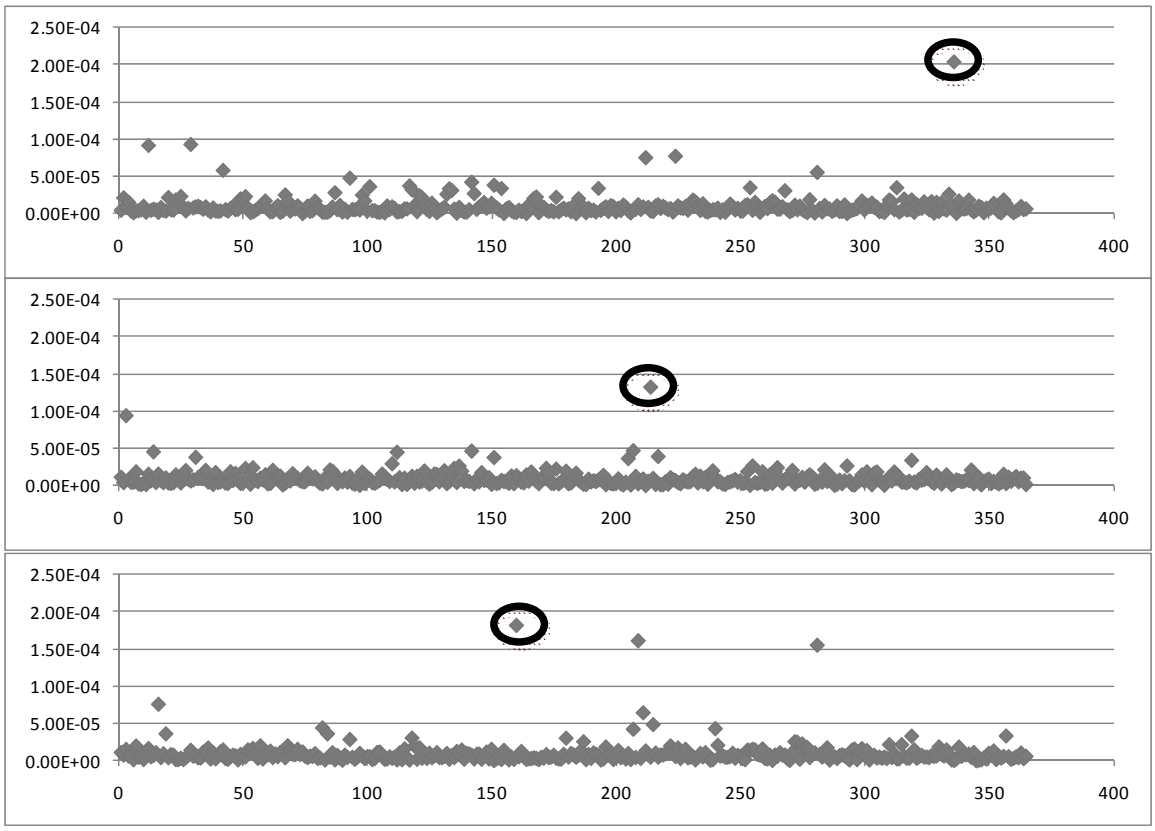

Figure 53. Exposure history (dietary doses of CPF (mg/kg) for each of 365 days) for three adults. Ovals indicate the maximum daily dose for each adult.

As indicated in Section 4, adults at the 99.9th percentile of the population are predicted by CARES to have a peak dose of 0.00012 mg/kg. A total of 499 individuals were identified who had one day during the 365-day period with an exposure equal to or slightly above the 99.9th percentile dose (0.00012 to 0.00024 mg/kg). For each of these individuals, the daily doses for the four days prior and four days subsequent to the high exposure day were identified (for a total of 9 days). Subsequent days were also included to investigate if the effect of the peak day could add to the effects of dose received on subsequent days. The result was the creation of 500 nine-day records where the fifth day had a dose at or slightly above the 99.9th percentile dose. The nine day exposure histories for the same three individuals are shown in Figure 54.

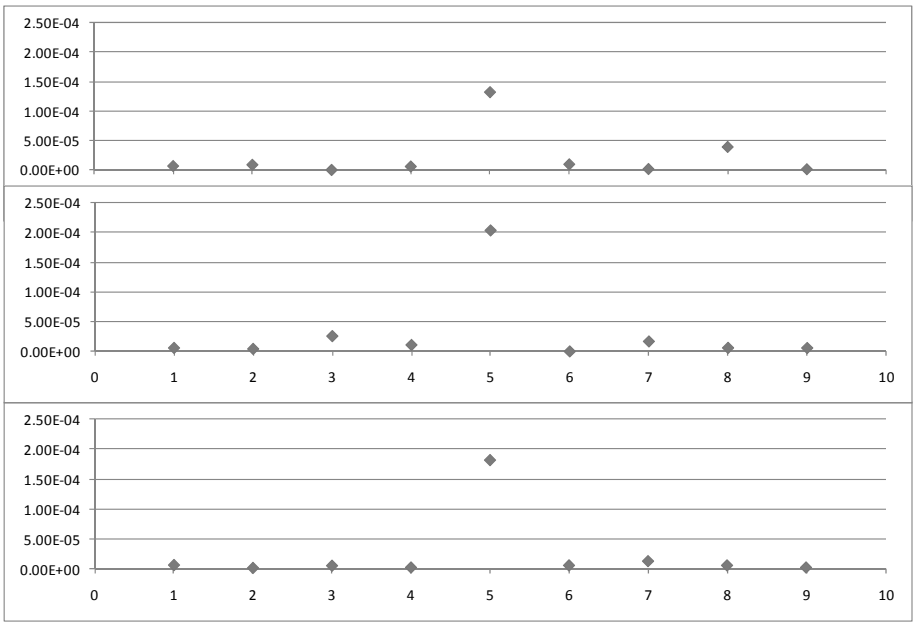

Figure 54. Dietary doses in mg/kg for the high exposure day and the four prior and subsequent days (same three adults as figure 53).

The 9-day exposure histories for the 499 adults were run through the source-to-outcome model and the peak RBC AChE inhibition levels were determined. In addition, the high days were also run through the source-to-outcome model as single day exposures and values of peak RBC AChE inhibition were determined. Figure 55 presents the cumulative distributions of the Peak AChE inhibition for both measures of exposure data. As the figure indicates, the impacts on RBC AChE from the high day plus the surrounding (+/- 4) days are very similar to the high day alone. The average impact of considering the contribution from the prior to subsequent days for the 500 individuals was a 9% increase in the estimate of the peak inhibition. This finding implies that for individuals receiving a large dose (relative to other individuals) the contributions from prior and subsequent days are minimal. A similar analysis for brain AChE showed an 11% average increase.

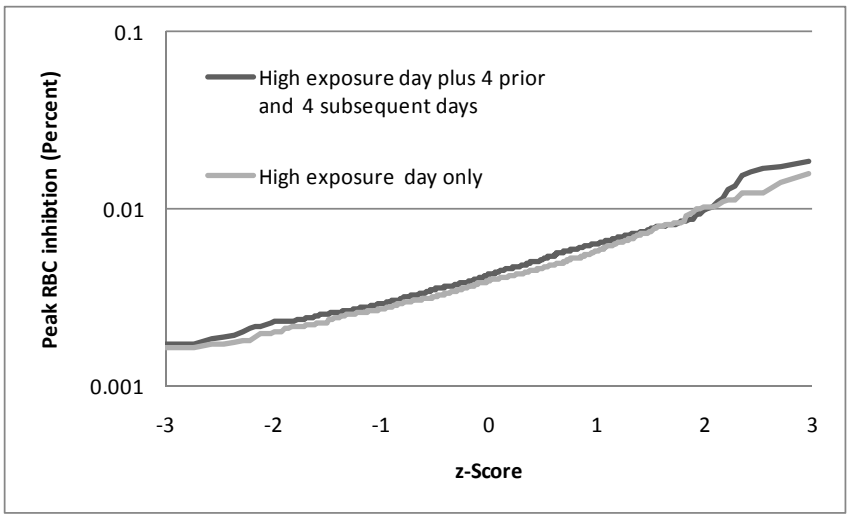

Figure 55. Cumulative distributions of 1) peak RBC AChE inhibition over the 9 day period in 500 adults where day five is the high exposure day (dose at or above the 99.9th percentile dose) and 2) peak RBC AChE inhibition for the high exposure day alone.

Section summary

This section has presented data from analyses where the source-to-outcome model and the Variation PBPK/PD model are used to investigate the issue of longitudinal exposure and its impact on four outcomes, CPF and CPF-oxon levels in blood and peak inhibition of RBC and brain AChE. The Variation model predicts that the effect of daily oral exposure to identical doses of CPF at current dietary results in effects that modestly accumulate over time (i.e., levels of RBC and brain inhibition increases by roughly a factor of three if an oral dose is repeated over multiple days). At the doses that are predicted from current dietary exposures (<0.0002 mg/kg), 90% of the increase in inhibition occurs over the first five days of exposure. In contrast, levels of CPF and CPF oxon in blood do not accumulate over time.

Three dietary exposure models were found to produce similar estimates of blood levels of CPF and CPF-oxon and similar estimates of peak inhibition in RBC and brain AChE. An evaluation of the predictions of the cumulative impact of dietary exposures over five days suggests that estimates of the upper portions of the distribution of the four parameters do not change if the duration of dietary simulations are extended beyond five

days. Finally, the model indicates for individuals at the extreme tail of the exposed population (the 99.9th percentile of dose) RBC inhibition is largely driven by the dose from a single day.

Based on these findings, we conclude that while repeated doses of equal size can result in higher inhibition rates over time, when there is large variation in day-to-day levels of dietary doses the impact of longitudinal exposures are minimized. This minimization is most apparent in the estimates of the individuals most exposed. As a result, if a person has a high level of exposure on a given day (in the top 0.1%), the impact on the four parameters are driven by the dose from that day.

These findings also suggests that the use of the five-day exposure histories produced by CARES or other dietary exposure software provide a reasonable basis for the evaluation of the impacts of longitudinal exposures to current dietary residue levels of CPF. The confidence in the predictions is higher for the upper percentiles of the exposed populations since these exposures are less dependent on longitudinal exposures (i.e., are more driven by single day above average exposures). Finally, these results explain why the three models of longitudinal exposures provide similar predictions of AChE inhibition at higher percentiles. The individuals at the higher percentiles were simply not affected by doses from prior days and differences in correlation between consecutive days would not affect the predicted blood levels or effects on AChE.

8. Evaluation in the uncertainty in the predictions of source-to-outcome model by comparison to measured values

Section overview

The predictions of the source-to-outcome model are subject to uncertainty that occurs from a number of factors including limitations in the fidelity of the model, uncertainty in the model inputs, and the relevance of the input data. Thus, the model is evaluated to determine the level of confidence in its output. The evaluation of uncertainty in the model is also a challenge because the model addresses multiple and diverse processes including variation in residues on food, food consumption rates, the conversion of oral doses to time histories of internal concentrations, and interactions with cholinesterase in blood and the brain. This section presents examples of how measured data from surveys can be used to evaluate the model predictions.

8.1 Finding data for model evaluations

The source-to-outcome model ideally should be evaluated by data that matches dietary levels of exposure to inhibition of AChE and BuChE levels. Such an exercise is not possible since any impact of current levels of CPF would not be detectable against the day-to-day variation in blood AChE or plasma BuChE. Without such data, the evaluation must rely on studies that evaluate the components of the model.

In the case of CPF, the monitoring data available for the evaluation of a source-to-outcome model are limited. While there are multiple sources of data that can be used, each of the sources has its particular limitations. In this section we discuss how to most effectively use the available data to evaluate the source-to-outcome and Variation models. In general, this is achieved when the model is used to mimic the conditions of the survey data.

To address this issue of model evaluation, we believe that multiple comparisons must be made that address specific steps in the source-to-outcome process. Figure 56 presents a

description of the major steps of the source-to-outcome model and the data that can be used to evaluate each of the steps.

Data on many of these steps have already been presented in this report. The process of modeling daily doses has been the subject of a number of reviews. The available software programs developed by multiple groups and using different methods for dose calculation have been shown to produce similar estimates of dietary exposure for pesticides (U.S. EPA, 2004; Xue, 2010). In this report we have shown that three of the current models produce similar estimates of the distribution of oral intakes of CPF in adults, children and infant (Table 5, Section 5).

The consistency indicates that the residue data were correctly entered and the models were run correctly. It also confirms that the use of the current models does not introduce modeling uncertainty (bias due to choice of dietary model in the analysis).

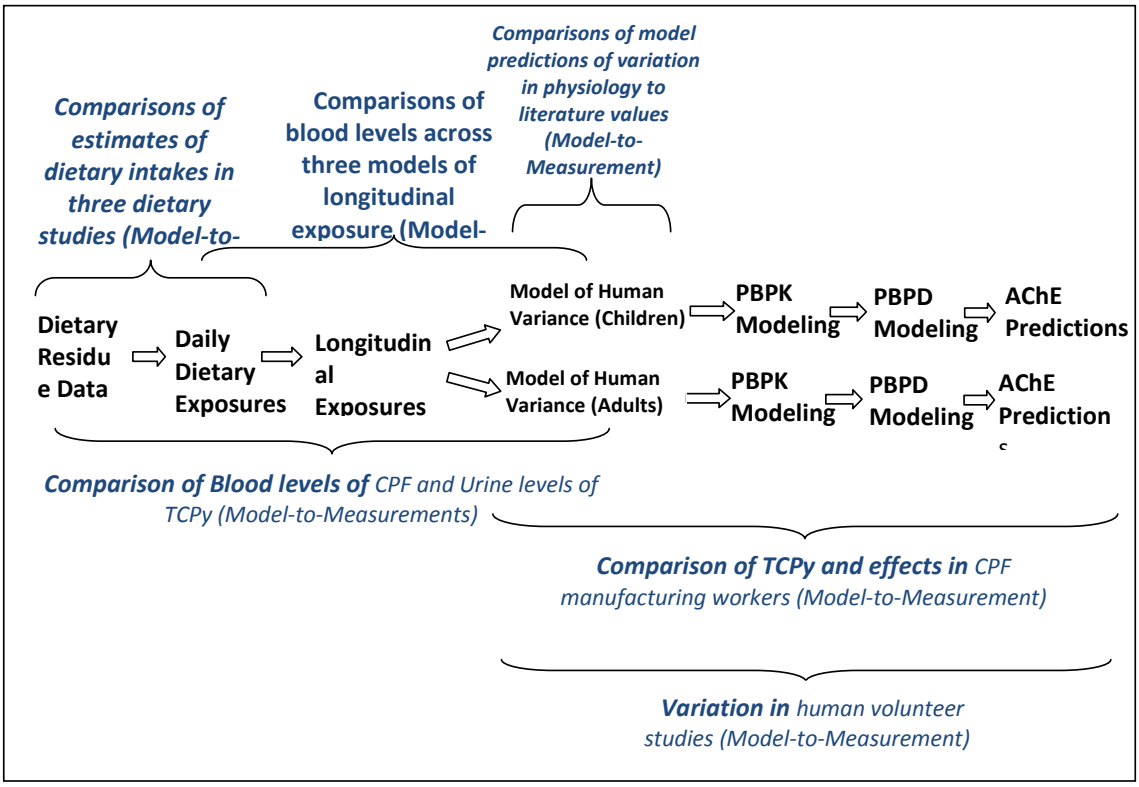

Figure 56. Steps in the Source-to-outcome model and analyses that provide a basis for the evaluation of the model output.

The second source of uncertainty, the development of estimates of longitudinal exposures, has been shown not to be an issue for dietary exposures to CPF. The impacts of repeated oral exposures on blood levels of CPF and CPF-oxon at dietary levels do not accumulate over time. The impact of repeated daily exposures on inhibition rates has been shown to be minimal for individuals with above average dietary exposures (see Section 7).

In Sections 3 and 4 of this report we have used the LifeStage model to predict the typical response in the groups (Figures 20-23) and the Variation model to predict the range of response observed across the individuals in Kisicki *et al.* (Figure 32). The predictions of the LifeStage and Variation PBPK/PD models are consistent with the observed levels BuChE inhibition in the Nolan *et al.* human volunteer study (Nolan *et al.*, 1984) and the TCPy blood levels and RBC AChE inhibition reported in the Kisicki *et al.* study (Kisicki *et al.*, 1999).

The LifeStage and Variation models have also demonstrated that their predictions of age related changes and interindividual variation in physiological parameters are also consistent with published data (Sections 3 and 4).

The following sections present a series of additional comparisons that provide further perspective on the predictions of the source-to-outcome and Variation models. In these comparisons the models are used to make predictions that can be directly compared to values reported in surveys of the public.

8.2 *Using biomonitoring data of CPF and its metabolites to evaluate the dietary and PBPK portions of the source-to-outcome model*

We use the source-to-outcome model to predict 1) blood levels of CPF in adults, 2) TCPy levels in urine in adults and children. These predictions are then compared to survey results. In addition, the model is used to investigate data on BuChE inhibition in workers.

Surveys of levels of pesticide metabolites in individuals are an important source of data for validation of dietary models. NHANES has been collecting blood samples for analysis of CPF levels in the 2007-2008 and 2009-2010 waves of sampling; however, these data have not been released as of this time.

There are two smaller studies that have measured levels of CPF in sera of pregnant women in New York City (Whyatt *et al.*, 2003; Whyatt *et al.*, 2009) and New Jersey (Barr, 2010). Table 7 presents the reported results of two surveys of blood levels in adult women at the time they gave birth (Barr, 2010; Whyatt *et al.*, 2009). Data were taken from both the mothers and from the cord blood. These survey data were taken from periods (after 2000) when CPF exposures were largely limited to dietary intake of food residues. The data on the Whyatt cohort are limited to values published in the peer review literature. The investigators of this cohort have not made their data available. Data on the Barr cohort were provided by Dr. Dana Barr.

The strategy used in performing this comparison has been to use the source-to-outcome model to produce estimates of the range of blood concentrations that would be found if a blood sample was taken any time during a 24 hour period after a dietary

exposure event. This was done by taking the values that occur at various points in time over a 24-hour period for 1,000 adults. The source-to-outcome model produces 96 estimates per 24-hour period (one every 15 minutes). The 96,000 values were ranked and the various percentiles, min, max, and geometric mean were determined. The 24 hours of data were taken from day 5 of a 5-day model simulation performed in a population of 30 year-old adults. If the last exposure event occurred no more than 8 hr before the time the blood was sampled, the predicted concentrations would be approximately 50% higher (data not shown).

The Variation model does not consider the impact of pregnancy on blood levels of CPF. Lowe *et al.*, 2009 investigated the impact of pregnancy on the ADME of CPF and found that blood levels would be increased by a factor 1.3 due to changes in the lipid levels during pregnancy. Therefore the predictions of CPF in blood from the source-to-outcome model were increased by a factor of 1.3.

Table 7. Comparison of measured blood CPF levels (ng/L) from selected biomonitoring studies with predictions from source-to-outcome model

	Source-to-outcome model[1]	Eaton *et al.* (2008)[2]	Whyatt *et al.* (2009)[2]		Barr et.al (2010)	
Exposure Date[3]	***2002-2010***	***2001-2002***	***2001-2004***		***2003-2004***	
Measurement	MB[4]	MB and CB[5]	CB	MB	CB	MB
Number of Individuals[5]	1000	76	65	92	148	138
Range						
Min	0.007	<LD[7]	<LD	<LD	<LD	<LD
Max	7	16	-[8]	-	1.8	10.1
Geometric Mean	0.2	0.5	-	-	1.5	4.2
Percentile						
10	0.05	-	<LD	<LD	<LD	<LD
25	0.09	-	<LD	<LD	<LD	<LD
50	0.2	-	<LD	<LD	<LD	<LD
75	0.4	-	<LD	<LD	1.3	<LD
90	0.7	-	2.3	1.5	1.7	<LD
95	1.0	-	2.5	2.5	1.8	<LD

[1] Model simulations were conducted using the adult data. Values based on randomly selected data points on day 5. Blood levels were adjusted up by 1.3 to reflect impact of pregnancy on CPF levels in blood as described by Lowe *et al.*, (2009).
[2] Summary data from the Whyatt studies were reported by both Eaton *et al.*, 2008 and Whyatt *et al.* 2009. Data for 2001 and 2002 are reflected in both sets of values.
[3] Date of that samples were taken for measured data or date of residue data used in dietary simulation
[4] Maternal Blood
[5] Cord Blood
[6] Number of simulated blood levels or number of measured values.
[7] Less than level of detection. Level of detection was reported by authors to range from 0.5 to 1.0 ng/L
[8] Indicates data not available

Table 7 indicates that that model predictions are relatively consistent with the limited monitoring data in pregnant women. This is encouraging since women of child-bearing age are one of the subpopulations of concern. However, because the surveys are limited in size and come from two adjacent states (New York and New Jersey) they are not ideal for evaluating the ability of the source-to-outcome model's to predict the distribution for other age groups and in other regions. In addition, the majority of the samples are below the

detection limit for the analytical methodology. When additional data become available they should be used to confirm the model predictions.

The second data set that can be used to evaluate the model's prediction are the data on urinary levels of TCPy in NHANES and other smaller biomonitoring studies. The use of TCPy in blood or urine as a direct measure of CPF is complicated by the fact that TCPy itself is present in the environment, and there are dietary residues of TCPy in many foods[14]. As a result, researchers have concluded that only 5 to 20% of TCPy observed in urine is from dietary intake of CPF residues (Barr *et al.*, 2005; Eaton *et al.*, 2008; Wilson *et al.*, 2003).

Figure 57 presents the predicted distribution of TCPy levels in the U.S. population in 2002 as determined by the NHANES survey of individuals over the age of 12 year. The data were below the level of quantification for 29% of the population and ranged from 0.43 to 27.5 ug/l. Using the estimates of 5-20% as the fraction of TCPy in adults that occurs from metabolism of CPF, a range of plausible TCPy values is specified. The predicted levels of TCPy in adult urine were determined based on the amount of TCPy removed on the fifth day of a 5 day simulation of dietary exposures in adults. The daily urine production for each individual was estimated using the individuals' body weights and assuming a daily urine production rate of 0.02 l/kg body weight (Brehrman RE, 2000; Snyder, 1975). The prediction of the distribution of TCPy in urine that occurs from dietary intake of CPF is presented in Figure 57 as the dashed line. The model predictions are consistent with the biomonitoring data for the median individuals, but tend to overestimate values for individuals with low TCPy urine levels and underestimate values for individuals with high TCPy levels. Current levels of dietary exposure of CPF are expected to be lower than levels in 2002 because of the changes in the regulation of the compound. This may explain why the predicted levels of TCPy from the source-to-outcome model are below the range suggested in the literature for the top of the cumulative distributions. However, any

14 These level of TCPy result from degradation of the parent CPF (and the related pesticide CPF-methyl in stored grain) after application but prior to consumption of food Barr, D. B., Angerer, J., 2006. Potential uses of biomonitoring data: A case study using the organophosphorus pesticides chlorpyrifos and malathion. Environmental Health Perspectives. 114**,** 1763-1769, Eaton, D. L., et al., 2008. Review of the toxicology of chlorpyrifos with an emphasis on human exposure and neurodevelopment. Crit Rev Toxicol. 38 Suppl 2**,** 1-125..

strong conclusions are prevented by the uncertainty in the fraction of the total TCPy in urine that comes from the metabolism of dietary intake of CPF.

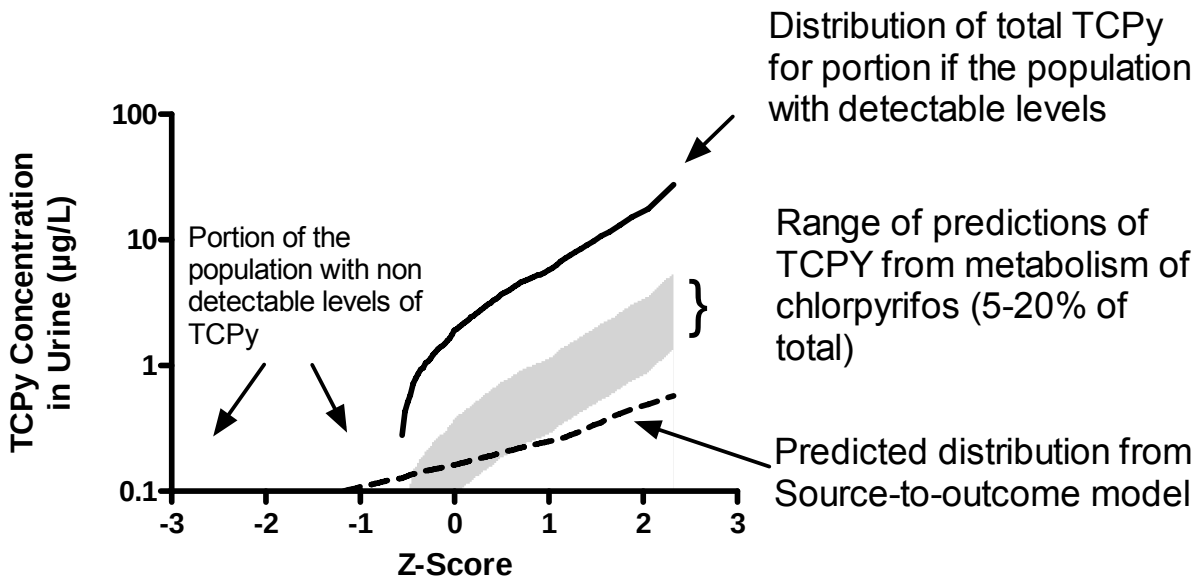

Figure 57. Cumulative distributions of predictions of current urinary levels of TCPy from the source-to-outcome model for adults, observed levels in the U.S. Population in the 2002 NHANES survey (30% of population have levels below the NHANES level of quantification and are not shown), and estimates of the portions of NHANES levels that come from CPF dietary exposures.

Table 8 compares the predicted levels of TCPy from the source-to-outcome model and the observed levels from two smaller studies (Curwin *et al.*, 2007; Lu *et al.*, 2008). The modeled predictions of TCPy range from 2% (adults) and 3-10% (children) of the observed values and are thus reasonably consistent with published findings of the fraction of TCPy that occurs from exposure to CPF.

Table 8. Comparison of selected measured urinary TCPy concentrations (μg/L) from selected biomonitoring studies with source-to-outcome model predictions

	Source-to-outcome model[1]	Curwin *et al.* (2007)	Lu *et al.* (2008)
	Median (90% CI)	**Geo. Mean (±Std. Dev.)**	**Mean (Range)**
Date[2]	2008-2009	2001	2003-2004
N	1000	Varies[2]	701
Men	-	12 (3.8-47)	-
Women	-	11 (1.8-35)	-
Women & Men	0.2 (0.08-0.3)	-	-
Children	0.5 (0.3-1.0)	16 (5.4-54)	5.1 (0-32)

[1] Source-to-outcome model simulations were conducted using the CARES model data. Day 5 values are presented.
[2] Date of sampling for measured data or date of exposure data simulated for source-to-outcome model
[3] 24 adult women, 24 adult men and 51 children
[4] Data not reported in published study

The results of the comparison of TCPy provide confirmation that the dietary and pharmacokinetic portions of the source-to-outcome model are producing estimates for adults that are reasonably consistent with the reported blood concentrations of CPF and urinary TCPy concentrations in adults and children. These results provide considerable support that the dietary and PBPK portions of the model are likely to be at the right order of magnitude in their predictions of body burdens of CPF and its metabolites.

8.3 PBPK/PD model predictions of the relationship between TCPy levels in urine and butyryl cholinesterase in plasma in occupationally exposed adults

In many instances data are available that are only partially relevant to a model's prediction. This subsection presents an example of how biomonitoring data from a study of workers could be used to evaluate the Variation model and the limitations of such a comparison.

Garabrant *et al.* (2009) published an analysis of data on RBC AChE and plasma BuChE cholinesterase collected from male and female workers in a plant manufacturing CPF as part of a regular industrial hygiene monitoring program. Unlike the general population, the majority of TCPy in the urine of the workers occupationally exposed to

CPF is the result of the workers' occupational exposure and not dietary residues of TCPy. In this group, TCPy can provide direct information on occupational CPF exposures (Garabrant *et al.*, 2009).

Figure 58, taken from the Garabrant *et al.* (2009) publication, depicts the observed BuChE levels for each worker (expressed as a percentage of each worker's baseline level) plotted against the worker's urinary levels of TCPy (normalized to creatinine). The TCPy urine levels in workers and controls range over three orders of magnitude and for workers with elevated levels are correlated with increased inhibition of plasma butyryl but not RBC acetyl cholinesterase.

The Variation PBPK/PD model was used to simulate the relation of TCPy in urine and BuChE in adults. The model was run for a group of 2,000 adults. The model assumed that the individuals were exposed for 5 days to the same bolus oral doses. The doses were varied across the adults in a log uniform distribution with doses ranging from 10 mg/kg to 0.001 mg/kg. The amounts of TCPy removed by the kidney on the fifth day were determined for each of the 2,000 adults. These data were used to estimate the concentration of TCPy in urine on a mg TCPy/gram creatinine basis. These estimates assume a daily urine production of 0.02 l/kg and creatinine levels in urine of 5-15 mg/l for adults. This estimate was plotted against BuChE activity. The model predictions are presented in Figure 58 as an overlay of the data reported by Garabrant *et al.* (2009).

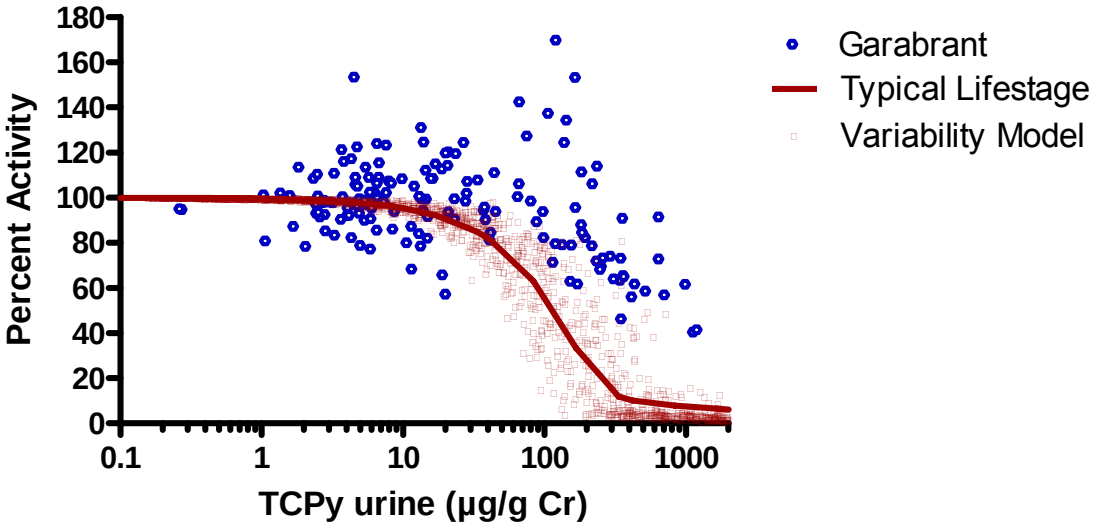

Figure 58. Observed relationships of cholinesterase inhibition and TCPy in urine for workers in a CPF manufacturing plant and for control workers. Predicted relationship (assuming major route of exposure is oral) using Variation PBPK/PD model.

As Figure 58 indicates, the Variation model's predictions of the relationship between BuChE inhibition in workers and elevated levels of TCPy in urine are a slight overestimate of the observed relationship in the Garabrant *et al.* study. The reason for the overestimation may be due to differences in the route or timing of the dose.

Since the study involved occupational exposures and not dietary exposures, route and timing of these exposures was not clearly defined. The Variation model predicts the response assuming a bolus oral dose. The workers' exposures are more likely to spread out over a workday and could occur by the dermal and/or inhalation routes. Such differences could change the relationship between BuChE and TCPy by reducing the peak concentration of CPF and CPF-oxon in blood by spreading the doses received over a longer period of time (e.g., the 8-hr workday).

Section summary

In this section and in Sections 3 and 4 we have reviewed the available human studies and biomonitoring data on CPF and its metabolites in the published literature. These data allow evaluation of each of the four steps in the total source-to-outcome process. These are:

1. Development of oral doses estimate for one day based on dietary residues
2. Characterizing longitudinal doses
3. Modeling the impact of oral doses on blood levels of CPF and CPF-oxon and TCPy levels in urine
4. Modeling the impacts on BuChE

The analyses presented in Sections 5 and 7 indicate that dietary modeling uncertainty and modeling longitudinal exposures are not major sources of uncertainty. The PBPK/PD modeling provided good fits to data in human volunteers, and the model's predictions are not inconsistent with data in workers (although the route of exposure for such workers is unclear). The data on biomonitoring evaluates the quality of the residue data and both the dietary and PBPK portion of the source-to-outcome model. The predictions are consistent with current studies of CPF in blood and TCPy in urine. These findings suggest that the model is predicting values that are of the right order of magnitude and could be within a factor of 2 or 3 of actual values. However, because of the limitations in the biomonitoring data, this consistency cannot be taken as proof that the source-to-outcome model is making predictions of impacts on cholinesterases that are less than an order of magnitude (+/- 3-fold) for the general population. Additional biomonitoring data will be necessary to determine if the source-to-outcome model's predictions are more precise.

9. *Model predictions of dietary dose impact on brain and RBC inhibition.*

Section overview

This section focuses on the predictions of the source-to-outcome model and their implications for public health assessment.

9.1 Model predictions

To evaluate the public health relevance of dietary intake on the general population, the source-to-outcome model was used to generate dietary estimates for three age groups: six month-olds, three year-olds, and thirty year-olds. These ages were selected to demonstrate the capabilities of the model. A complete risk assessment would address other ages as well. One thousand individuals were modeled for each age group with dietary doses determined over a 5-day period for each individual (from CARES). The peak values of blood CPF, CPF-oxon, RBC AChE inhibition and brain AChE inhibition were determined for day five of the assessment (Figures 59 and 60).

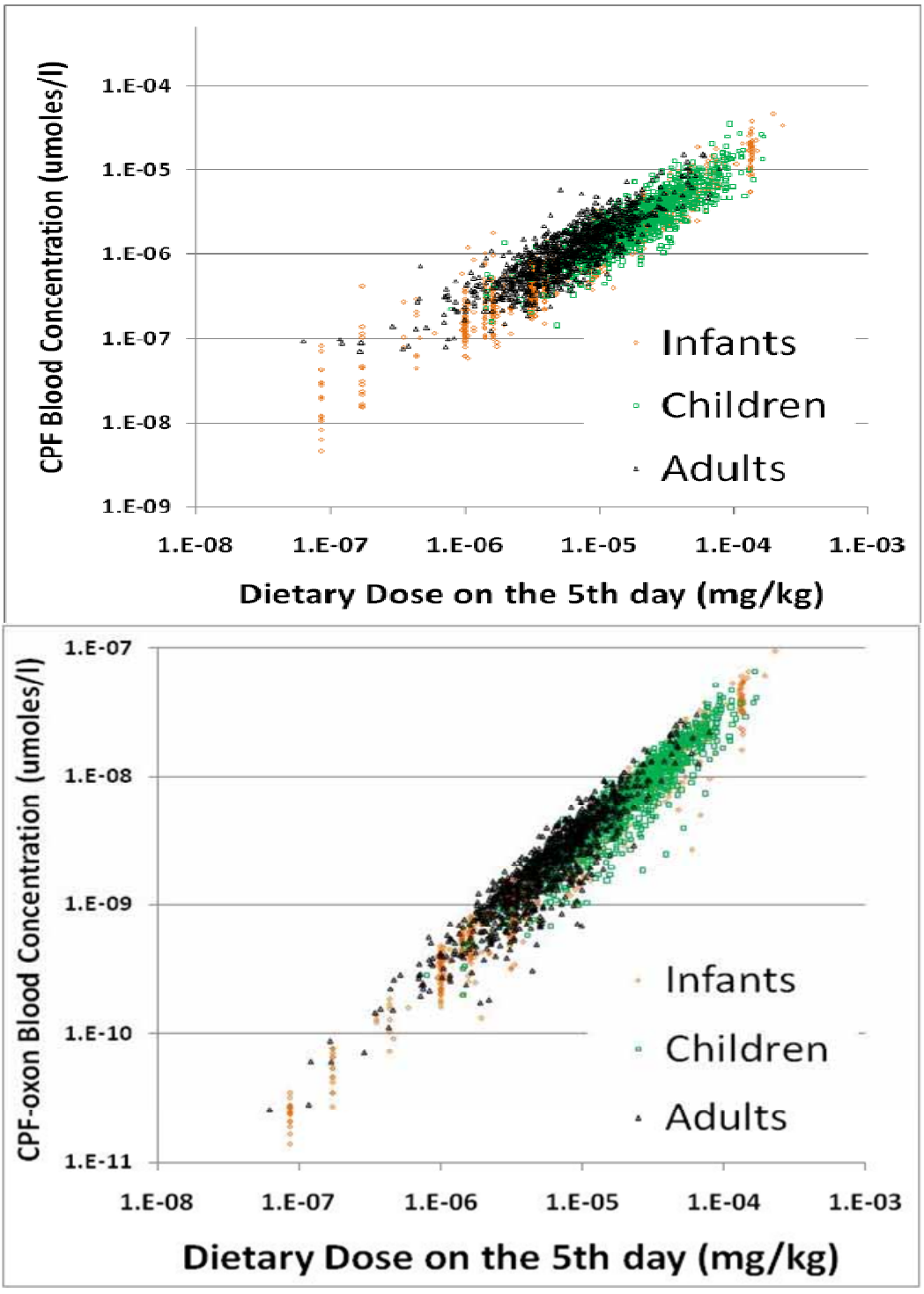

Figure 59. Predicted blood concentrations of CPF and CPF-oxon on the 5th day of simulated daily dietary exposures in 1,000 adults (30 years), 1,000 children (3 years), and 1,000 infants (6 months).

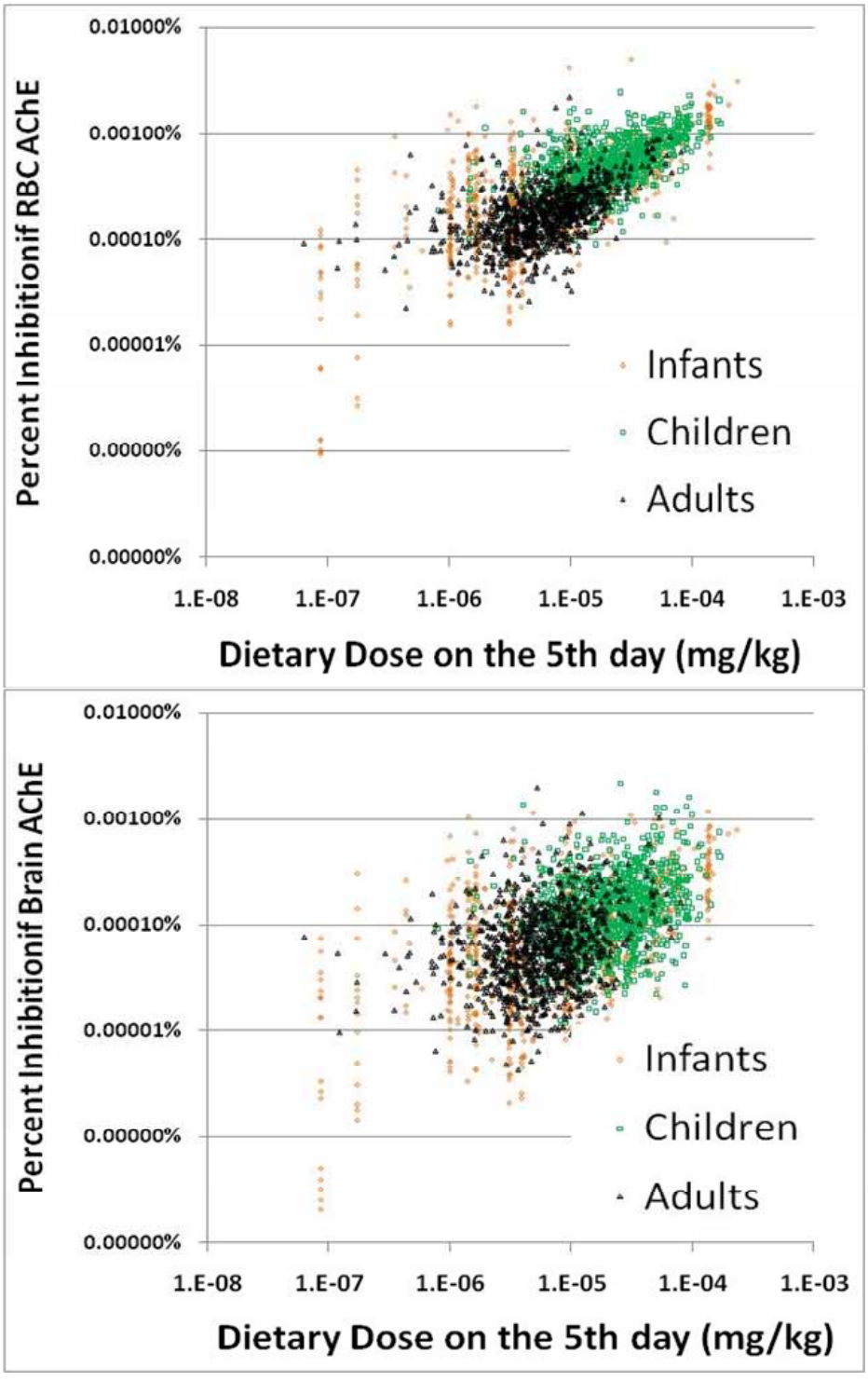

Figure 60. Predicted RBC and brain AChE inhibition on the 5th day of simulated daily dietary exposures in 1,000 adults (30 years), 1,000 children (3 years), and 1,000 infants (6 months).

As discussed in Section 7 of this report, by day five of a simulation, the model predictions should reflect the impact of an individual's current day's dose and all of the individual's prior days' exposures (quasi steady-state). Thus these predictions should be a reflection of the current impact of dietary residues. The results of the modeling suggest that the current dietary exposures are resulting in blood levels of CPF that range from 10^{-7} to 10^{-4} µmoles/l in infants or 10 -0.01 ng/l (ppt). The range of levels is about five fold lower in adults or 2 - 0.002 ng/l (ppt). As indicated in Section 8, these levels are consistent with the limited monitoring data currently available. The RBC and brain inhibition on day 5 are less than 0.01% for all of the simulated individuals.

The vertically aligned clusters in the estimates for the infants are the result of the dietary exposure model predicting very similar doses for multiple infants. This may reflect dietary records indicating the consumption of standard amounts of a highly processed blended food (such a one jar of a specific type of baby food). The impact of this can also be seen in the "stair step" shape of the dose distribution for infants shown in Figure 43.

Figures 61 and 62 describe the relationship between the predictions of the impacts of dietary exposures in infants in the context of the dose response "clouds" presented in **Section 4**. Figure 61 overlays data on CPF and CPF-oxon presented in Figure 59 onto Figure 40. Figure 62 over lays data from figure 60 on to the data presented in Figures 41 and 42).

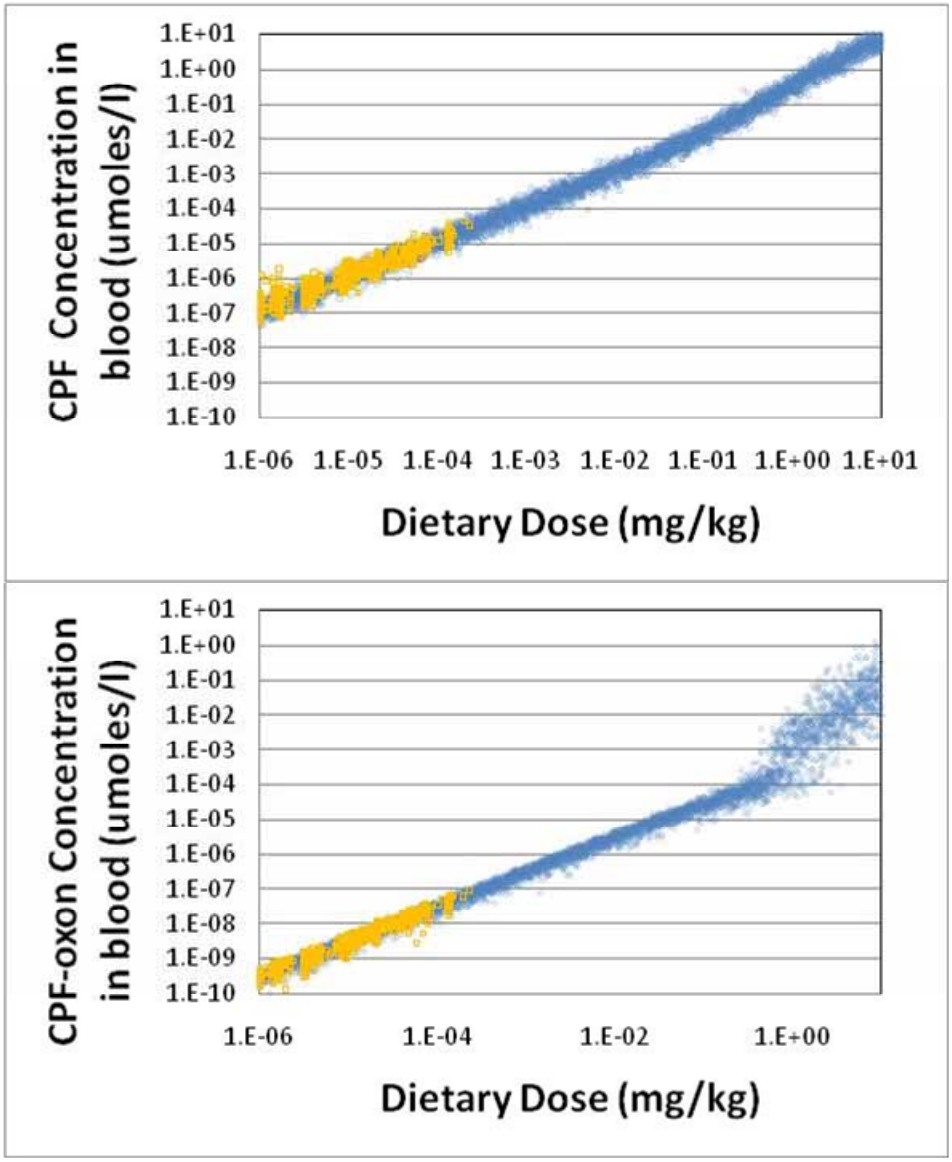

Figures 61. Predicted blood concentrations of CPF and CPF-oxon RBC predicted to occur on day 5 of a 5-day simulation of dietary exposures (yellow) and after a single exposure to a wide range of doses (blue) in infants (6 months).

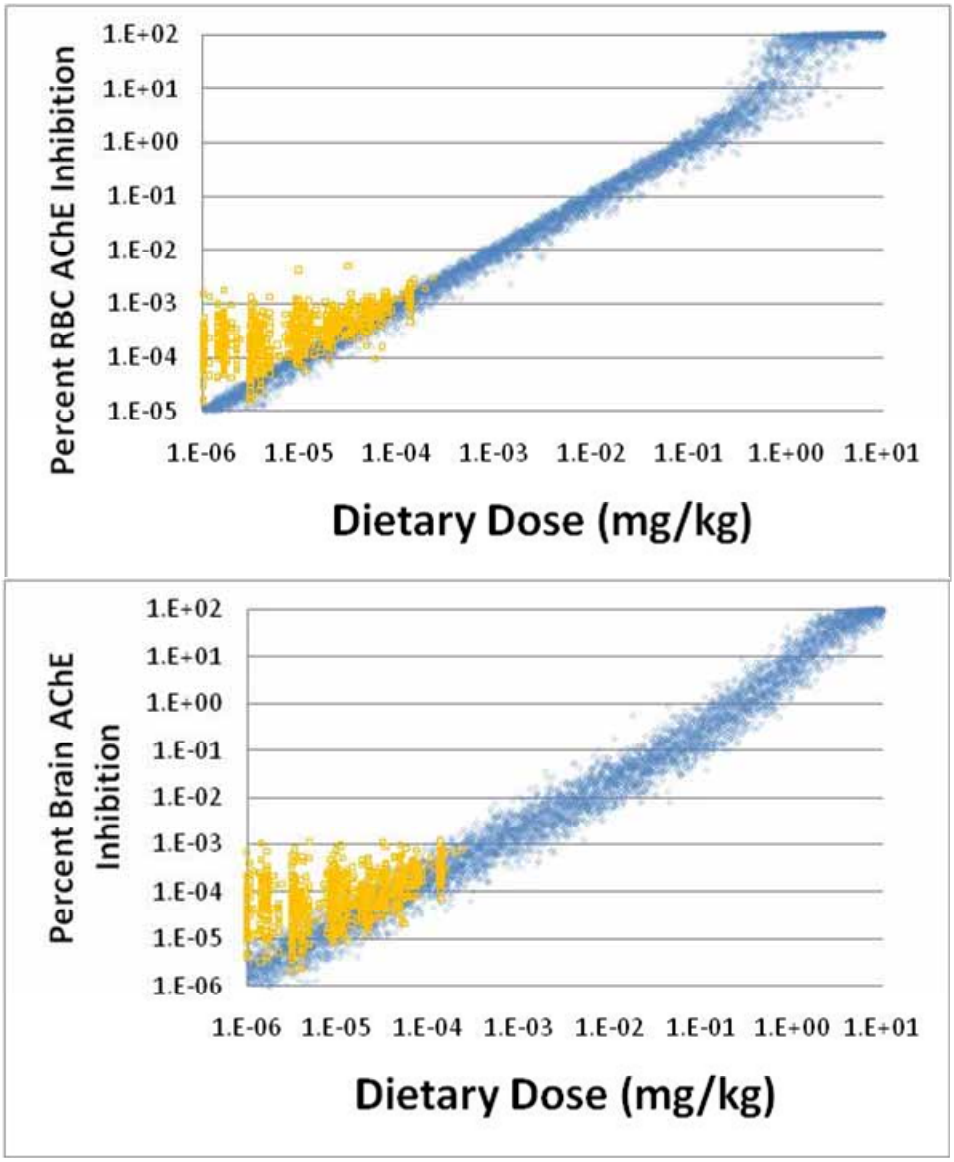

Figures 62. Predicted RBC and brain AChE inhibition predicted to occur on day 5 of a 5 day simulation of dietary exposures (yellow) and after a single exposure to a wide range of doses (blue) in infants (6 months).

The comparisons presented in Figures 61 and 62 place the predicted impacts of diet into the framework of predictions of human response and show the impact of longitudinal exposures on the response. The predictions of the blood levels of CPF and CPF-oxon look very similar to the levels predicted by a single dose (Figure 61). In contrast, the RBC and brain inhibition in Figure 62 are often higher than expected from a single day's dose. This

increase is due to residual inhibition predicted to carry over from prior days. As discussed in Section 7, this impact is limited to lower dietary doses. At dietary doses at the top end of the range, the observed responses on day 5 are similar to the responses from a single day's dose. While not shown, similar patterns were observed for children and adults.

Section summary

The most straightforward approach for the use of the source-to-outcome model is to use the model to assess the impacts of current dietary residue levels on public health. This can be done by using the relevant data on dietary residues and predicting the impact on AChE for different populations. Such an evaluation would consider factors such as the relationship between various levels of inhibition of RBC and brain AChE and the frequency of the occurrence of apical effects in populations of different ages. In addition, the confidence in the predictions of the source-to-outcome model needs to be considered.

In this section, we have attempted to use the source-to-outcome model in a fashion that would support this use. Specifically,

1. The model has been used to determine the distribution of impacts of current exposures in three age populations, adults, children, and infants.
2. The model was run for a sufficient duration such that the predictions for the population reflects quasi-steady state conditions.
3. Data were generated on multiple key events that could be used to evaluate the potential for the occurrence of apical effects from inhibition of cholinesterase.
4. Supporting information on CPF and CPF-oxon pharmacokinetics are provided.
5. Data are provided in a format that discloses the variation in response as well as the variation in dose.

This source to outcome model has enabled us to simulate effects from exposures well below outcomes that can be visualized experimentally. AChE activity is sufficiently variable that it is difficult to demonstrate treatment-related inhibition less than 10 or 20%. Therefore, the model was used to estimate the effects the might occur following much

lower exposures. Finally, the value of the source-to-outcome model is accentuated when the model is used as a tool for exploring the processes that drive the source-to-outcome pathway rather than just as a risk "calculator" where the only thing of interest is the "answer". In this paper we have used the source-to-outcome model to explore several issues of importance for the evaluation of CPF. These include the role that longitudinal exposure to time-varying doses plays in estimating upper bounds to risk (Section 7), the evidence that variations in metabolism rather than physiology or level of physical activity are important drivers of sensitivity to CPF's effects on cholinesterases (Section 4), and the finding that interindividual variation in RBC inhibition is dose-dependent.

10 Using the source-to-outcome model to estimate compound and age-specific uncertainty factors

Section overview

The source-to-outcome model was also used to derive values for the interspecies (UF_A) and interindividual[15] (UF_H) uncertainty factors for two age groups. EPA and other organizations have developed guidance for the replacement of all or part of the values of the interindividual UF_H and UF_A using chemical specific data and PBPK models (Lipscomb, 2006; WHO, 2006). This guidance indicates that each uncertainty factor can be divided into two sub-factors, one for kinetic and a second for the dynamic components of the uncertainty factor. Unlike PBPK models, the source-to-outcome model predicts both measures of internal dose (CPF and CPF-oxon in blood) and inhibition of RBC and brain AChE. Thus the source-to-outcome model addresses both the kinetic and dynamic portions of the uncertainty factors. As a result, values are proposed for the total (kinetic plus dynamic portions) of UF_H and UF_A.

In this section we explore how the source-to-outcome model could be used to determine the compound and age-specific UF_H and UF_A. We make a number of assumptions that have regulatory decision-making implications, although such considerations are outside the remit of this paper and its focus. These assumptions are made for the purpose of this illustration only. For example, we use the key event of RBC AChE inhibition as the basis for the point of departure (POD). The aPAD for CPF is currently set using three uncertainty factors, the 10 for the UF_A, 10 for the UF_H, and for infants, children, and women of childbearing age a value of 10 for the FQPA factor (Figure 63).

15 Also referred to as the intraspecies uncertainty factor.

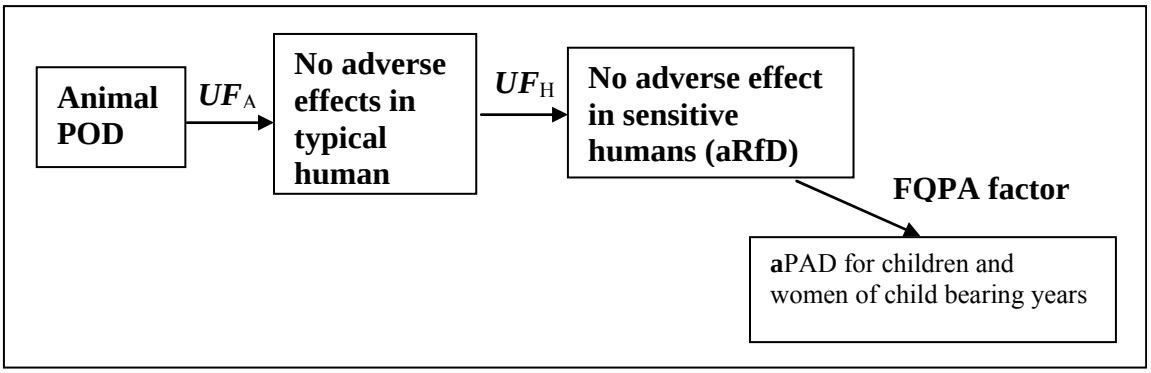

Figure 63. The relationship between the POD, aRfD, and aPAD

The equation used to set the values for the aRfD and aPAD are:

$$aRfD = \frac{PoD}{UF_A \times UF_H}$$

$$aPAD = \frac{RfD}{FQPA\_factor}$$

Historically, the interindividual uncertainty factor also considered sensitive subpopulations including subpopulations based on age. The source-to-outcome model allows the development of age-specific uncertainty factors that extrapolate from age-specific animal data to humans of a corresponding age. In this project we develop age-specific values for two age groups; adults 30 years old and infants six months of age. Because the model allows calculation of uncertainty factors at specific ages, there is no need to consider extrapolation from adults to children as part of the determination of the interindividual uncertainty factor. While not explored here, this approach envisions the future development of values of UF_A and UF_H for other ages (e.g., the elderly).

Example development of interspecies (UF_A) uncertainty factor for adults and infants

For the purpose of illustrating how the results from a source-to-outcome model can be used to derive interspecies factors, this project investigates the values for UF_A based on the premise that a that the POD is based on RBC AChE inhibition data from the recent study by Marty and Andrus (2010). Attachment G provides a copy of the study summary for this effort.

The recent study by Marty and Andrus (2010) measured blood and brain AChE inhibition in rats. The study included measurements with adults and pups (PND 11). In this analysis we focus on the results of the one day study (acute exposure). In this study adult rats were administered a single dose of the compound using corn oil as vehicle. As discussed above, the effects from dietary exposures can be treated as individual acute exposures if the focus of the assessment is to characterize risks from the highest exposed individuals. This suggests that the use of single dose studies is appropriate for evaluating cholinesterase inhibition associated with CPF.

In the Marty and Andrus study, initial scoping studies identified the time to peak inhibition for the animals. The animals were sacrificed at the time of peak inhibition and RBC and brain AChE inhibition levels were determined. BMD and BMDL doses for RBC and brain AChE inhibition were developed using these data (Reiss *et al.*, 2010). A copy of this report is provided in Attachment H.

The acute RBC AChE inhibition $BMDL_{10}$ is assumed to be the basis for the POD for both adults and pups. Separate analyses were performed on male and female pups; the lower of the two gender specific values of $BMDL_{10}$ (males) reported by (Reiss *et al.*, 2010) is used as the basis of this analysis. The final values of the POD for adults and pups are 0.52 mg/kg and 0.36 mg/kg respectively.

The adult rat and pup data (large red squares) are overlaid on the dose response "clouds" of adults and infants (originally presented in Figures 41 and 42 in Section 4) to show the relationship between the animal data and the predicted responses in humans (Figure 64). The animal data reflects the findings in dose groups where the animals were

statistically different from controls. At lower doses, RBC AChE inhibition was not statistically significant. The simulated dose response in adult and infant humans and the observed responses in the test animals are similar and fall within the range of variation in human response. The typical infant appears to be more sensitive than the rat pup. The typical human adult is also more sensitive than the adult rat.

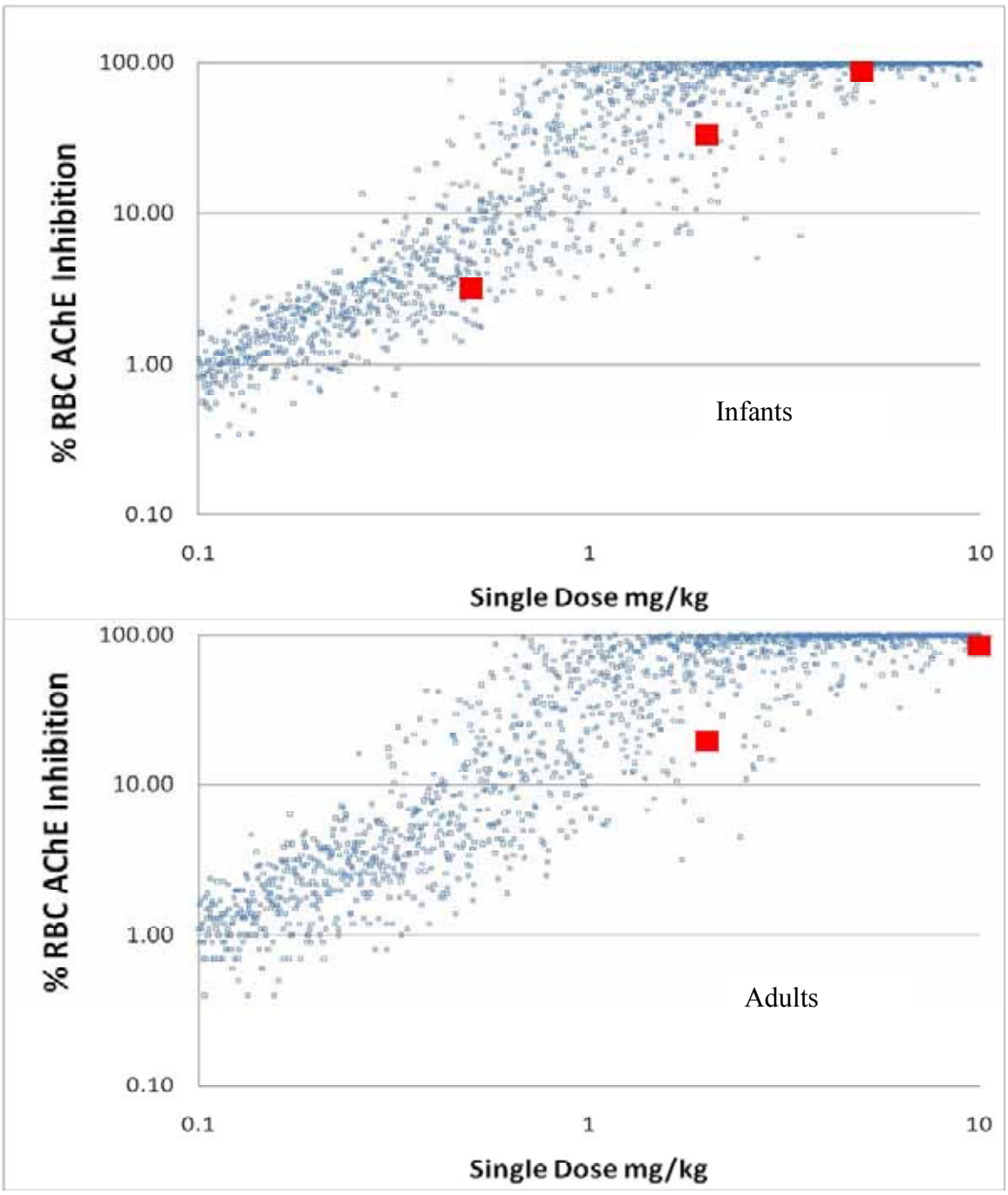

Figure 64. Comparison of test animal data (Marty and Andrus, 2010) and simulations of variation in human response. The blue cloud is repeated from earlier figures and presents the outline of CPF response in populations of infants (6 months) and adults (30 years) exposed to a range of doses. Test animal data in adult rats and PND 11 rat pups indicated by large red squares. The data suggest that animals are less sensitive than most, but not all humans.

In this analysis, the value of the interspecies uncertainty factor UF_A is determined by matching the simulation of humans to the specific dose regime, metric of response, and subsequent data analysis used to derive the POD values. This approach allows a direct comparison of the dose associated with the POD as measured in the test animal to the dose causing a corresponding effect in humans. The data on PND 11 pups are used to estimate a value for UF_H for infants and the data on adult rats are used to estimate UF_H values for adults.

In this illustration the source-to-outcome models are used to match the animal data by making the following decisions:

1. Since the animal study is a single bolus dose in adults and pups, the source-to-outcome model assumes a single dose.
2. The study design attempted to identify the peak levels of inhibition in the animals; therefore, the simulation models are used to determine peak levels of inhibition in each simulated individual.
3. The study design included eight test animals per dose group. The mean AChE activity levels in the group were compared to AChE activities in controls. Therefore, the simulation model is used to create sets of eight humans and the mean inhibition for the group is determined.
4. The values of BMD_{10} and $BMDL_{10}$ for RBC AChE inhibition were derived using the general dose response model developed by EPA for the organophosphate cumulative risk assessment (Reiss *et al.* 2010). Therefore, the source-to-outcome model is used to determine doses that correspond to the BMD and BMDL values. Specifically,

    a. 4,000 groups of 8 individuals are created and their response of each individual to a specific dose is modeled using the Variation PBPK/PD model. The mean inhibition levels for each group of humans is then determined. The results are a distribution of group mean responses.

    b. This process is repeated for multiple doses (D_i).

c. The median value of the distribution of the group means, (M_i) for dose D_i is assumed to be equivalent to the BMD_{Mi}.

d. Values of BMD_{10} are determined by interpolation from values of M_i greater and less than 10%.

e. A similar approach is used for deriving the equivalent to $BMDL_{10}$. In the case of BMDL the upper 95 percentile of the distribution of group means is used instead of the median estimate.

The results of this exercise are dose estimates that directly correspond to the BMD and BMDL. Assuming that the value of $BMDL_{10}$ is used as the hypothetical POD, the value of UF_A is given by:

$$UF_A = \frac{PoD}{PoD_H}$$

where, POD is the $BMDL_{10}$ in either adult rats or pups and POD_{10} is the equivalent $BMDL_{10}$ in simulated output of the source-to-outcome models for adults and infants.

The simulations for infants are overlaid on the one day dose response cloud for RBC inhibition (Figure 65). The Variation model was run for groups of 5,000 infants at doses of 0.1, 0.2, 0.5, and 1.0 mg/kg. The ranges of RBC inhibition at each dose are presented in the figure as a series of vertical lines, one at each of the four doses. A series of 5,000 groups of 8 individuals were created by sampling from the 5,000 individuals (with replacement). The means for the 5,000 groups are plotted for each dose. These appear as sets of black circles at the four doses. Note that the ranges of responses in the distribution of the 8-person group means are smaller than the range of responses of the individuals. The reason for this is that the variation in mean responses in groups of 8 is less than for single individuals (regression to the mean).

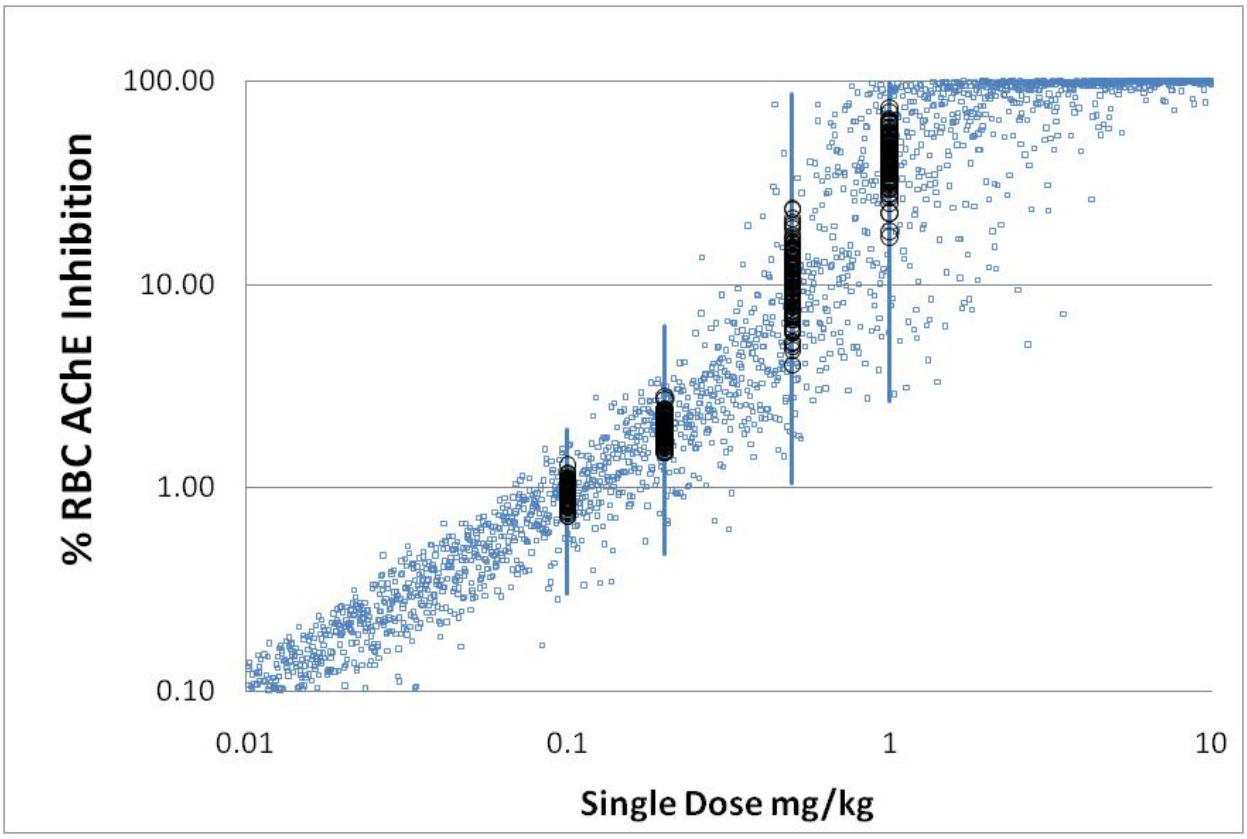

Figure 65.The range of % RBC inhibition in different simulated populations of infants exposed to a single daily dose of CPF. The blue cloud is repeated from earlier figures and presents the outline of CPF dose response in populations of infants exposed to a range of doses. The ranges of predicted responses for 5,000 simulated infants at four dose rates (0.1, 0.2, 0.5, and 1.0 mg/kg) are given by the vertical light blue lines. The black circles show the range of mean responses in groups of eight infants (corresponding to the groups of eight test animals used in the Marty and Andrus, 2010).

The values of the human equivalent of $BMDL_{10}$ are determined by interpolation. In Figure 66 the same data on the distributions of the individual and mean values for groups of 8 are plotted. This plot is not in log-log space as is the prior plot. The 95th percentiles of the distributions of the 8-person group mean responses at each dose are identified and a solid line is created that connects the values. The human equivalents of the $BMDL_{10}$ is determined to be 0.33 mg/kg, based on interpolation of the 95th percentile values of the

distribution of the observed at 0.2 and 0.5 mg/kg to determine the dose that causes a 10% inhibition in 95 % of the groups. The value is marked by a thick red circle on the figure.

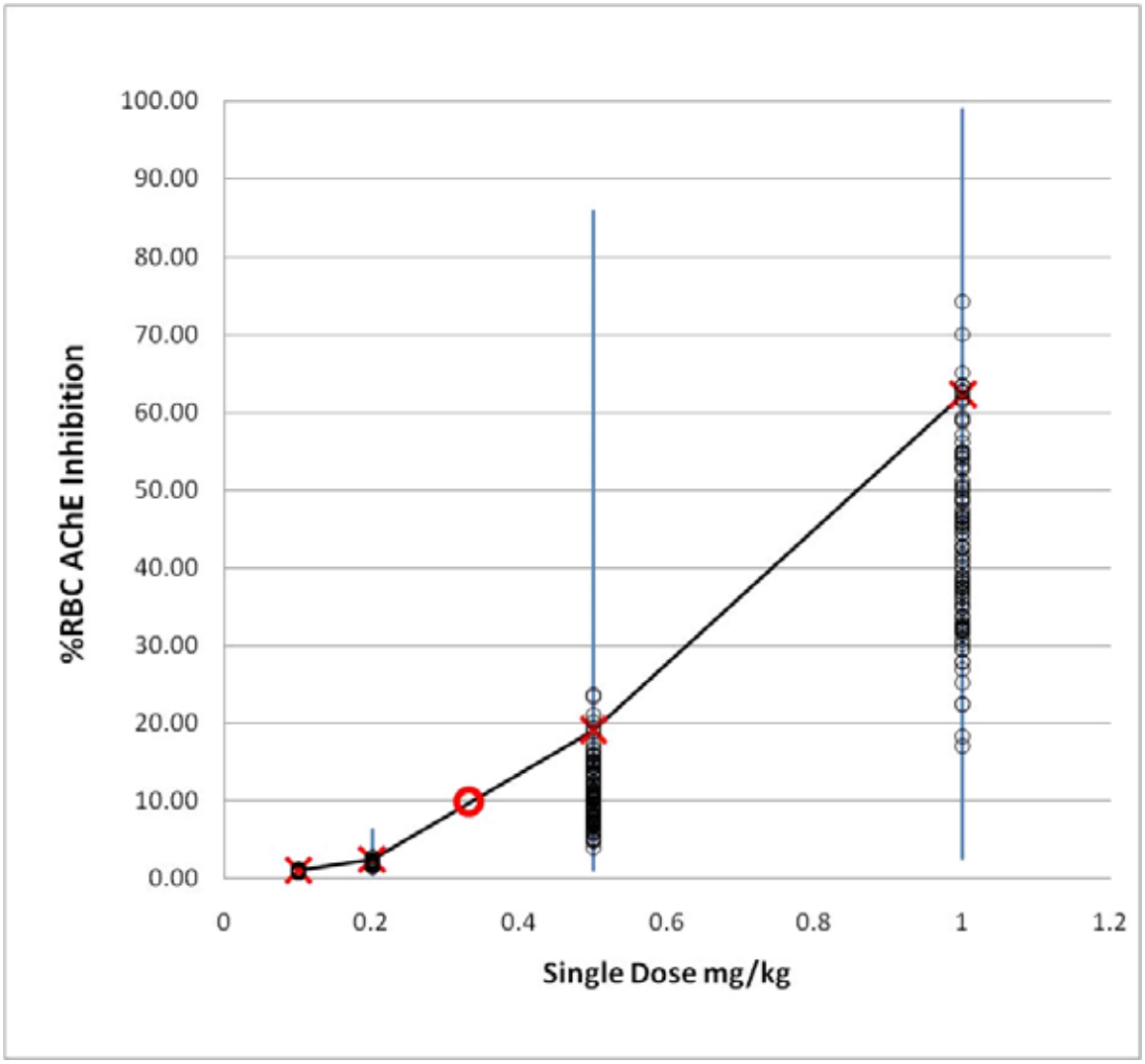

Figure 66. Derivation of human equivalent dose to an animal BMDL10. The mean responses in groups of eight infants (corresponding to the groups of eight test animals used in the Marty and Andrus, 2010) are designated by the black circles with the corresponding ranges of predicted responses for the simulated infants given by the vertical lines (blue). The 95th percentile values of group means (shown by the red Xs and connected by the solid black line) were used to calculate the $BMDL_{10}$ in the test animals (0.33 mg/kg, marked with the red circle).

Using the reported BMDL in rats and the value of the human equivalent, the value of UF_A for infants is:

UF_A (Infants) = 0.36 (mg/kg/d) / 0.33 (mg/kg/d)

UF_A (Infants) = 1.1

While not shown, the value of UF_A for adults derived using this method is 1.7.

Example development of interindividual (UF_H) uncertainty factor for adults and infants

The interindividual uncertainty factor is intended to address differences in the relative sensitivity of individuals to CPF for the different age groups. This factor is defined using the source-to-outcome model's ability to assess variation in sensitivity in different age groups at different doses. (Lipscomb, 2006) and (WHO, 2006) recommend that the value of the UF_A should be determined based on the distribution of the ratios of the administered doses that produce the same internal dose at the target organ across individuals. Separate ratios should be determined for a variety of percentiles of the populations. This illustration uses the 95th and 99th percentiles.

The determination of the UF_H also requires an assumption of a level of RBC inhibition is acceptable in the general population. In this assessment a value of 10% is used. Other values could be used.

The values for UF_H for the two age groups are calculated based on two endpoints. The first is the human equivalent of the $BMDL_{10}$. This endpoint was established in the definition of UF_A in the prior subsection. The second measure is the dose that does not result in a peak RBC AChE inhibition of more than 10%. In this assessment such a dose is considered to be a POD for sensitive humans ($POD_{sensitiveH}$). The value of UF_A is then defined as the ratio of the human equivalent of the $BMDL_{10}$ to a dose where there is a 95% (or 99%) confidence that an individual has less than a 10% peak RBC AChE inhibition (POD for the sensitive human or $POD_{sensitiveH}$).

$$UF_H = \frac{PoD_H}{PoD_{SenstiveH}}$$

The values of $POD_{sensitiveH}$ were determined by calculating the level of inhibition for the 95th and 99th percentiles of the peak RBC AChE inhibition levels for the 5,000 individuals. The method used to determine the values of $POD_{sensitiveH}$ was also used to calculated the levels of inhibition for the 95 and 99th percentiles of the population at different doses and then to interpolate to find the doses where 95 and 99% of the population would have less than a 10% peak inhibition.

Figure 67 shows how this interpolation was performed. The data from Figure 62 is again presented; however, the 95th and 99th percentiles of the values of the response for the individuals are determined and connected by dotted lines. The doses that occur where these lines cross the 10% inhibition level are the two values of $POD_{sensitiveH.}$

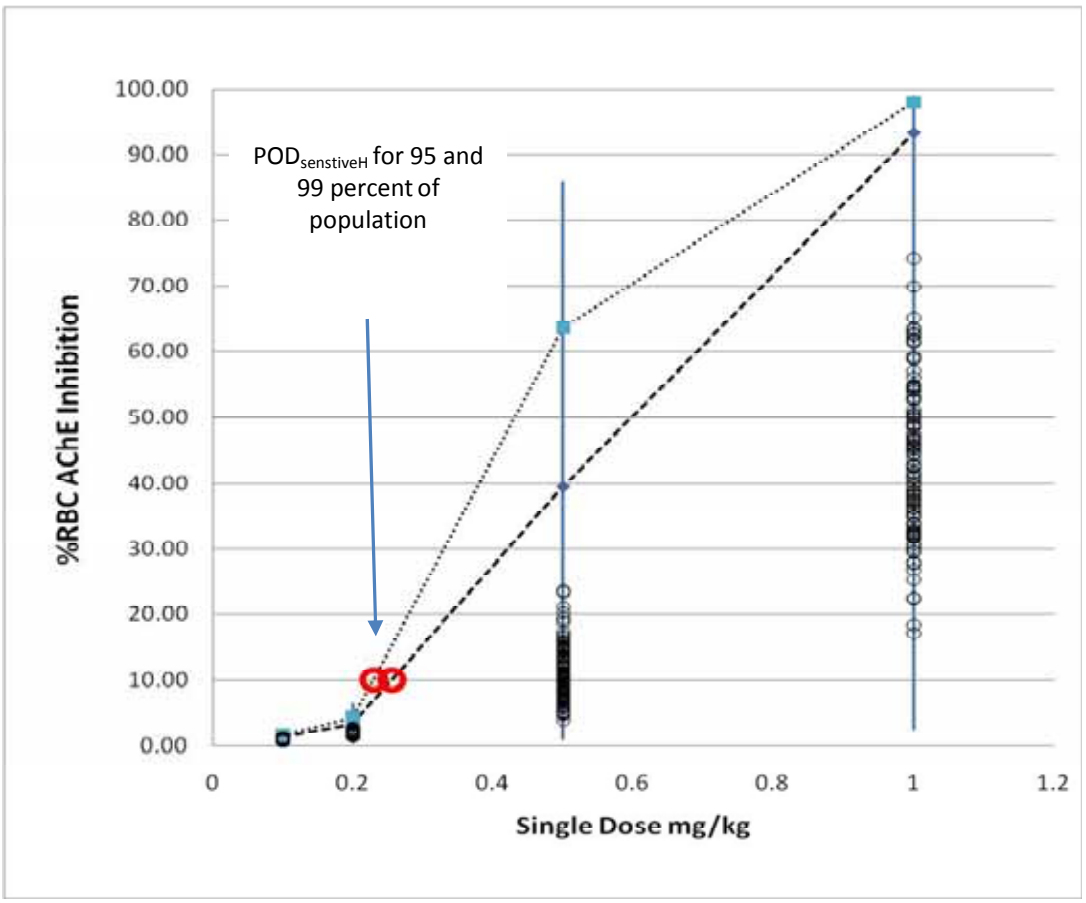

Figure 67. Determination of $POD_{sensitiveH}$ by interpolation of values of the 95 and 99th percentiles of the responses in simulated infants at various doses. The ranges of individuals' responses at four dose rates (0.1, 0.2, 0.5, and 1.0 mg/kg) are given by the vertical light blue lines. The black circles show the range of mean responses in groups of eight infants (see the derivation of UF_A above). The thick red circles indicate the single daily doses that are predicted to have peak RBC inhibitions of l0% or less for 95 and 99% of the population (0.24 and 0.22 mg/kg respectively) .

The values of $POD_{sensitiveH}$ for the 95th and 99th percentiles for both infants and adults (calculations not shown) are given in Table 9. The values of the POD_H were developed using the approach described in the previous portion of this section and are 0.30 mg/kg/d for adults and 0.33 mg/kg/d for the infants. Using the above equation and these doses, the values of UF_H were determined for the 95th and 99th percentiles of the population and for each age group and are given in Table 9. The values of UF_H for the 95th and 99th

percentiles are very similar. This occurs because the variation in response at doses of 0.1 to 0.3 mg/kg in both adults and infants are small (See Figures 42 and 43 in Section 4).

Table 9. Values of POD for sensitive humans and UF_H values for adults and infants

Adults (30 years)	
$POD_{SenstiveH}$ (95%)	$POD_{SenstiveH}$ (99%)
0.26 mg/kg	0.23 mg/kg
Infants (6 Months)	
$POD_{SenstiveH}$ (95%)	$POD_{SenstiveH}$ (99%)
0.24 mg/kg	0.22 mg/kg
Adults (30 years)	
UF_H (95%)	UF_H (99%)
1.3	1.4
Infants (6 Months)	
UF_H (95%)	UF_H (99%)
1.3	1.5

Section summary

In summary, the source-to-outcome models indicate that the two age groups of humans (adults and infants) have RBC AChE inhibition responses that are similar to the test animals. In fact, the animal data fall within the range of human variation in response. In addition, the level of variation in response across the populations of infants and adults are modest at doses that cause a 10% RBC inhibition level is small. As a result the predicted values for both UF_A and UF_H for both adults and infants are less than 2.

11 Summary

In this paper we have sought to describe the methodologies and data used to create a model that captures the events in the pathway that begins with data on residue levels and ends with predictions of cholinesterase inhibition across the U.S. population, a source-to-outcome model. As indicated in the introduction this is not a complete risk assessment for CPF and as such it does not purport to address all of the toxicological issues for the compound. The focus of the case study is on the use of linked exposure and PBPK/PD models to address the potential for the occurrence of apical effects that are produced by a specific mechanism, by a specific route of exposure, from a specific source.

The source-to-outcome model described in this case study consists of two commercially available software programs. The first component is a dietary software program. The dietary exposure software used here is CARES but any of the existing programs that can produce estimates of longitudinal dietary exposures could be used. The second program is the Variation model a program created to run on acslXtreme a publically available software platform for PBPK modeling.

The process for creation of the source-to-outcome model has been outlined in detail in the report and this process can be applied to other chemicals with other endpoints. This process begins by understanding the mode of action by which a chemical exerts its toxicity. Key events in the toxicity pathway are identified that are as close to the initial interaction between the initial biological targets/molecules in the body and the chemical or its active metabolite. Once the key events are determined, a PBPK/PD model is developed and used to predict the dose response for each key event (see Section 3).

With a PBPK/PD model of the dose to key event process in place, a sensitivity analysis is performed that identifies the factors that drive variation in response to a given dose of a chemical (see Section 4). These driving factors require data on interindividual variation across the population of interest. These data and data on correlation between

values in individuals are identified from the published literature or are created using *in vitro* measurements.

With these data, simulation models of the variation in response in the key event can be created (see Section 4). These models define dose and the individual in very specific ways. The exposure portions of the source-to-outcome models need to be matched to the specific needs of the PBPK/PD models of variation. In this project an existing dietary model was used to characterize exposure (see Section 5). The linkage between the two models was achieved by a careful consideration of physiology of the exposure event (Section 6) and data in human studies.

In the development of this project, one concept that has been repeatedly used is the need to tailor the level of complexity to the importance of a process. For example, earlier efforts to link diet and PBPK models have expended considerable resources on modeling the timing of exposures within a day (Xue, 2010). Our analysis of CPF indicated that the assumption that an entire dose on a single day occurred at one eating event was a reasonable first assumption. This allowed the project to avoid the complexity of modeling intakes over multiple eating events. In a similar fashion, we found that the level of activity had little impact on variation in metabolism or increased sensitivity to CPF's effects on AChE. Thus the modeling efforts did not include any attempt to model actual patterns of human activity using data such as activity diaries.

The evaluation of the uncertainty in a source-to-outcome model's predictions and the determination of the confidence that can be placed in the predictions is a challenge. The levels of the predictions of the model vary with the age, endpoint, and questions that the model attempts to answer. In Sections 3, 4, 5 and 8 we have investigated the ability of the model to address predictions of the change in AChE inhibition and interim findings such as distribution of daily dose, blood concentrations of parent and metabolites, and predictions of variation in physiology. These predictions can be evaluated using other modeled and measured data. In general, we have demonstrated that the various predictions of the source-to-outcome model are consistent with measured data in the literature. However, we also found that the model-to-measurement comparisons were limited by the relevance of the

measurement data. Data often came from small surveys from specific locations and limited age ranges (women of child bearing age), had significant confounding factors (other sources of TCPy in diet), or reflected exposures that differed from diet (e.g., worker studies). Because of this, we conclude that the final predictions of impacts of AChE in the general population are within an order of magnitude but additional representative data are required in order to determine if the models are in fact more precise.

Once the source-to-outcome model is completed, it can be used in a variety of ways. We believe that the value of a source-to-outcome model is fully realized when the model is used as a tool for exploring the processes that determine the source-to-outcome pathway rather than just as a risk "calculator." In this project the source-to-outcome model has been used in a number of ways and has demonstrated a number of novel and potentially valuable findings.

- The variation portion of the model was used to investigate the role of different factors in affecting adult and child sensitivity to CPF (see Section 4). The models found that variation in metabolism but not variation in physiology or level of physical activity were important for infants. For adults, variation in physiology had some effect but was still minor compared to metabolism.

- The source-to-outcome allowed the investigation of the impact of repeated doses of CPF on blood levels of CPF and CPF–oxon and the impact on cholinesterases (see Section 7). This work indicated that neither CPF nor CPF-oxon accumulated over time. The cumulative impact of RBC inhibition (inhibition seen at 1 day of dosing versus 30 days) was significant at doses of 0.5 mg/kg with as much as a 20-fold increase in response. But at the dose levels that currently occur from exposure to dietary residues the impact was much more modest (i.e., a 3-fold). In contrast increases in brain AChE inhibition were at most 3-fold across all doses.

- When day-to-day variation in dietary exposure was considered, the increase in impact from one to multiple days was found to be very small for dietary exposures (Section 7). The population reached quasi-steady state within 3 days. More importantly the impact of multi-day exposures was much smaller for individuals with high exposures. The

impact of dietary exposures on the RBC and brain AChE inhibition for these individuals was dominated (90% of the impact) by the dose received from a single day.

- Interspecies variation in response was investigated by comparing the predicted responses humans to the observed responses in rats. The findings suggest that rats are only slightly less sensitive than humans.

- Interindividual variation in response to CPF was explored using the Variation model. The impact on RBC AChE inhibition was found to be dose dependent. At dietary levels the difference between the responses of the typical and sensitive individual (resulting from differences in metabolism, physiology, and activity) was less than 2.

The source-to-outcome model was used to evaluate the impact of the current dietary exposure on RBC and brain AChE inhibition. This was done in two ways. First the model investigated the impacts in three age groups after quasi-steady state conditions were obtained (see Section 9). The peak inhibitions did not exceed 0.01% inhibition for either RBC or brain inhibition. The second way the models were used was to determine age-specific values for the interspecies and interindividual uncertainty factors (Section 10). This assessment found that models prediction of variation in response overlapped with the responses seen in recent animal studies (Attachment G). In addition, human variation in response was found to be modest (less than a factor of 2 between the responses in a typical adult or infant and a sensitive adult or infant) for doses that cause 10% or less RBC AChE inhibition in humans. As a result, the values of UF_A and UF_H calculated were small and ranged between 1 and 2.

The exercise in this paper has achieved the goals set out in the introduction. We have identified a key event, AChE inhibition, and constructed models of interindividual variation in both dose and response. The models have been evaluated and have been used to make quantitative predictions of the AChE inhibition in the exposed population using an example pesticide. In addition, the modeling has operated as a framework that has allowed diverse information from *in vitro* studies of metabolism, biomonitoring studies in humans, test animal data, and statistical tools to come together to provide quantitative guidance on the impacts posed by a chemical to the general U.S. population.

Acknowledgements

Early efforts on development of this project occurred as a result of an American Chemistry Council LRI project 'Demonstrating Scientific Advances in Human Health Risk Assessment Practice' (MTH-07-01), and thanks for the support of the ACC are warmly offered.

The authors acknowledge contributions to the experimental, modeling, and reporting phases of this project. For experimental contributions, we thank Dr. Susan Marty. For modeling contributions, we thank Dr. Carl Schnelle.

Attachments

Attachment A:

Report on *in vitro* human metabolism results, in draft manuscript format

Attachment B:

Philpott, P. (2009) "June 24-25, 2009 EPA Human Studies Review Board Meeting Report." Memo and final report (40 pages).

Attachment C:

Copy of Model code for: acslXtreme Lifestage model and associated m files

Attachment D:

Cleveland, C.B. (2010) "2010 Update of the Acute Dietary Risk Assessment for Chlorpyrifos." Dow AgroSciences. Final report 101760 (140 pages).

Attachment E:

Copies of inputs files used in dietary models

Attachment F:

Copies of input files for PBPK/PD model runs

Attachment G:

Marty, M.S. and Andrus, A.K. (2010) "Comparison of Cholinesterase (ChE) Inhibition in Young Adult and Preweanling CD Rats after Acute and Repeated Chlorpyrifos or Chlorpyrifos-oxon Exposures." Dow AgroSciences. Public release summary (7 pages).

Attachment H:

Reiss, R., *et al.* (2010) "Benchmark Dose Modeling for Cholinesterase Inhibition from Exposure to Chlorpyrifos and Chlorpyrifos-Oxon." Dow AgroSciences. Public release summary (4 pages).

References

Akaike, H., 1974. A New Look at the Statistical Model Identification. I.E.E.E. Transactions on Automatic Control. AC 19**,** 716-723.

Akaike, H., 1976. Canonical Correlation Analysis of Time Series and the Use of an Information Criterion. in: Lainotis, R. K. M. a. D. G., (Ed.), System Identification: Advances and Case Studies. Academic Press, New York, pp. 52-107.

Albers, J. W., et al., 2010. Paraoxonase status and plasma butyrylcholinesterase activity in chlorpyrifos manufacturing workers. Journal of Exposure Science and Environmental Epidemiology. 20**,** 79-100.

Alcorn, J., et al., 2007. Evaluation of the assumptions of an ontogeny model of rat hepatic cytochrome P450 activity. Drug Metab Dispos. 35**,** 2225-31.

Alcorn, J., McNamara, P. J., 2002. Ontogeny of hepatic and renal systemic clearance pathways in infants - Part I. Clinical Pharmacokinetics. 41**,** 959-998.

Amitai, G., et al., 1998. Inhibition of acetylcholinesterase and butyrylcholinesterase by chlorpyrifos-oxon. Biochemical Pharmacology. 56**,** 293-299 %U http://www.ncbi.nlm.nih.gov/pubmed/9744565.

Andersen, M. E., 1995. Development of physiologically based pharmacokinetic and physiologically based pharmacodynamic models for applications in toxicology and risk assessment. Toxicology Letters. 79**,** 35-44.

Andersen, M. E., 2003. Toxicokinetic modeling and its applications in chemical risk assessment. Toxicology Letters. 138**,** 9-27.

Andersen, M. E., et al., 1994. Gas uptake studies of deuterium isotope effects on dichloromethane metabolism in female B6C3F1 mice in vivo. Toxicology and Applied Pharmacology. 128**,** 158-165.

Bakke, J. E., Price, C. E., 1976. Metabolism of O,O-dimethyl-O-(3,5,6-trichloro-2-pyridyl) phosphorothioate in sheep and rats and of 3,5,6-trichloro-2-pyridinol in sheep. Journal of Environmental Science and Health. Part. B, Pesticides, Food Contaminants, and Agricultural Wastes. 11**,** 9-22 %U http://www.ncbi.nlm.nih.gov/pubmed/58885.

Ballantyne, B., Marrs, T. C., 1992. Clinical and experimental toxicology of organophosphates and carbamates. Butterworth Heinemann %@ 9780750602716.

Barr, D., Ananth CV, Yan X, Lashley S, Smulian JC, Ledoux TA, Hore P, Robson MG., 2010. Pesticide concentrations in maternal and umbilical cord sera and their relation to birth outcomes in a population of pregnant women and newborns in New Jersey. Science of The Total Environment. 408**,** 790-795.

Barr, D. B., et al., 2005. Concentrations of selective metabolites of organophosphorus pesticides in the United States population. Environmental Research. 99**,** 314-326.

Barr, D. B., Angerer, J., 2006. Potential uses of biomonitoring data: A case study using the organophosphorus pesticides chlorpyrifos and malathion. Environmental Health Perspectives. 114**,** 1763-1769.

Barter, Z. E., et al., 2008. Covariation of Human Microsomal Protein Per Gram of Liver with Age: Absence of Influence of Operator and Sample Storage May Justify Interlaboratory Data Pooling. Drug Metabolism and Disposition. 36**,** 2405-2409.

Bjorkman, S., 2005. Prediction of drug disposition in infants and children by means of physiologically based pharmacokinetic (PBPK) modelling: theophylline and midazolam as model drugs. Br J Clin Pharmacol. 59**,** 691-704.
Blesch, K. S., et al., 2003. Clinical pharmacokinetic/pharmacodynamic and physiologically based pharmacokinetic modeling in new drug development: the capecitabine experience. Invest New Drugs. 21**,** 195-223.
Bois, F., Jamei M, Clewell H, 2010. PBPK modelling of inter-individual variability in the pharmacokinetics of environmental chemicals. Toxicology. doi:10.1016/j.tox.2010.06.007.
Bois, F. Y., 1999. Analysis of PBPK models for risk characterization. Ann.N.Y.Acad.Sci. 895**,** 317-337.
Brehrman RE, K. R., Jenson HB,, 2000. Nelson Textbook of Pediatrics 16th Edition. W.B. Saunders, Philadelphia.
Brown DM, D. M., Lindsted SL, Rhomber LR, Belites RP, 1997. Physiological Parameter Values for Physiologically Based Pharmacokinetic Models,. Toxicology and Industrial Health, . 13**,** 77.
Busby-Hjerpe, A. L., et al., 2010. Comparative pharmacokinetics of chlorpyrifos versus its major metabolites following oral administration in the rat. Toxicology. 268**,** 55-63.
Carr, R. L., Nail, C. A., 2008. Effect of different administration paradigms on cholinesterase inhibition following repeated chlorpyrifos exposure in late preweanling rats. Toxicological Sciences. 106**,** 186-192.
Chambers, J. E., Chambers, H. W., 1989. Oxidative desulfuration of chlorpyrifos, chlorpyrifos-methyl, and leptophos by rat brain and liver. Journal of Biochemical Toxicology. 4**,** 201-203 %U http://www.ncbi.nlm.nih.gov/pubmed/2481746.
Chambers, J. E., Levi, P. E., 1992. Organophosphates: chemistry, fate, and effects. Academic Press %@ 9780121673451.
Chambers, J. E., et al., 1994. Role of detoxication pathways in acute toxicity levels of phosphorothionate insecticides in the rat. Life Sciences. 54**,** 1357-1364 %U http://www.ncbi.nlm.nih.gov/pubmed/7514706.
Chiu, W. A., et al., 2007. Evaluation of physiologically based pharmacokinetic models for use in risk assessment. Journal of Applied Toxicology. 27**,** 218-237.
Choi, K., et al., 2006. Metabolism of chlorpyrifos and chlorpyrifos oxon by human hepatocytes. Journal of Biochemical and Molecular Toxicology. 20**,** 279-291 %U http://www.ncbi.nlm.nih.gov/pubmed/17163483.
Clewell, H. J., et al., 2005. Evaluation of physiologically based pharmacokinetic models in risk assessment: An example with perchloroethylene. Critical Reviews in Toxicology. 35**,** 413-433.
Cole, T. B., et al., 2005. Toxicity of chlorpyrifos and chlorpyrifos oxon in a transgenic mouse model of the human paraoxonase (PON1) Q192R polymorphism. Pharmacogenet.Genomics. 15**,** 589-598.
Conolly, R. B., et al., 2004. Human respiratory tract cancer risks of inhaled formaldehyde: Dose-response predictions derived from biologically-motivated computational modeling of a combined rodent and human dataset. Toxicological Sciences. 82**,** 279-296.
Corley, R. A., et al., 2005. DEVELOPMENT OF A PHYSIOLOGICALLY BASED PHARMACOKINETIC MODEL FOR ETHYLENE GLYCOL AND ITS

METABOLITE, GLYCOLIC ACID, IN RATS AND HUMANS. Toxicological Sciences.
Costa, L. G., et al., 2005. Modulation of paraoxonase (PON1) activity. Biochem Pharmacol. 69, 541-50.
Croom, E. L., et al., 2010. Human variation in CYP-specific chlorpyrifos metabolism. Toxicology. 276, 184-91.
Crop Life America, 2002. Cumulative and Aggregate Risk Evaluation System, Technical Manual.
Curwin, B. D., et al., 2007. Urinary pesticide concentrations among children, mothers and fathers living in farm and non-farm households in iowa. Ann Occup Hyg. 51, 53-65.
Davis, K. A., et al., 2009. Racial Differences in Paraoxonase-1 (PON1): A Factor in the Health of Southerners? Environmental Health Perspectives. 117, 1226-1231.
DeWoskin, R. S., Thompson, C. M., 2008. Renal clearance parameters for PBPK model analysis of early lifestage differences in the disposition of environmental toxicants. Regulatory Toxicology and Pharmacology. 51, 66-86.
Dixit, R., et al., 2003. Toxicokinetics and physiologically based toxicokinetics in toxicology and risk assessment. Journal of Toxicology and Environmental Health-Part B-Critical Reviews. 6, 1-40.
Durango Software, DEEM (TM) dietary exposure analysis system Vol. 2010, 2010, pp. Web page of Durango software.
Eaton, D. L., et al., 2008. Review of the toxicology of chlorpyrifos with an emphasis on human exposure and neurodevelopment. Crit Rev Toxicol. 38 Suppl 2, 1-125.
el Masri, H. A., et al., 1995. Physiologically based pharmacokinetic/pharmacodynamic modeling of chemical mixtures and possible applications in risk assessment. Toxicology. 105, 275-282.
Foxenberg, R. J., et al., 2007. Human hepatic cytochrome P450-specific metabolism of parathion and chlorpyrifos. Drug Metabolism and Disposition. 35, 189-193.
Furlong, C. E., et al., 2005. Role of paraoxonase (PON1) status in pesticide sensitivity: genetic and temporal determinants. Neurotoxicology. 26, 651-659.
Furlong, C. E., et al., 2000. The PON1 gene and detoxication. Neurotoxicology. 21, 581-587.
Garabrant, D. H., et al., 2009. Cholinesterase inhibition in chlorpyrifos workers: Characterization of biomarkers of exposure and response in relation to urinary TCPy. J Expo Sci Environ Epidemiol. 19, 634-42.
Gearhart, J. M., et al., 1993. Variability of physiologically based pharmacokinetic (PBPK) model parameters and their effects on PBPK model predictions in a risk assessment for perchloroethylene (PCE). Toxicology Letters. 68, 131-144.
Ginsberg, G., Neafsey P, Hattis D, Guyton KZ, Johns DO, Sonawane B., 2010. Genetic polymorphism in paraoxonase 1 (PON1): Population distribution of PON1 activity. Journal Toxicol Environ Health B Crit Rev. . 12, 34.
Griffin, P., et al., 1999. Oral and dermal absorption of chlorpyrifos: a human volunteer study. Occupational and Environmental Medicine. 56, 10-13 %U http://www.ncbi.nlm.nih.gov/pubmed/10341740.
Grigoryan, H., et al., 2009. Mass spectral characterization of organophosphate-labeled lysine in peptides. Analytical Biochemistry. 394, 92-100 %U http://www.ncbi.nlm.nih.gov/pubmed/19596251.

Grigoryan, H., et al., 2008. Mass spectrometry identifies covalent binding of soman, sarin, chlorpyrifos oxon, diisopropyl fluorophosphate, and FP-biotin to tyrosines on tubulin: a potential mechanism of long term toxicity by organophosphorus agents. Chemico-Biological Interactions. 175**,** 180-186 %U http://www.ncbi.nlm.nih.gov/pubmed/18502412.

Hellmig S, V. S. F., Gadow C, Katsoulis S, Hedderich J, Fölsch UR, Stüber E, 2006. Gastric emptying time of fluids and solids in healthy subjects determined by 13C breath tests: influence of age, sex and body mass index. Journal of Gastroenterology and Hepatology 21**,** 6.

ICRP, 2003. Basic Anatomical and Physiological Data for Use in Radiological Protection: Reference Values, 89.

ILSI, Cumulative and Aggregate Risk Evaluation System (CARES)™. Vol. 2009, 2009.

Janssen, I., et al., 2000. Skeletal muscle mass and distribution in 468 men and women aged 18-88 yr. J Appl Physiol. 89**,** 81-8.

Johnson, T. N., et al., 2006. Prediction of the clearance of eleven drugs and associated variability in neonates, infants and children. Clinical Pharmacokinetics. 45**,** 931-956.

Kaushik, R., et al., 2007. Concentration-dependent interactions of the organophosphates chlorpyrifos oxon and methyl paraoxon with human recombinant acetylcholinesterase. Toxicology and Applied Pharmacology. 221**,** 243-250.

Kisicki, J. C., et al., A Rising Dose toxicology Study to Determine the No-Observable-Effect-Levels (NOEL) for Erythrocyte Acetylcholinesterase (AChE Inhibitino and Cholinergic Signs and Symptoms of Chlorpyrifos at Three Dose levels. The Toxicology Research Laboratory: Health and Environmental Research Laboratories, The DOW Chemical Company, 1999.

Koukouritaki, S. B., et al., 2004. Developmental expression of human hepatic CYP2C9 and CYP2C19. Journal of Pharmacology and Experimental Therapeutics. 308**,** 965-974.

Kousba, A., et al., 2004. In vitro interactions between organophosporous pesticides and consequences of pre-treatment with nicotine and alcohol on in vitro pesticide metabolism in rats. Drug Metabolism Reviews. 36**,** 268-268.

Kousba, A. A., et al., 2007. Age-related brain cholinesterase inhibition kinetics following in vitro incubation with chlorpyrifos-oxon and diazinon-oxon. Toxicological Sciences. 95**,** 147-155.

Krishnan, K., Johanson, G., 2005. Physiologically-based pharmacokinetic and toxicokinetic models in cancer risk assessment. J.Environ.Sci.Health C.Environ.Carcinog.Ecotoxicol.Rev. 23**,** 31-53.

Lafortuna, C. L., et al., 2005. Gender variations of body composition, muscle strength and power output in morbid obesity. Int J Obes (Lond). 29**,** 833-41.

Lassiter, T. L., et al., 1999. Gestational exposure to chlorpyrifos: dose response profiles for cholinesterase and carboxylesterase activity. Toxicological Sciences. 52**,** 92-100.

Lee, S., et al., 2009. Effects of nicotine exposure on in vitro metabolism of chlorpyrifos in male Sprague-Dawley rats. Journal of toxicology and environmental health. Part A. 72**,** 74-82 %U http://www.ncbi.nlm.nih.gov/pubmed/19034796.

Licata, A. C., et al., 2001. A physiologically based pharmacokinetic model for methyl tert-butyl ether in humans: implementing sensitivity and variability analyses. Toxicological Sciences. 62**,** 191-204.

LifeLine, Designing Exposure Models that Support PBPK/PBPD Models of Cumulative Risk. 2004.
LifeLine, Technical Manual LifeLine™ Version 4.3 Software, The LifeLine Group Inc., 2006.
Lipscomb, J. C., Use of Physiologically Based Pharmacokinetic Models to Quantify the Impact of Human Age and Interindividual Differences in Physiology and Biochemistry Pertinent to Risk. In: Office of Research and Development, N CEA, (Ed.), 2006.
Lowe, E. R., et al., 2009. The Effect of Plasma Lipids on the Pharmacokinetics of Chlorpyrifos and the Impact on Interpretation of Blood Biomonitoring Data. Toxicological Sciences. 108**,** 258-272.
Lu, C., et al., 2008. Dietary intake and its contribution to longitudinal organophosphorus pesticide exposure in urban/suburban children. Environ Health Perspect. 116**,** 537-42.
Lu, C., et al., 2010. The implications of using a physiologically based pharmacokinetic (PBPK) model for pesticide risk assessment. Environ Health Perspect. 118**,** 125-30.
Luecke, R. H., et al., 2007. Postnatal growth considerations for PBPK modeling. Journal of Toxicology and Environmental Health-Part a-Current Issues. 70**,** 1027-1037.
Marty, M. S., et al., 2007. The effect of route, vehicle, and divided doses on the pharmacokinetics of chlorpyrifos and its metabolite trichloropyridinol in neonatal Sprague-Dawley rats. Toxicological Sciences. 100**,** 360-373.
Mattsson, J. L., et al., 2000. Lack of differential sensitivity to cholinesterase inhibition in fetuses and neonates compared to dams treated perinatally with chlorpyrifos. Toxicological Sciences. 53**,** 438-446.
McDowell, M., Fryar, CD, Hirsch, R, Ogden CL, Anthropometric Reference Data for Children and Adults: U.S. Population, 1999–2002. In: CDC, N. D., (Ed.), 2005, pp. 32.
Medinsky, M. A., 1995. The application of physiologically based pharmacokinetic/pharmacodynamic (PBPK/PD) modeling to understanding the mechanism of action of hazardous substances. Toxicology Letters. 79**,** 185-191.
Mendrala, A. L., Brzak, K. A., Chlorpyrifos: Part A-- Concentration-Time Course of Chlorpyrifos and Chlorpyrifos-Oxon in Blood (in Rats): Lab Project Number: 971187A. Unpublished study prepared by The Dow Chemical Company. 63 p. (MRID 44648102). The Dow Chemical Company, 1998.
Moreira, E. G., et al., 2010. Toxicogenomic profiling in maternal and fetal rodent brains following gestational exposure to chlorpyrifos. Toxicol Appl Pharmacol. 245**,** 310-25.
Mutch, E., Williams, F. M., 2006. Diazinon, chlorpyrifos and parathion are metabolised by multiple cytochromes P450 in human liver. Toxicology. 224**,** 22-32.
National Research Council, 2007. Toxicity Testing in the 21st Centryu a Vision and a Strategy. National Academies Press, Washington, DC.
National Research Council, 2008. Science and Decisions: Advancing Risk Assessment. Committee on Improving Risk Analysis Approaches Used by the U.S. EPA. National Research Council, Washington, DC.
Nigg, H. N., Knaak, J. B., 2000. Blood cholinesterases as human biomarkers of organophosphorus pesticide exposure. Reviews of Environmental Contamination and Toxicology. 163**,** 29-111.
Nolan, R. J., et al., Chlorpyrifos: Tissue Distribution and Metabolism of Orally Administered Carbon 14-Labeled Chlorpyrifos in Fischer 344 Rats: Laboratory Project Study ID: K-044793-(76). Unpublished study prepared by The Dow Chemical Company. 41 p. [MRID 40458901]. The Dow Chemical Company, 1987.

Nolan, R. J., et al., 1984. Chlorpyrifos: pharmacokinetics in human volunteers. Toxicology and Applied Pharmacology. 73**,** 8-15.
Nomura, D. K., Casida, J. E., 2010. Activity-Based Protein Profiling of Organophosphorus and Thiocarbamate Pesticides Reveals Multiple Serine Hydrolase Targets in Mouse Brain†. Journal of Agricultural and Food Chemistry. null-null.
Noort, D., et al., 2009. Covalent binding of organophosphorothioates to albumin: a new perspective for OP-pesticide biomonitoring? Archives of Toxicology. 83**,** 1031-1036 %U http://www.ncbi.nlm.nih.gov/pubmed/19575182.
Peters, S. A., Hultin, L., 2008. Early identification of drug-induced impairment of gastric emptying through physiologically based pharmacokinetic (PBPK) simulation of plasma concentration-time profiles in rat. Journal of Pharmacokinetics and Pharmacodynamics. 35**,** 1-30.
Poet, K. S., et al., 2002. Physiologically based pharmacokinetic/pharmacodynamic modeling of organophosphate pesticides for biologically based risk assessments. Epidemiology. 13**,** S240-S240.
Poet, T. S., et al., 2003. In vitro rat hepatic and intestinal metabolism of the organophosphate pesticides chlorpyrifos and diazinon. Toxicological Sciences: An Official Journal of the Society of Toxicology. 72**,** 193-200 %U http://www.ncbi.nlm.nih.gov/pubmed/12655035.
Ray, A., et al., 2010. Dose-related gene expression changes in forebrain following acute, low-level chlorpyrifos exposure in neonatal rats. Toxicology and Applied Pharmacology. 248**,** 144-155 %U http://www.ncbi.nlm.nih.gov/pubmed/20691718.
Reddy, M. B., et al., 2005. Physiologically Based Pharmacokinetic Modeling: Science and Applicaitons. John Wiley and Sons, Hoboken, NJ.
Reitz, R. H., et al., 1988. Physiologically based pharmacokinetic modeling with methylchloroform: Implications for interspecies, high dose/low dose, and dose route extrapolations. Toxicology and Applied Pharmacology. 95**,** 185-199.
Richter, R. J., Furlong, C. E., 1999. Determination of paraoxonase (PON1) status requires more than genotyping. Pharmacogenetics. 9**,** 745-53.
Sams, C., et al., 2004. Biotransformation of chlorpyrifos and diazinon by human liver microsomes and recombinant human cytochrome P450s (CYP). Xenobiotica. 34**,** 861-73.
Sangster, J., LOGKOW Databank. A databank of evaluated octanol-water partition coefficients (Log P) on microcomputer diskette. Montreal, Quebec, Canada: Sangster Research Laboratories (as referenced in the PhysProp Database of US EPA KowWin program (v1.67a)). 1994.
Schwartz, G., 1978. Estimating the Dimension of a Model. Annals of Statistics. 6**,** 461-464.
Slikker, W., et al., 2005. Improving predictive modeling in pediatric drug development: Pharmacokinetics, pharmacodynamics, and mechanistic modeling. Neuroprotective Agents. 1053**,** 505-518.
Smith, G. N., et al., 1967. METABOLISM Investigations on Dursban Insecticide. Metabolism of [36Cl]0,O-Diethyl 0-3,5,6-Trichloro-2-pyridyl Phosphorothioate in Rats. Journal of Agricultural and Food Chemistry. 15**,** 132-138 %U http://dx.doi.org/10.1021/jf60149a017.
Snyder, W., 1975. Report of the Task Group on Reference Man. Elsevier Science Limited, Oxford, UK.
Sultatos, L. G., 1994. Mammalian toxicology of organophosphorus pesticides. Journal of Toxicology and Environmental Health. 43**,** 271-289.

Sunaga, M., et al., 1989. [Metabolism and urinary excretion of chlorpyrifos in rats]. Nippon Eiseigaku Zasshi. Japanese Journal of Hygiene. 43**,** 1124-1129 %U http://www.ncbi.nlm.nih.gov/pubmed/2473231.

Tan, Y. M., et al., 2006. Reverse dosimetry: interpreting trihalomethanes biomonitoring data using physiologically based pharmacokinetic modeling. J.Expo.Sci.Environ.Epidemiol.

Tang, J., et al., 2001. Metabolism of chlorpyrifos by human cytochrome P450 isoforms and human, mouse, and rat liver microsomes. Drug Metab Dispos. 29**,** 1201-1204.

Tardif, R., et al., 2002. Impact of human variability on the biological monitoring of exposure to toluene: I. Physiologically based toxicokinetic modelling. Toxicology Letters. 134**,** 155-163.

Tateishi, T., et al., 1997. A comparison of hepatic cytochrome P450 protein expression between infancy and postinfancy. Life Sciences. 61**,** 2567-2574.

Teeguarden, J. G., Barton, H. A., 2004. Computational modeling of serum-binding proteins and clearance in extrapolations across life stages and species for endocrine active compounds. Risk Analysis. 24**,** 751-770.

Thompson, C. M., et al., 2010. Mass spectrometric analyses of organophosphate insecticide oxon protein adducts. Environmental Health Perspectives. 118**,** 11-19 %U http://www.ncbi.nlm.nih.gov/pubmed/20056576.

Timchalk, C., et al., 2002a. Monte Carlo analysis of the human chlorpyrifos-oxonase (PON1) polymorphism using a physiologically based pharmacokinetic and pharmacodynamic (PBPK/PD) model. Toxicology Letters. 135**,** 51.

Timchalk, C., et al., 2002b. A Physiologically based pharmacokinetic and pharmacodynamic (PBPK/PD) model for the organophosphate insecticide chlorpyrifos in rats and humans. Toxicological Sciences. 66**,** 34-53.

Timchalk, C., Poet, T. S., 2008. Development of a physiologically based pharmacokinetic and pharmacodynamic model to determine dosimetry and cholinesterase inhibition for a binary mixture of chlorpyrifos and diazinon in the rat. Neurotoxicology. 29**,** 428-443.

Timchalk, C., et al., 2005. Pharmacokinetic and pharmacodynamic interaction for a binary mixture of chlorpyrifos and diazinon in the rat. Toxicology and Applied Pharmacology. 205**,** 31-42.

Timchalk, C., et al., 2006. Age-dependent pharmacokinetic and pharmacodynamic response in preweanling rats following oral exposure to the organophosphorus insecticide chlorpyrifos. Toxicology. 220**,** 13-25.

Treluyer, J. M., et al., 1997. Developmental expression of CYP2C and CYP2C-dependent activities in the human liver: in-vivo/in-vitro correlation and inducibility. Pharmacogenetics. 7**,** 441-452.

U.S. EPA, A Model Comparison: Dietary (Food and Water) Exposure in DEEM/Calendex, CARES, and LifeLine. 2004.

U.S. EPA, Guidelines for Carcinogen Risk Assesment. In: Forum, R. A., (Ed.), 2005.

Welsch, F., et al., 1995. Physiologically based pharmacokinetic models applicable to organogenesis: extrapolation between species and potential use in prenatal toxicity risk assessments. Toxicology Letters. 82-83**,** 539-547.

WHO, CHEMICAL-SPECIFIC ADJUSTMENT FACTORS FOR INTERSPECIES DIFFERENCES AND HUMAN VARIABILITY:
GUIDANCE DOCUMENT FOR USE OF DATA IN DOSE/CONCENTRATION–RESPONSE ASSESSMENT. 2006, pp. 100.

Whyatt, R. M., et al., 2003. Contemporary-use pesticides in personal air samples during pregnancy and blood samples at delivery among urban minority mothers and newborns. Environ Health Perspect. 111**,** 749-56.
Whyatt, R. M., et al., 2009. A biomarker validation study of prenatal chlorpyrifos exposure within an inner-city cohort during pregnancy. Environ Health Perspect. 117**,** 559-67.
Wilson, N. K., et al., 2003. Aggregate exposures of nine preschool children to persistent organic pollutants at day care and at home. Journal of Exposure Analysis and Environmental Epidemiology. 13**,** 187-202.
Xue, J., Zartarian V., and Nako S., The Stochastic Human Exposure and Dose Simulation Model for Multimedia, Multipathway Chemicals (SHEDS-Multimedia):Dietary Module SHEDS-Dietary version 1 Draft Technical Manual June 16, 2010. In: US Environmental Protection Agency, O. o. R. a. D., National Exposure Research, US Environmental Protection Agency, Office of Pesticide Programs, Laboratory, Eds.), 2010.
Yang, D., et al., 2008. Chlorpyrifos and chlorpyrifos-oxon inhibit axonal growth by interfering with the morphogenic activity of acetylcholinesterase. Toxicol Appl Pharmacol. 228**,** 32-41.
Yang, R. S., et al., 1995. The use of physiologically-based pharmacokinetic/pharmacodynamic dosimetry models for chemical mixtures. Toxicology Letters. 82-83**,** 497-504.
Young, J. F., et al., 2009. Human Organ/Tissue Growth Algorithms that Include Obese Individuals and Black/White Population Organ Weight Similarities from Autopsy Data. Journal of Toxicology and Environmental Health-Part a-Current Issues. 72**,** 527-540.
Zemke, A. C., et al., 2009. Molecular Staging of Epithelial Maturation Using Secretory Cell-Specific Genes as Markers. American Journal of Respiratory Cell and Molecular Biology. 40**,** 340-348.